การแสดงออกและลักษณะสมบัติของแอลฟากลูโคซิเดสจาก *Weissella confusa* BBK-1

นางสาวลลิตา ศิลปสม

จุฬาลงกรณ์มหาวิทยาลัย
CHULALONGKORN UNIVERSITY

บทคัดย่อและแฟ้มข้อมูลฉบับเต็มของวิทยานิพนธ์ตั้งแต่ปีการศึกษา 2554 ที่ให้บริการในคลังปัญญาจุฬาฯ (CUIR)
เป็นแฟ้มข้อมูลของนิสิตเจ้าของวิทยานิพนธ์ ที่ส่งผ่านทางบัณฑิตวิทยาลัย
The abstract and full text of theses from the academic year 2011 in Chulalongkorn University Intellectual Repository (CUIR)
are the thesis authors' files submitted through the University Graduate School.

วิทยานิพนธ์นี้เป็นส่วนหนึ่งของการศึกษาตามหลักสูตรปริญญาวิทยาศาสตรมหาบัณฑิต
สาขาวิชาชีวเคมีและชีววิทยาโมเลกุล ภาควิชาชีวเคมี
คณะวิทยาศาสตร์ จุฬาลงกรณ์มหาวิทยาลัย
ปีการศึกษา 2560

ลิขสิทธิ์ของจุฬาลงกรณ์มหาวิทยาลัย

EXPRESSION AND CHARACTERIZATION OF α-GLUCOSIDASE FROM *Weissella confusa* BBK-1

Miss Lalita Silapasom

จุฬาลงกรณ์มหาวิทยาลัย
CHULALONGKORN UNIVERSITY

A Thesis Submitted in Partial Fulfillment of the Requirements
for the Degree of Master of Science Program in Biochemistry and Molecular Biology
Department of Biochemistry
Faculty of Science
Chulalongkorn University
Academic Year 2017
Copyright of Chulalongkorn University

Thesis Title	EXPRESSION AND CHARACTERIZATION OF α-GLUCOSIDASE FROM *Weissella confusa* BBK-1
By	Miss Lalita Silapasom
Field of Study	Biochemistry and Molecular Biology
Thesis Advisor	Assistant Professor Kuakarun Krusong, Ph.D.
Thesis Co-Advisor	Professor Piamsook Pongsawasdi, Ph.D.

Accepted by the Faculty of Science, Chulalongkorn University in Partial Fulfillment of the Requirements for the Master's Degree

..... Dean of the Faculty of Science

(Associate Professor Polkit Sangvanich, Ph.D.)

THESIS COMMITTEE

..... Chairman

(Assistant Professor Kanoktip Packdibamrung, Ph.D.)

..... Thesis Advisor

(Assistant Professor Kuakarun Krusong, Ph.D.)

..... Thesis Co-Advisor

(Professor Piamsook Pongsawasdi, Ph.D.)

..... Examiner

(Assistant Professor Rath Pichyangkura, Ph.D.)

..... External Examiner

(Associate Professor Jarunee Kaulpiboon, Ph.D.)

จุฬาลงกรณ์มหาวิทยาลัย
CHULALONGKORN UNIVERSITY

ลลิตา ศิลปสม : การแสดงออกและลักษณะสมบัติของแอลฟากลูโคซิเดสจาก *Weissella confusa* BBK-1 (EXPRESSION AND CHARACTERIZATION OF α-GLUCOSIDASE FROM *Weissella confusa* BBK-1) อ.ที่ปรึกษาวิทยานิพนธ์หลัก: ผศ. ดร.เกื้อการุณย์ ครูส่ง, อ.ที่ปรึกษาวิทยานิพนธ์ร่วม: ศ. ดร.เปี่ยมสุข พงษ์สวัสดิ์, 134 หน้า.

แอลฟากลูโคซิเดส [EC 3.2.1.20] คือ เอนไซม์ที่ตัดจากด้านปลายเข้ามาทีละหน่วย ซึ่งเร่งปฏิกิริยาการสลายพันธะจากปลายด้านนอนรีดิวซ์ซิงค์ของสารตั้งต้นให้ผลิตภัณฑ์คือกลูโคส นอกจากนี้แอลฟากลูโคซิเดสยังมีความสามารถในการโยกย้ายหมู่ฟังก์ชั่นทำให้เกิดการสร้างผลิตภัณฑ์ที่หลากหลายจำพวกสารประกอบที่มีกลูโคสเป็นองค์ประกอบ เช่น แป้งและไกลโคเจน งานวิจัยนี้มีจุดมุ่งหมายในการแสดงออกและศึกษาลักษณะสมบัติของแอลฟากลูโคซิเดสจาก *Weissella confusa* BBK-1 (*Wc*AG) ยีน *Wc*AG แสดงออกใน modified pET28b โดยยีนมีขนาด 1775 คู่เบส ภาวะที่เหมาะสมในการแสดงออกของ *Wc*AG คือเลี้ยงเซลล์ในอาหารเหลว (LB broth) ที่มีกลูโคสความเข้มข้นร้อยละ 1 และเหนี่ยวนำด้วย IPTG ความเข้มข้น 0.4 มิลลิโมลาร์ ณ อุณหภูมิ 20 องศาเซลเซียสเป็นเวลา 20 ชั่วโมง รีคอมบิแนนท์ *Wc*AG ที่มี his-tag ด้านปลาย C ถูกทำให้บริสุทธิ์โดยใช้คอลัมน์ His-Trap ได้ค่าแอกทิวิตีจำเพาะเท่ากับ 45.29 ยูนิตต่อมิลลิกรัมโปรตีน มีความบริสุทธิ์เพิ่มขึ้น 2.93 เท่าและมีแอกทิวิตีคงเหลือทั้งหมดร้อยละ 21.65 *Wc*AG มีมวลโมเลกุลประมาณ 124 กิโลดาลตันประกอบด้วยโปรตีน 2 หน่วยย่อย สำหรับปฏิกิริยาไฮโดรไลซิสอุณหภูมิและค่า pH ที่เหมาะสมในการเร่งปฏิกิริยาคือ 50 องศาเซลเซียสและ pH 6.0 ตามลำดับ การตรวจสอบเสถียรภาพของ *Wc*AG พบว่ามีความเสถียรในช่วงอุณหภูมิ 4 - 40 องศาเซลเซียสในฟอสเฟตบัฟเฟอร์ pH 6.0-8.0 โดยสารตั้งต้นที่ดีที่สุดสำหรับปฏิกิริยาไฮโดรไลซิสคือมอลโทไตรโอส (G3) และปฏิกิริยาการโยกย้ายหมู่คือมอลโทส (G2) โดยปฏิกิริยาไฮโดรไลซิสมีลำดับความชอบของสารตั้งต้นเรียงจากมากไปน้อยคือ มอลโทไตรโอส (G3) มอลโทเตตระโอส (G4) มอลโทเพนตะโอส (G5) มอลโทเฮกซะโอส (G6) และมอลโทส (G2) จากการศึกษาจลนศาสตร์ของ *Wc*AG เมื่อใช้มอลโทไตรโอสเป็นสารตั้งต้นพบว่าค่า K_m, k_{cat}และ k_{cat}/K_mคือ 2.67 มิลลิโมลาร์,14.096 วินาที$^{-1}$และ5.279 (วินาที·มิลลิโมลาร์)$^{-1}$ ตามลำดับ ค่า K_m, k_{cat}และ k_{cat}/K_m เมื่อใช้มอลโทสเป็นสารตั้งต้นคือ 16.22 มิลลิโมลาร์, 0.738 วินาที$^{-1}$และ 0.046 (วินาที·มิลลิโมลาร์)$^{-1}$ตามลำดับ ภาวะที่สังเคราะห์มอลโทออลิโกแซคคาไรด์ได้ผลผลผลิตสูงสุดคือการบ่มปฏิกิริยาโดยใช้มอลโทสความเข้มข้น 200 มิลลิโมลาร์กับ *Wc*AG ความเข้มข้น 0.4 ยูนิตต่อมิลลิมิตร ณ อุณหภูมิ 37 องศาเซลเซียสเป็นเวลา 24 ชั่วโมง โดยที่ปฏิกิริยาการโยกย้ายหมู่สามารถสังเคราะห์ผลิตภัณฑ์ได้ 4 ชนิด การวิเคราะห์ผลิตภัณฑ์โดยใช้เทคนิค HPAEC-PAD พบว่าผลิตภัณฑ์ที่สังเคราะห์ได้คือ ไอโซมอลโทส พาโนสและมอลโทออลิโกแซคคาไรด์อีกสองชนิดที่ยังไม่สามารถระบุได้

ภาควิชา	ชีวเคมี	ลายมือชื่อนิสิต .....
สาขาวิชา	ชีวเคมีและชีววิทยาโมเลกุล	ลายมือชื่อ อ.ที่ปรึกษาหลัก .....
ปีการศึกษา	2560	ลายมือชื่อ อ.ที่ปรึกษาร่วม .....

5872041723 : MAJOR BIOCHEMISTRY AND MOLECULAR BIOLOGY

KEYWORDS: ALPHA-GLUCOSIDASE / MALTOOLIGOSACCHARIDES PRODUCT / WEISSELLA CONFUSA BBK-1 / TRANSGLYCOSYLATION

LALITA SILAPASOM: EXPRESSION AND CHARACTERIZATION OF α-GLUCOSIDASE FROM *Weissella confusa* BBK-1. ADVISOR: ASST. PROF. KUAKARUN KRUSONG, Ph.D., CO-ADVISOR: PROF. PIAMSOOK PONGSAWASDI, Ph.D., 134 pp.

Alpha-glucosidase [EC 3.2.1.20; α-D-glucoside glucohydrolase] is an exohydrolase which catalyzes non-reducing end of substrates to release D-glucose. In addition, alpha-glucosidase also displays a transferase activity, which bring about the formation of α-glucosylated compounds such as soluble starch and glycogen. This research aims to express and characterize α-glucosidase from *Weissella confusa* BBK-1 (*Wc*AG). *WcAG* gene was expressed in modified pET28b vector. This gene contained an open reading frame of 1,775 bps. Optimum expression condition of *Wc*AG was cultured in LB medium containing 1% (w/v) glucose and induced with 0.4 mM IPTG at 20°C for 20 h. The recombinant *Wc*AG containing his-tag at the C-terminus was successfully purified by His-Trap column with the specific activity of 45.29 U/ml, purification fold of 2.93 increased with 21.65% yields of total activity. *Wc*AG had molecular mass of 124 kDa and existed as dimer in native form. For hydrolysis activity, the optimum temperature and pH were at 50 ºC and pH 6.0, respectively. Temperature and pH stability of *Wc*AG were in range of 4 to 40 °C, and pH 6.0-8.0 in phosphate buffer, respectively. The most suitable substrate for hydrolysis activity of *Wc*AG was maltotriose (G3) while maltose (G2) was for transglycosylation activity. For hydrolysis activity, the order of preferable substrate was maltotriose (G3), maltotetraose (G4), maltopentaose (G5), maltohexaose (G6) and maltose (G2), respectively. For kinetic study of *Wc*AG, the apparent K_m, k_{cat} and k_{cat}/K_m values for G3 substrate were 2.67 mM, 14.096 s^{-1} and 5.279 $(s{\cdot}mM)^{-1}$, respectively. The apparent K_m, k_{cat} and k_{cat}/K_m values for G2 substrate were 16.22 mM, 0.738 s^{-1} and 0.046 $(s{\cdot}mM)^{-1}$, respectively. The optimal maltooligosacharide production was obtained of incubation using 200 mM of G2 with 0.4 unit/ml of *Wc*AG at 37 ºC for 24 h. Four products were obtained from transglycosylation activity including product I, II, III and IV. Identification of all products using HPAEC-PAD revealed that product I was isomaltose, product II was panose while product III and IV still cannot be identified.

Department:	Biochemistry	Student's Signature	.....
Field of Study:	Biochemistry and Molecular Biology	Advisor's Signature	.....
		Co-Advisor's Signature	.....
Academic Year:	2017		

ACKNOWLEDGEMENTS

Firstly, I would like to express my sincere gratitude to my advisor Assistant Professor Kuakarun Krusong, for the continuous support of my master study and related research, for her patience, motivation, and immense knowledge. Her guidance helped me in all the time of research and writing of this thesis. I could not have imagined having a better advisor and mentor for my master study. In addition, this is also including my co-advisor, Professor Piamsook Pongsawasdi, who give a valuable comment and support me.

Besides my advisor, sincerely thanks and appreciation are due to Assistant Professor Kanoktip Packdibamrung, Assistant Professor Rath Pichyangura and Associate Professor Jarunee Kaulpiboon for their encouragement, valuable suggestion, insightful comment which incented me to widen my research from various perspectives and dedication their valuable time for thesis examination.

My sincere thanks also goes to member in 705, 709 and 618 room with their help and support me. This research was funded by Thailand Research Fund IRG5780008 and Special Task Force for Activating Research, Faculty of Science, Chulalongkorn University for Structural and Computational Biology Research Group GSTAR 59-012-23-001. And also, thanks to Chulalongkorn University Graduate Scholarship to commemorate the 72nd Anniversary of His Majesty King Bhumibol Adulyadej for partially financial support to me. Without they precious support it would not be possible to conduct this research.

Last but not the least, I would like to thank my family for supporting me spiritually throughout writing this thesis and my my life in general and cheer me up all the time when I have got a problem or I was tired. This is valuable for me to go through all tasks and complete my master degree.

จุฬาลงกรณ์มหาวิทยาลัย
CHULALONGKORN UNIVERSITY

CONTENTS

Page

THAI ABSTRACT iv

ENGLISH ABSTRACT v

ACKNOWLEDGEMENTS vi

CONTENTS vii

LIST OF TABLES x

LIST OF FIGURES xi

ABBREVIATIONS xviii

CHAPTER I INTRODUCTION 1

1.1 Glycosyltransferases and glycosidases as catalysts 1

1.2 α-Glucosidase 3

1.3 Classification 4

1.4 GH 13 α-glucosidases 5

1.5 GH 31 α-glucosidase 13

1.6 Enzymatic and chemical production of oligosaccharides 14

1.7 Applications 16

1.8 *Weissella confusa* 17

1.9 Objectives 17

CHAPTER II MATERIALS AND METHODS 18

2.1 Equipment 18

2.2 Chemicals 20

2.3 Enzymes and restriction enzymes 22

2.4 Bacterial strains 22

2.5 Analysis of *Wc*AG sequence 23

2.6 Optimization of *Wc*AG expression 23

2.7 Purification of *Wc*AG by His-Trap column chromatography 24

2.8 Protein determination 24

2.9 Characterization of *Wc*AG 25

2.10 Optimization of transglycosylation activity 29

จุฬาลงกรณ์มหาวิทยาลัย
CHULALONGKORN UNIVERSITY

Page

2.11 Large scale production of maltooligosaccharide products 30

2.12 Isolation of maltooligosaccharide products.....30

2.13 HPAEC-PAD analysis of maltooligosaccharide products 31

CHAPTER III RESULTS 32

3.1 Sequence analysis of α–glucosidase from *Weissella confusa* BBK-1 32

3.2 Expression of α–glucosidase from *Weissella confusa* BBK-1 38

3.3 Purification of *Wc*AG 50

3.4 Characterization of *Wc*AG 54

3.5 Optimization of transglycosylation reaction 70

3.6 Large scale production and isolation of maltooligosaccharide products 77

3.7 Characterization of maltooligosaccharide products 77

CHAPTER IV DISCUSSION.....82

CHAPTER V CONCLUSIONS.....103

REFERENCES.....105

APPENDICES.....116

APPENDIX 1 Preparation of SDS-polyacrylamide gel electrophoresis 117

APPENDIX 2 Preparation of buffer for crude enzyme preparation 120

APPENDIX 3 Preparation of purification buffer.....121

APPENDIX 4 Preparation of Bradford' s solution 123

APPENDIX 5 Restriction map of modified pET-28b vector 124

APPENDIX 6 Standard curve for protein determination by Bradford's assay 126

APPENDIX 7 Standard curve for protein determination by glucose oxidase assay.....127

APPENDIX 8 Calculation for percentage relative activity 128

APPENDIX 9 Standard curve of molecular weight protein from SDS-PAGE.....129

APPENDIX 10 Standard curve for protein determination by gel filtration chromatography.....130

APPENDIX 11 Abbreviation of amino acid residue found in protein 131

จุฬาลงกรณ์มหาวิทยาลัย
Chulalongkorn University

Page

REFERENCES.....132

VITA.....134

จุฬาลงกรณ์มหาวิทยาลัย
CHULALONGKORN UNIVERSITY

LIST OF TABLES

Table 1. 1 Amino-acid residues related with substrate specificity and transglycosylation activity in GH13 α-glucosidase (Table from Okuyama et al., 2016) 11

Table 3. 1 Purification table of *Wc*AG by His-Trap column. 54

Table 3. 2 Substrate preference of *Wc*AG[a]. 63

Table 3. 3 Summary of kinetic parameters of *Wc*AG hydrolysis activity using maltose and maltotriose as substrates. 69

Table 4. 1 Properties parameters for hydrolysis activity of α-glucosidase from various strains. 91

Table 4. 2 Kinetic parameters of hydrolysis activity from various strains using maltose as substrate. 96

Table 4. 3 Kinetic parameters of hydrolysis activity from various strains using maltotriose as substrate. 97

จุฬาลงกรณ์มหาวิทยาลัย
CHULALONGKORN UNIVERSITY

LIST OF FIGURES

Figure 1. 1 Catalytic reactions of α-glucosidase. The upper is hydrolysis and lower reactions is transglycosylation activity.R_1 represent α-glucosaccharide, α-glucan and maltooligosaccharide unit. HO-R_2 represent acceptor substrate for transglycosylation.....4

Figure 1. 2 Three dimensional structures of GH13 α-glucosidases. (A) Overall structure of HaG and maltose complex (PDB, 3WY4). (B) Overall structure of SmDG and isomaltotriose complex (PDB, 2ZID). Domain A red; domain B green; domain C orange; domain B blue; β→α loop 1, 2, 5, 6, and 7,cyan; and β→α loop 4, magenta. The substrates bound to the enzymes are shown by green stick. Calcium ion bound to the β→α loop 1 of domain A is indicated by a green sphere. It is thought to regulate the thermostability based on the kinetic experiment (Kobayashi et al., 2011); (C) closeup view of the *Sm*DG active site. Isomaltotriose covers from subsite -1 to -2. The inactive mutant enzyme (E236Q) was used to trap the Michaelis complex. (Figure from Okuyama et al., 2016).....6

Figure 1. 3 Multiple alignment of GH13 α-glucosidases. Amino-acid sequences of GH13 α-glucosidases were aligned using the MAFFTash. 8

Figure 1. 4 Typical process of chemical production a disaccharides (Figure from Nilsson, 1988). 15

Figure 3. 1 Nucleotide sequence of *WcAG* gene with *Nco*I and *Xho*I restriction sites (underlined), respectively. Bold three codons of ATG and TGA indicated start and stop codon, respectively.....33

Figure 3. 2 Deduced amino acid sequence of *Wc*AG.....34

Figure 3. 3 Structural analysis of *Wc*AG sequence.....34

จุฬาลงกรณ์มหาวิทยาลัย
CHULALONGKORN UNIVERSITY

Figure 3. 4 Multiple sequence alignment of *Wc*AG comparing to α–glucosidases from other organisms 36

Figure 3. 5 Phylogenetic tree showed the relationship of *Wc*AG with others organisms. 37

Figure 3. 6 (A) 10% SDS-PAGE of *Wc*AG expressed at 30 ºC, 1 mM IPTG induction at 0 to 24 h. (B) 10% SDS-PAGE of *Wc*AG expressed at 37 ºC, 1 mM IPTG induction at 0 to 24 h.....39

Figure 3. 7 (A) 10% SDS-PAGE of *Wc*AG expressed at 30 ºC, 0.1 mM IPTG induction at 0 to 24 h. (B) 10% SDS-PAGE of *Wc*AG expressed at 30 ºC, 0.5 mM IPTG induction at 0 to 24 h. (C) 10% SDS-PAGE of *Wc*AG expressed at 30 ºC, 1 mM IPTG induction at 0 to 24 h. 40

Figure 3. 8 (A) 10% SDS-PAGE of *Wc*AG expressed at 16 ºC, 0.1 mM IPTG induction at 0 to 24 h. (B) 10% SDS-PAGE of *Wc*AG expressed at 16 ºC, 0.5 mM IPTG induction at 0 to 24 h. (C) 10% SDS-PAGE of *Wc*AG expressed at 16 ºC, 1 mM IPTG induction at 0 to 24 h. 41

Figure 3. 9 (A) 10% SDS-PAGE of *Wc*AG expressed at 16 ºC, 1 mM IPTG induction at 0 to 20 h. (B) 10% SDS-PAGE of *Wc*AG expressed at 16 ºC, 1 mM IPTG induction at 24 h.....42

Figure 3. 10 (A) 10% SDS-PAGE of *Wc*AG expressed at 12 ºC, 0.4 mM IPTG induction at 0 to 24 h. (B) 10% SDS-PAGE of *Wc*AG expressed at 20 ºC , 0.4 mM IPTG induction at 0 to 24 h.....43

Figure 3. 11 (A) 10% SDS-PAGE of *Wc*AG expressed at 25 ºC, 0.1 mM IPTG induction at 0 to 24 h. (B) 10% SDS-PAGE of *Wc*AG expressed at 25 ºC, 0.4 mM IPTG induction at 0 to 24 h.....44

จุฬาลงกรณ์มหาวิทยาลัย
CHULALONGKORN UNIVERSITY

Figure 3. 12 (A and B) 10% SDS-PAGE of *Wc*AG expressed at 20 ºC , 0.1 mM IPTG induction at 0 to 24 h. (C and D) 10% SDS-PAGE of *Wc*AG expressed at 20 ºC, 0.2 mM IPTG induction at 0 to 24 h. (E and F) 10% SDS-PAGE of *WcAG* expressed at 20 ºC, 0.4 mM IPTG induction at 0 to 24 h. 45

Figure 3. 13 (A) 10% SDS-PAGE of *Wc*AG expressed at 20 ºC with 0.1 mM L-arginine, 0.4 mM IPTG induction at 0 to 24 h. (B) 10% SDS-PAGE of *Wc*AG expressed at 20 ºC with 0.25 mM L-arginine, 0.4 mM IPTG induction at 0 to 24 h. (C) 10% SDS-PAGE of *Wc*AG expressed at 20 ºC cultivation with 0.1 mM D-sorbitol, 0.4 mM IPTG induction at 0 to 24 h. (D) 10% SDS-PAGE of *Wc*AG expressed at 20 ºC cultivation with 0.5 mM D-sorbitol, 0.4 mM IPTG induction at 0 to 24 h. (E) 10% SDS-PAGE of *Wc*AG expressed at 16 ºC with 0.5 mM TritonX-100, 0.4 mM IPTG induction at 0 to 24 h. (F) 10% SDS-PAGE of *Wc*AG expressed at 16 ºC with 0.1 mM Tween-20, 0.4 mM IPTG induction at 0 to 24 h. 47

Figure 3. 14 10% SDS-PAGE of *Wc*AG expressed at 20 ºC, 0.4 mM IPTG induction at 20 h and resuspended in 50-500 ml of 50 mM phosphate buffer pH 7.4/cell culture in 1 L of LB medium. 49

Figure 3. 15 10% SDS-PAGE of *Wc*AG expressed at 20 ºC, 0.4 mM IPTG induction at 20 h and resuspended in 0.01-1% of Triton-X100. Red arrow indicated the expected *Wc*AG size of 62.0 kDa. 50

Figure 3.16 A 10% SDS-PAGE analysis of *Wc*AG purified by His-Trap column. 51

Figure 3.16 B Determining the molecular weight of *Wc*AG by SDS-PAGE. 52

Figure 3. 17 10% SDS-PAGE (A) and Western blot (B) analysis of *Wc*AG. 53

จุฬาลงกรณ์มหาวิทยาลัย
CHULALONGKORN UNIVERSITY

Figure 3. 18 Effect of temperature on hydrolysis activity. Purified *Wc*AG was incubated with 50 mM maltotriose in phosphate buffer pH 6.0 for 10 min at various temperatures. Free glucose, by-product of the reaction, was detected by glucose oxidase method, measuring at A_{505}.....55

Figure 3. 19 Effect of temperature on *Wc*AG stability assayed by hydrolysis method. *Wc*AG was pre-incubated at different temperatures for 1 h. Purified *WcAG* was incubated with 50 mM maltotriose in phosphate buffer pH 6.0 for 10 min at 50 ºC. Free glucose, by-product of the reaction, was detected by glucose oxidase method, measuring at A_{505} 56

Figure 3. 20 Effect of pH on hydrolytic activity. Purified *Wc*AG was incubated with 50 mM maltotriose in buffers with various pHs for 10 min at 50 ºC. Free glucose, by-product of the reaction, was detected by glucose oxidase method, measuring at A_{505}.....57

Figure 3. 21 Effect of pH on *Wc*AG stability assayed by hydrolytic method. *Wc*AG was pre-incubated at different temperatures for 60 min. Purified *Wc*AG was incubated with 50 mM maltotriose in 50 mM phosphate buffer pH 6.0 for 10 min at 50 ºC. Free glucose, by-product of the reaction, was detected by glucose oxidase method, measuring at A_{505}. A —●— indicates acetate buffer pH 3-6 , a ---▲--- indicates phosphate buffer pH 6-8 and – · ■ · – · indicates Tris-HCl pH 8-9. 58

Figure 3. 22 Effect of ions towards hydrolysis activity of *Wc*AG. Bar graph calculated from mean ± S.D. of three replicates of hydrolysis activity. Activity of *Wc*AG without ion was set as 100%. The letters indicated significant differences accepted at *p*-value = 0.01. 59

จุฬาลงกรณ์มหาวิทยาลัย
CHULALONGKORN UNIVERSITY

Figure 3.23 A Purification profile of *Wc*AG by gel filtration. The x-axis indicated elution time. 60

Figure 3.23 B Calibration curve for determining molecular weight of *Wc*AG by gel filtration chromatography. X-axis represented $K_{average}$ and Y-axis represented the log molecular weight. Marker proteins; Thyroglobulin (bovine)(670 kDa), γ-globulin (bovine)(158 kDa), Ovalbumin (chicken)(44 kDa), Myoglobin (horse)(17 kDa) and Vitamin B12(1.35 kDa).....61

Figure 3. 24 Half-life of *Wc*AG assayed by hydrolytic method. *Wc*AG was pre-incubated at 50 ºC for 10 min. Purified *Wc*AG was incubated with 50 mM maltotriose in phosphate buffer pH 6.0 at various times. Free glucose, by-product of the reaction, was detected by glucose oxidase method, measuring at A_{505}.....62

Figure 3. 25 TLC chromatogram of reaction product of *Wc*AG incubated with maltose (G2), maltotriose (G3) and maltotetraose (G4) as substrate. Solvent system was butanol : acetic acid : water (3:3:2, v/v). Dash box indicated glucose, the product from hydrolysis activity and square dot box indicated maltose, the product from hydrolysis activity. 65

Figure 3. 26 TLC chromatogram of reaction product of *Wc*AG incubated with maltopentaose (G5), maltohexaose (G6) and maltoheptaose (G7) as substrate. Solvent system was butanol : acetic acid : water (3:3:2, v/v). Dash box indicated glucose, the product from hydrolytic activity and square dot box indicated maltose, the product from hydrolytic activity. 66

Figure 3.27 A Michealis-Menten plot of *Wc*AG hydrolysis activity using maltotriose as substrate. The K_m and V_{max} values of *Wc*AG for G3 as substrate were 2.67 mM and 6.821 mM, respectively. 67

จุฬาลงกรณ์มหาวิทยาลัย
CHULALONGKORN UNIVERSITY

Figure 3.27 B Lineweaver-Burk plot of *Wc*AG hydrolysis activity using maltotriose as substrate. 68

Figure 3.28 A Michealis-Menten plot of *Wc*AG activity using maltose as substrate. The K_m and V_{max} values of *Wc*AG for G2 as substrate were 16.22 and 0.357 mM, respectively. 68

Figure 3.28 B Lineweaver-Burk plot of *Wc*AG activity using maltose as substrate. 69

Figure 3. 29 (A and B) TLC of transglycosylated products for 0.04 U/ml and 0.4 U/ml of *Wc*AG incubated with 100 mM maltose for 16 h....71

Figure 3. 30 TLC of transglycosylated products for various *Wc*AG concentrations incubated with 100 mM maltose at 37 ºC for 16 h....72

Figure 3.31 A TLC of transglycosylated products for *Wc*AG 0.4 U/ml incubated with various maltose concentrations at 37 ºC for 16 h. 74

Figure 3.31 B TLC of transglycosylated products for 0.04 and 0.4 U/ml *Wc*AG incubated at 18, 30 and 37 ºC for 24 h....75

Figure 3. 32 TLC of transglycosylated products for 0.4 U/ml *Wc*AG incubated with 200 mM maltose at 37 ºC at various times....76

Figure 3. 33 HPAEC-PAD chromatogram of crude maltooligosaccharide products....77

Figure 3. 34 TLC of purified transglycosylated products by Biogel P2 column ...78

Figure 3. 35 HPAEC-PAD analysis of peak I compared with standard isomaltose from CarboPac® PA1 analytical column. 79

Figure 3. 36 HPAEC-PAD analysis of peak II compared with standard panose from CarboPac® PA1 analytical column. 79

จุฬาลงกรณ์มหาวิทยาลัย
CHULALONGKORN UNIVERSITY

Figure 3. 37 HPAEC-PAD analysis of peak III from CarboPac® PA1 analytical column. 80

Figure 3. 38 HPAEC-PAD analysis of peak IV from CarboPac® PA1 analytical column. 81

Figure 4. 1 Structural modeling of alpha amylase. The α-helices and β-sheets are presented in red and cyan, respectively. The oxygen atoms are in red, the nitrogen atoms are in light blue, the carbon atoms are in yellow-green, and the sulfur atoms are in yellow (Figure from Yang et al., 2012).....84

Figure 4. 2 Structural modeling of alpha amylase. The catalytic residues Asp 248, Glu 278, and Asp 340 are shown in a "CPK" (Corey-Pauling-Koltun) representation. ---indicated distances from the respective catalytic residues to Met 145, Met 214, Met 229, Met 247, and Met 317. The oxygen atoms are in red for Met and dark purple for catalytic residues, the nitrogen atoms are in purple for Met and dark purple for catalytic residues, the carbon atoms are in green, and the sulfur atoms are in yellow. (Figure from Yang et al., 2012). 85

Figure 4. 3 Possible transglycosylated products of *Wc*AG using maltose as substrate 102

ABBREVIATIONS

A	Absorbance
AGase	Alpha-glucosidase
APS	Ammonium persulfate
BSA	Bovine serum albumin
°C	Degree Celsius
C	Carbon
cm	Centimeter
CtMGAM	C-terminal subunit of maltase-glucoamylase
CtSI	C-terminal subunit of sucrose-isomaltase
DG	Dextran glucosidase
E. coli	*Escherichia coli*
g	Gram
GAA	Human acid α-glucosidase
Gal/GalNAc	*Galactose*/N-acetyl D-galactosamine
GH	Glycoside hydrolase family
h	Hour
HaG	*Halomonas sp.* α-glucosidase

จุฬาลงกรณ์มหาวิทยาลัย
CHULALONGKORN UNIVERSITY

HPAEC-PAD	High-Performance Anion-Exchange Chromatography with Pulsed Amperometric Detection
k_{cat}	Turnover number
K_m	Michaelis-Menten constant
L	Litre
M	Molar
mA	Milliampare
mg	Milligram
MGAM	Maltase-glucoamylase
min	Minute
ml	Millilitre
mM	Millimolar
n.d.	Not detectable
NaOH	Sodium hydroxide
NDP-sugars	sugar nucleotides
NtMGAM	N-terminal subunit of maltase-glucoamylase
NtSI	N-terminal subunit of sucrose-isomaltase
O16G	Oligo-1,6-glucosidase
PAGE	Polyacrylamide gel electrophoresis

จุฬาลงกรณ์มหาวิทยาลัย
Chulalongkorn University

PCR	Polymerase chain reaction
rpm	round per minute
SDS	Sodium dodecyl sulfate
SI	Sucrose-isomaltase
*Sm*DG	*Streptococcus mutans* dextran glucosidase
TEMED	Tetramethyl ethylenediamine
U	Unit enzyme
V_{max}	Maximum velocity

จุฬาลงกรณ์มหาวิทยาลัย
CHULALONGKORN UNIVERSITY

CHAPTER I

INTRODUCTION

1.1 Glycosyltransferases and glycosidases as catalysts

1.1.1 Glycosyltransferase

Glycosyltransferase (EC 2.4) catalyses the stereospecific and regiospecific transfer of saccharide moieties from glycosyl donor such as activated nucleotide sugar to saccharide and nonsaccharide acceptors. Transfer of the sugar residue forms glycosidic bonds which occurs either the retention or the inversion of the configuration of the anomeric carbon. Definition of regiospecificity and stereospecificity are mean the high catalysts which can be obtained have an attractive characters and the high selectivity for the acceptor substrate. Glycosyltransferases were classified by the sugar transfer from donor to acceptor and by an acceptor specificity (Breton et al., 2006).

Large family of glycosyltransferases are important in all domains of life for the biosynthesis of glycoconjugates and complex carbohydrates. Glycosyltransferases are present in both prokaryotes and eukaryotes. Glycosylation reactions in bacterial cell are vital in many essential biological processe such as adhesion and signaling. In eukaryotic cells, most of the glycosylation reactions occur in the golgi apparatus which generates the variety of oligosaccharide structures. In animals, glycosyltransferases transfer galactose/N-acetyl D-galactosamine (Gal/GalNAc) units to the cell surface of glycolipids and glycoproteins which are the component of ABO blood groups. Glycosyltransferase from animals are present in low concentrations and also bound to intracellular membranes. Therefore, they require special purification technique (Beyer et al., 1981; Paulson, 1989). In plants cell, glycosyltransferases play a crucial function including the attachment of sugar moieties to various small molecules such as

flavonoids and hormones, the addition of N-linked glycans to glycoproteins, and the biosyntheses of cell wall polysaccharides using sugar nucleotides (NDP-sugars) as donors, and transfer the sugar residue to acceptors to form glycosidic bonds (Drickamer and Taylor, 1998).

1.1.2 Glycosidase

Glycosidase can be divided into two types. The first one is exoglycosidase that has an ability to hydrolyze glycosidic linkages at non-reducing end of saccharide chains. Another one is endoglycosidase which catalyzes oligosaccharide substrate. Type of exo or endo-glycosidase depending on the region where it attack in chain of substrate. Exoglycosidase catalyzes at the end of sugar chains to release particular monosaccharides from non-reducing termini of oligosaccharides, whereas endoglycosidase catalyzes at the middle of the chain to release an individual monomer (Kobata, 2013). This enzyme is found in viruses, microorganisms, plants and animal. Glycosidases were identified by specificity properties for the glycosyl unit of the donor and properties of their stereospecificity. However, most of glycosidases show less specificity to its substrate proof selectivity than glycosyltransferase does. Therefore, glycosidase is suitable for the production of various glycosides using less cost investment. So, variety of linkages can derived by different sources of the enzyme. The hydrolytic activity of glycosidases also be used for preparation of oligosaccharides or peptides from larger structural substrate such as starch (Tomasik and Horton, 2012). Properties of glycosyltransferases and glycosidases indicated the type of enzyme used and the synthetic goal. Therefore, glycosidases are appropriate for shorter oligosaccharides while glycosyltransferases are used for synthesis of production of higher oligosaccharides (Nilsson, 1988; van den Eijnden et al., 1986).

จุฬาลงกรณ์มหาวิทยาลัย
CHULALONGKORN UNIVERSITY

1.2 α-Glucosidase

Alpha-glucosidase (EC 3.2.1.20) is an enzyme that catalyzes substrate from non-reducing ends and releases glucose as by-product. In natural, α-glucosidase found in many organisms such as mammals, insects, plants, fungi and bacteria because this enzyme has an important function in physiological roles to produce glucose in the amylolytic metabolism pathway. Substrates of this enzyme are in types of α-glucosides, α-glucans, and α-linked oligosaccharides. Alpha-glucosidase has two mains activity including hydrolysis and transglycosylation activity. Definition of hydrolysis activity means the enzyme hydrolyzes terminal non-reducing (1,4) linked α-glucose residues to release a single α-glucose molecule while transglycosylation activity means the enzyme bring a donor to form bond with an acceptor together, which results in the formation of various α-glucosylated compounds such as glycogen and soluble starch (Shimba et al., 2009). Moreover, α-glucosidase has a wide range of substrate for hydrolysis activity. Some of these enzymes favor α-linked di-, oligo-, and polyglucans, while others preferentially are on heterogeneous substrates such as sucrose and aryl glucosides (Paulson, 1989; Schauer, 1982). Furthermore, α-glucosidase also displays transferase activity which forms α-glucosylated compounds such as soluble starch and glycogen (Cihan et al., 2012; Zhang et al., 2011). In case of high substrate concentrations, the enzyme also shows transglycosylation activity to synthesize oligosaccharides as presented in Figure 1.1.

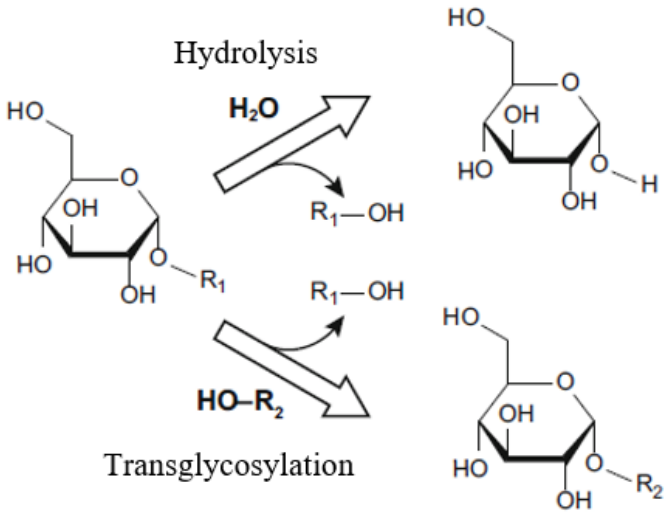

Figure 1. 1 Catalytic reactions of α-glucosidase. The upper is hydrolysis and lower reactions is transglycosylation activity. R_1 represent α-glucosaccharide, α-glucan and maltooligosaccharide unit. HO-R_2 represent acceptor substrate for transglycosylation. (Figure from Okuyama et al., 2016)

1.3 Classification

Based on the basis of substrate specificity, α-glucosidases are classified into three types (I, II and III). Type I α-glucosidase prefer to hydrolyze heterogeneous substrates which has heteroside linkage such as aryl-glucosides and sucrose to homogeneous substrate which has holoside linkage e. g. maltooligosaccharides, α-glucans and α-glucobioses. Type II enzyme show high activity on maltose and isomaltose while displays low activity towards aryl-glucosides. Type III enzyme not only displays similar substrate specificity as type II enzyme does but also hydrolyzes polysaccharides such as amylose and starch (Nimpiboon et al., 2011; Yamamoto et al., 2004). The difference between type II and type III, therefore, is the ability to hydrolyze polysaccharide substrate. The former has a minimum activity on α-glucan, whlie the

latter has a high activity. Type I α-glucosidase is found in *Saccharomyces cerevisiae* (Dušan et al., 2014), *Thermus thermophilus* TC11 (Zhou et al., 2015) and *Apis cerana japonica* (Wongchawalit et al., 2006), while type II α- glucosidase exists in *Arthrobacter* sp.DL001 (Zhou et al., 2012), *Pseudoalteromonas* sp. K8 (Li et al., 2016) and *Apis mellifer* (Pontoh, 2001). Type III α-glucosidase is presented in plants and animals such as *Apis mellifera* L., *Apis cerana indica* Fabricus (Kaewmuangmoon et al., 2012), *Spinacia oleracea* L. (Sugimoto et al., 1995), *Allium fistulosum* L. (Suzuki and Uchida, 1984) and shows activities on starch and glycogen (Li et al., 2016; Nishimoto et al., 2001). Based on primary structural classification, α-glucosidase is classified into two families including glycosidehydrolase family (GH) 13 and 31. Type I is in GH 13 group, while type II and III are GH 31 members (Nakai et al., 2005; Okuyama et al., 2016).

1.4 GH 13 α-glucosidases

1.4.1 Structure and common characteristics of GH13 α-glucosidase

The sequence of GH13 α- glucosidase is closely releated to oligo- 1,6-glucosidase (EC 3.2.1.10; O16G) and dextran glucosidase (glucan 1,6- α-glucosidase; EC 3. 2. 1. 70; DG). This enzyme belongs to subfamilies GH13_17, GH13_23, GH13_30, and GH13_31 (Stam et al., 2006). Evidence from published three-dimensional structures have been reveals the enzyme core structure consisting of three domain A, B and C (Figure 1.2A, B) (Shirai et al., 2008) (Møller et al., 2012). Domain A is a catalytic domain fromd by (β/α) 8-barrel fold. The catalytic domain of both GH13 and GH31 α- glucosidases are construced by (β/α) 8-barrel fold as well (Bojsen et al., 1999).

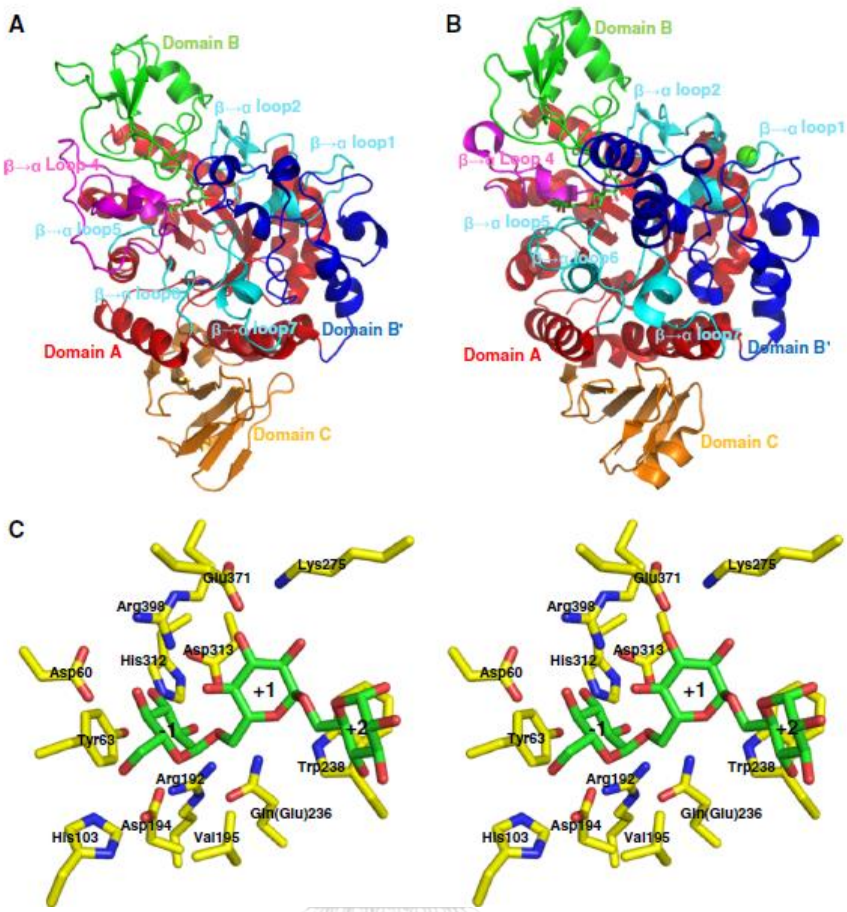

Figure 1. 2 Three dimensional structures of GH13 α-glucosidases. (A) Overall structure of HaG and maltose complex (PDB, 3WY4). (B) Overall structure of SmDG and isomaltotriose complex (PDB, 2ZID). Domain A red; domain B green; domain C orange; domain B blue; β→α loop 1, 2, 5, 6, and 7,cyan; and β→α loop 4, magenta. The substrates bound to the enzymes are shown by green stick. Calcium ion bound to the β→α loop 1 of domain A is indicated by a green sphere. It is thought to regulate the thermostability based on the kinetic experiment (Kobayashi et al., 2011); (C) closeup view of the *Sm*DG active site. Isomaltotriose covers from subsite -1 to -2. The inactive

จุฬาลงกรณ์มหาวิทยาลัย
CHULALONGKORN UNIVERSITY

mutant enzyme (E236Q) was used to trap the Michaelis complex. (Figure from Okuyama et al., 2016)

GH 13 enzyme has four conserved regions including region I, II, III, and IV. Conserved region II and III comprises catalytic nucleophile residue (Asp) and general acid-base catalytic residue (Glu) located at C-terminal ends of the fourth and fifth β-strands of domain A, respectively (MacGregor et al., 2001). Domain B comprising several α-helices and β-strands is located between the third β-strand and the third α-helix of domain A. In addition, outer site of the active site pocket has a part of domain B. The last one is domain C which is formed by anti-parallel β-sheets next to the domain A. GH13 α-glucosidases is different from GH13 endo-type enzyme because GH13 α-glucosidase consists of two extra α-helices on β/α loop 8 of domain A located on the main parts of domain B but GH13 endo-type enzyme has a cleft-shaped substrate binding sites (Kadziola et al., 1994; Lawson et al., 1994; Matsuura et al., 1984; Wiegand et al., 1995).

The conserved His (Figure 1.3, region I), Arg (Figure 1.3, region II), and His (Figure 1.3, region IV) residues of GH 13 enzyme can from hydrogen bond with non-reducing end of glucosyl residue of the Tyr on β→α loop 2 on domain A and the subsite-1 of substrate (Figure 1.2C) (Hondoh et al., 2008; Watanabe et al., 1997). Salt-bridge is generated by Asp and Arg to recognize the non-reducing end of substrate which have an interaction with the 4-OH of the glucosyl residue. Moreover, Asp and Arg residues are also available in the other GH13 exo-type enzymes (Mirza et al., 2001; Ravaud et al., 2007).

จุฬาลงกรณ์มหาวิทยาลัย
CHULALONGKORN UNIVERSITY

Figure 1. 3 Multiple alignment of GH13 α-glucosidases. Amino-acid sequences of GH13 α-glucosidases were aligned using the MAFFTash.

- *Sm*DG, *Streptococcus mutans* DG (GenBank ID: BAE79634.1);
- *La*DG, *Lactobacillus acidophilus* DG (GenBank ID: AAV42157.1);
- *Bc*O16G, *Bacillus cereus* O16G (GenBank ID: CAA37583.1);
- *Bs*O16G, *Bacillus subtilis* O16G (GenBank ID: CAB15461.1);
- *Sc*O16G, *Saccharomyces cerevisiae* isomaltase (GenBank ID: BAA07818.1);
- *B*SAMaG, *Bacillus* sp. SAM1606 α-glucosidases (GenBank ID: CAA54266.1);
- *Sc*aG, *S. cerevisiae* maltase (GenBank ID: CAA85264.1);
- *G*staG, *Geobacillus stearothermophilus* α- glucosidases (Gen- Bank ID: BAA12704.1);

- *Gs*aG, *Geobacillus* sp. HTA426 α-glucosidases (GenBank ID: BAE48285.1);
- *H*aG, *Halomonas* sp. H11 α-glucosidases (GenBank ID: BAL49684.1);
- HBGI, *Apis mellifera* α-glucosidases I (GenBank ID: BAE86926.1);
- HBGII, *Apis mellifera* α-glucosidases II (GenBank ID:BAE86927.1);
- HBGIII, *Apis mellifera* α-glucosidases III (GenBank ID:BAE11466.1).

*Sm*DG, *La*DG, *Bc*O16G, *Bs*O16G, and *Sc*O16G are specific to α-(1,6)-glucosidic linkage, and *Sc*aG, *Gs*taG, *Gs*aG, *H*aG, HBGI, HBGII, and HBGIII have high activities toward α-(1,4)-linked substrates. *B*SAMaG has a high activity toward both α-(1,6)- and α-(1,4)-linked substrates. Conserved regions and β→α loop 4 are indicated by red and green boxes, respectively. Amino-acid residues responsible for the α-(1,6)-glucosidic-linkage specificity are indicated by inverted triangles (Figure from Standley et al., 2007).

Some GH13 α-glucosidases such as neopullulanase (Hondoh et al., 2003), cyclodextrin glucanotransferase (Lawson et al., 1994), trehalulose synthase (Ravaud et al., 2007), and α-amylase (Koropatkin and Smith, 2010) require calcium ion bound to the β/α loop 1 of domain A (Hondoh et al., 2008; Shirai et al., 2008; Yamamoto et al., 2010). The calcium ion binding site binds to domain B to maintain the active site's structure (Machius et al., 1998). The evidence from kinetic analysis using *Streptococcus mutans* DG (*Sm*DG) presented that calcium ion enhanced thermal stability by bound to β→α loop 1. It can be infered that calcium ion is involved in enzyme stability under high temperature (Kobayashi et al., 2011).

จุฬาลงกรณ์มหาวิทยาลัย
CHULALONGKORN UNIVERSITY

1.4.2 Substrate chain-length specificity of GH13 α-glucosidases

The substrate chain-length specificity of GH13 exo-glucosidase has a variety. Short-chain substrates are highly selective for α-glucosidase and oligo-1,6 glucosidase. For example, *Halomonas* sp. α-glucosidase is specific to disaccharide (Ojima et al., 2012). The result from analyzing amino acid sequences together with three-dimensional structures of GH13 exo-glucosidases indicated that the length of β→α loop 4 of domain A differed rely on the substrate chain-length specificity. Therefore, the tendency for long chain substrate preference may contain short β→α loop 4. Previousely, the substitution of Trp238 with smaller amino-acid residue in *Streptococcus mutans* dextran glucosidase displays lowering in catalytic efficiency toward isomaltooligosaccharides as shown in Table 1.1 (Okuyama et al., 2016). The lower preference long-chain substrates presented that the hydrolytic activity on long-chain substrates was related with this residue and the short β→α loop 4. Besides, the interactions of Arg212 and Asn243 via hydrogen bonds of glucosyl residue at subsite +2 resulted in increasing affinity towards long-chain substrates (Møller et al., 2012).

จุฬาลงกรณ์มหาวิทยาลัย
CHULALONGKORN UNIVERSITY

Table 1. 1 Amino-acid residues related with substrate specificity and transglycosylation activity in GH13 α-glucosidase (Table from Okuyama et al., 2016)

Enzyme	Amino acid	β → α loop	Subsite	Function
*Sm*DG	Val195	4	+1	Specificity to α-(1 → 6)-glucosidic linkage
	Trp238	5	+1 and +2	Selectivity to long-chain substrates and transglucosylation activity
	Phe262	6	None[a]	Regulating orientation of Trp238
	Lys275	6	+1	Specificity to α-(1 → 6)-glucosidic linkage
	Glu371	8[b]	+1	Specificity to α-(1 → 6)-glucosidic linkage
L. acidophilus DG	Arg212	4	+2	Selectivity to long-chain substrates
	Asn243	5	+2	Selectivity to long-chain substrates
Bacillus sp. SAM1606 AGase	Gly273	5	+1	Selectivity to trehalose and maltose
S. cerevisiae isomaltase	Gln279	5	+1	Specificity to α-(1 → 6)-glucosidic linkage
Halomonas sp. AGase	Phe297	6	+1	Specificity to α-(1 → 4)-glucosidic linkage
HBG-I	Pro233	4	+1	Selectivity to α-(1 → 4)-glucosidic linkage in transglucosylation
	His234	4	+1	High selectivity to maltose
HBG-II	Asn226	4	+1	Selectivity to α-(1 → 6)-glucosidic linkage in transglucosylation
	His227	4	+1	High selectivity to maltose
HBG-III	Pro226	4	+1	Selectivity to α-(1 → 4)-glucosidic linkage in transglucosylation
	Tyr227	4	+1	High selectivity to sucrose

[a] Phe262 has no direct interaction with the substrate

[b] Corresponds to domain B′

1.4.3 Transglycosylation of GH13 α-glucosidases

α- Glucosidase has ability in catalyze transglycosylation. The process of transglycosylation begins with transfering of glucosyl residue to a hydroxyl group of the acceptor at non-reducing end of substrate. Then enzyme was used as biocatalyst in production of oligosaccharides. *Halomonas* sp. glucosidase has a high disaccharide specificity and hardly produce trisaccharides so it is an efficient enzyme that using maltose as a glucosyl donor (Ojima et al., 2012).

Moreover, α- glucosidase from *Xanthomonas campestris* which belongs to GH13_23, can produce glucoside through transglycosylation using L-menthol, (+)-catechin, and hydroquinone as acceptor (Kurosu et al., 2002; Nakagawa et al., 2000; Sato et al., 2000). The research revealed that transglycosylation activity was controlled by amino-acid residues forming substrate binding sites. The substitution of Trp238 in *Streptococcus mutans* dextran glucosidase with group of non-aromatic amino acid

จุฬาลงกรณ์มหาวิทยาลัย
CHULALONGKORN UNIVERSITY

residues such as Asn, Pro, and Ala, which constructed subsites +1 and +2, inhibits transglycosylation activity on the p-nitrophenyl α-glucoside (Saburi et al., 2006).

In addition, glycosidase, glucoamylase and cellulase were mutated by replacing catalytic carboxylate with cysteine sulfinate (–SOO-) resulted in alteration of enzymatic properties. This enhances adds the catalytic activity of glucoamylase and increase cellulase activity at acidic pH (Cockburn et al., 2010; Fierobe et al., 1998). Cysteine sulfinate substitution of *Streptococcus mutans* dextran glucosidase definitely inhibits catalytic activity on ρ-nitrophenyl α-glucoside, but increases transglycosylation activity (Saburi et al., 2013). Mutated enzyme carrying cysteine sulfinate expresses higher transglycosylation activity both on ρ-nitrophenyl α-glucoside and natural substrate such as isomaltooligosaccharide. Therefore, this process can support enhancing of transglycosylation activity more than using synthetic substrates which composed of good leaving groups.

1.4.4 Honeybee α-glucosidase

European honeybee (*Apis mellifera*) has three α-glucosidase isozymes including HBG-I, HBG-II, and HBG-III (Nishimoto et al., 2001; Takewaki et al., 1980). Expressions of these three enzyme occured in different organs at different stages of bees' life (Kubota et al., 2004). Firstly, HBG-I presents in the ventriculus. Secondly, HBG-II is localized in the ventriculus and the hemolymph. Finally, HBG-III is generated by the hypopharyngeal glands into the nectar which is directly related in honey formation by the hydrolysis of sucrose in the nectar. In general, the α-glucosidase in honey is indicated to be HBG-III as consider from enzymatic properties. The expression level of the gene encoding HBG-III is found only in worker bees. The function of the hypopharyngeal glands is changed to produce royal jelly in nurse bees

จุฬาลงกรณ์มหาวิทยาลัย
CHULALONGKORN UNIVERSITY

(Kubo et al., 1996). Juvenile hormones and ecdysone have an effect on functional and physiological transition of the hypopharyngeal glands. It is controlled by the actions of the HBG-III gene's expression level (Ueno et al., 2015). The enzymes from three honeybee are belonged to GH13 subfamily 17 (GH13_17). It contains α-glucosidase from insects such as bees, mosquitos, and flies. However, there have not yet been reported about the three-dimensional structures of the proteins in this subfamily.

Substrate specificity of the three α-glucosidase from honeybee is maltotriose while nigerose, isomaltose, and soluble starch are poor substrates. HBG-I and HBG-II are monomeric enzymes which show non-Michaelis–Menten kinetics. There are also identified as allosteric enzymes (Kimura et al., 1990; Takewaki et al., 1993). Whereas, HBG-III follows typical Michaelis–Menten kinetics. Transglycosylation acyivity of α-glucosidase from honeybee is high. Particularly, regioselectivity of α-1,4-glycosidic linkages is predominant (Kimura et al., 1990).

1.5 GH 31 α-glucosidase

GH 31 is a variety family comprising hydrolases, transglycosidases and lyases. Carbohydrate Active Enzymes (CAZy) database (http:// www.cazy.org/)(Lombard et al., 2013) indicated that members of GH31 consisted of α-glucosidase, α-1,3-glucosidase, α-xylosidase, 3-α-isomaltosyltransferase, 1,4-α-glucan 4-α-glucosyltransferase, α-galactosidase, and α-1,4-glucan lyase. GH31 α-glucosidase functions in vital biological processes. It has an important function in the formation of initiate glycoproteins in the endoplasmic reticulum. Most GH 31 α-glucosidase can digest starch to glucose, the smallest product. For example, the mammalian small

intestine contains sucrase–isomaltase (SI) and maltase–glucoamylase (MGAM) that function on degradation of dietary starch.

Two catalytic subunits of SI and MGAM are N-terminal subunit (N-terminal-SI and N-terminal-MGAM) and C-terminal subunit (C-terminal-SI and C-terminal-MGAM). Each catalytic subunits is a member of GH31 subunit , but shows differance substrate selectivity, especially possessed α-(1,4)-specificity (Nichols et al., 2003). Two catalytic subunit are mainly function on hydrolysis of α-(1,4)-linkages but different for degree of polymerization (DP) of substrate. N-terminal-MGAM prefer hydrolyzing substrates with lower DP than C-terminal-MGAM (Quezada et al., 2008; Ren et al., 2011). C-terminal-SI acts on α(1↔2)β linkages in sucrose (Takesue et al., 2001) while N-terminal-SI catalyze of α-(1,6)-glucosidic linkages (Sim et al., 2010).

1.6 Enzymatic and chemical production of oligosaccharides

1.6.1 Chemical method

Chemical methods for synthesis of oligosaccharides are continuously developed (Nilsson, 1988; Schmidt, 1986). Nevertheless, there are drawback and pose some problem. The research points out unsuitability of chemicals method in the process of oligosaccharide production. Chemicals method is complicate because it has many protection and deprotection steps which are essential for regioselective synthesis as shown in Figure 1.4. Moreover, structural of carbohydrates contain multiple hydroxyl groups of similar reactivity as well. The size of the oligosaccharide has an effect to increase the number of steps. Therefore, production of a disaccharide may desire five to seven steps while a trisaccharide may require more than ten steps. In addition, the providing of correct anomer in stereospecific reactions are often difficult and amount of total product is rather less. (Iijima and Ogawa, 1988)

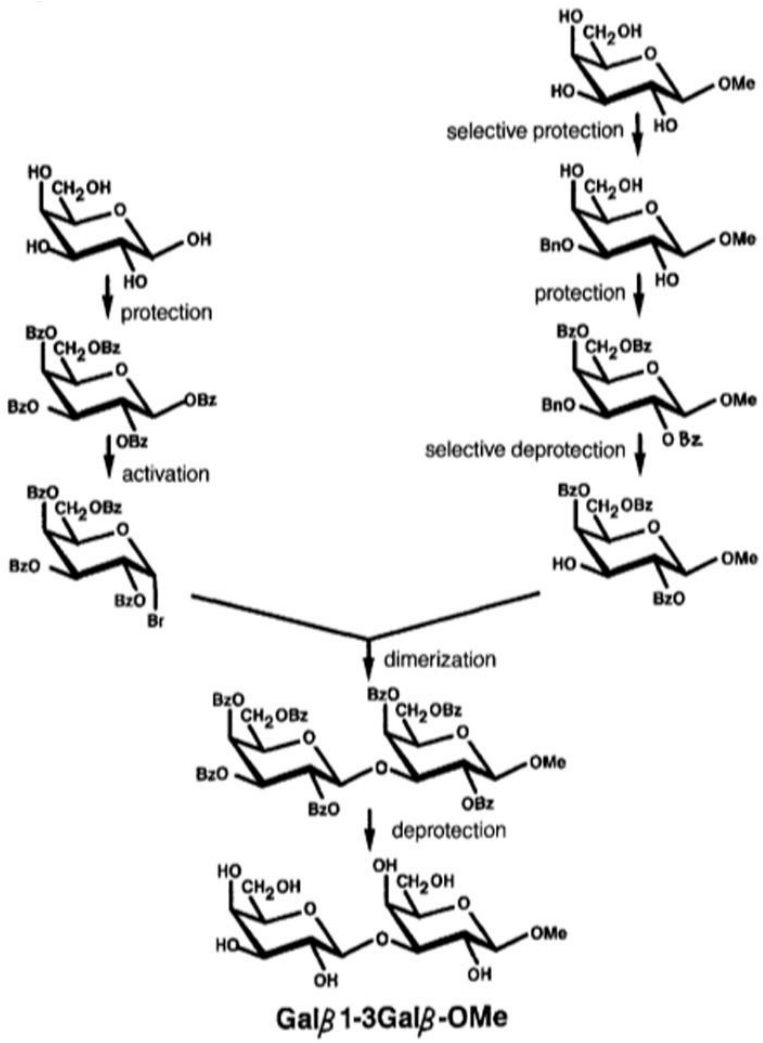

Figure 1. 4 Typical process of chemical production a disaccharides (Figure from Nilsson, 1988).

จุฬาลงกรณ์มหาวิทยาลัย
CHULALONGKORN UNIVERSITY

1.6.2 Enzymatic method

In the production of organic compounds, enzymatic method is the best alternative method which was used more than decade (Jones and Francis, 1984). Enzymatic method has a wide variety of regiospecific and often highly regioselective reactions which it can be catalysed very efficiently without protection of the hydroxyl groups. Therefore, outstanding points of enzymatic method is composed of two ways. Firstly, reaction occur under mild conditions often at room temperature and nearly

neutral pH. Secondly, it can be avoided organic solvents and hazardous chemicals such as dithiothreitol (DTT) and tris(2-carboxyethyl)phosphine (TCEP) which prevent thiol dimerization. The enzymes were divided into 2 types according to the process of complex oligosaccharides production which consists of glycosyltransferases (EC 2.4) and glycosidases (EC 3.2).

1.6.3 Combinating of chemical and enzymatic method

Oligosaccharides were synthesized by combinating both a chemical and enzymatic methods. Chemical methods usually synthesized nitrophenyl glycosides, which used as a substrate in glycosidase catalysed reactions. Glycosidases hydrolyze polysaccharide to give useful material for organic synthesis and also produce oligosaccharide which is a precursor for the process of organic synthesis (Mori et al., 1999). So, organic synthesis has an importance role for production of sugar analogs and derivatives. Moreover, glycosidase and glycosyltransferases were applied in synthesis of oligosaccharide glycosides with various noncarbohydrate aglycons such as allyl, benzyl, nitrophenyl (Nilsson, 1988).

จุฬาลงกรณ์มหาวิทยาลัย
CHULALONGKORN UNIVERSITY

1.7 Applications

Alpha- glucosidases have been used in food industries. Transglycosylation activity of the α- glucosidases has been applied in industries to produce isomaltooligosaccharides and also conjugated sugars, aiming to improve their chemical properties and physiological functions (Ravaud et al., 2007; Yoshinaga et al., 1999). Industrial applications are interested in the production of oligosaccharides with various types of α-(1,2)-, α-(1,3)-, or α-(1,6) linkages. Furthermore, the products provide benefits to human health such as being prebiotics that can improve gastrointestinal

conditions and promoting of mineral absorption in human body (Fernández et al., 2007). In humans body, a tissue acid α-glucosidase (GAA) deficiency leads to glycogen-storage disease (Pompe disease type II) (Hers, 1963). Therefore, α-glucosidase is used to produce variety of glycoconjugated products such as complex carbohydrates and glycoconjugated vitamins and drugs (Fernández et al., 2007; Hung et al., 2005).

1.8 *Weissella confusa*

Weissella confusa is a gram-positive bacterium with a short rod-shaped. *W. confusa* was isolated from a nutrient-rich environments such as vegetable products, fermented foods (Björkroth et al., 2002), kimchi (Lee et al., 2005), sourdough and fermented soya (Malik et al., 2009). In addition, *W. confusa* was found in breast milk (Martín et al., 2007) and acted as a normal microbiota of human intestines (Walter et al., 2001) with probiotic properties (Nam et al., 2002).

1.9 Objectives

Previous research successfully cloned an α-glucosidase gene from *W. confusa* BBK-1 into pET28b vector. This research aims to characterize α-glucosidase from *W. confusa* BBK-1 (*Wc*AG).

1. To express *Wc*AG in *Escherichia coli* BL21(DE3).
2. To purify the recombinant *Wc*AG by His-Trap column.
3. To characterize properties of the recombinant α-glucosidase.
4. To synthesize maltooligosaccharide products and to identify the product pattern of this enzyme.

CHAPTER II

MATERIALS AND METHODS

2.1 Equipment

Autoclave: Model H-88LL (Kokusan Ensinki Co., Ltd, Japan)

Autopipette (Pipetman, Gilson, France)

Balance: PB303-L (Mettler Toledo, Switzerland)

Biogel P2 polyacrylamide beads (BIO-RAD, USA)

Biophotometer (Eppendorf, Germany)

Centrifuge: Sorvall Legend XTR (Thermo Fisher Scientific, USA)

Centrifuge: 5804 R (Eppendorf, Germany)

Centrifuge: Avanti J-30I (Beckman Coulter, USA)

Electrophoresis units:

- Power supply (BIO-RAD, USA)
- Short plates (BIO-RAD, USA)
- Spacer plates (BIO-RAD, USA)

FPLC ÄKTA (Amersham Pharmacia Biotech Unit, USA)

- Column: Amersham Biosciences His-trap FF™
- Detector: UPC-900
- Pump: P-920
- Fraction collector: Frac-900

FPLC ÄKTA start (GE Healthcare Life Sciences, England)

Freezer (- 20 °C) (Whirlpool, USA)

Gel Document (SYNGENE, England)

Hot plate: C-MAG HS7 (IKA, Germany)

High Performance Anion Exchange Chromatography (HPAEC): DX- 600 (Dinox Corp., Sunnydale USA)

- Column: Carbopac® PA-1™ 4 × 250 mm
- Pulsed amperometry detector (PAD): DIONEX ED40
- Autosampler: DIONEX AS40
- Column oven: DIONEX ICS-3000 SP

Hiprep 16/60 sephacryl S-200 High Resolution (GE Healthcare, England)

Incubator (Memmert, Germany)

Incubator box (Hercuvan, USA)

Incubator shaker Innova™ 44 (New Brunswick Scientific, USA)

Incubator shaker Innova™ 4000 (New Brunswick Scientific, USA)

Incubator shaker Innova™ 4080 (New Brunswick Scientific, USA)

Incubator shaker (Kühner, Switzerland)

Laminar flow Bio Clean Bench (SANYO, Japan)

Magnetic stirrer: Model Fisherbrand (Fisher Scientific, USA)

Membrane filter: polyethersulfone (PES), pore size 0.22, 0.45 µm, Whatman™ (GE Healthcare, England)

Microcentrifuge (TOMY SEIKO, Japan)

pH meter (Mettler Toledo, Switzerland)

Peristatic pump (Cloe-Parmer, USA)

Shaking waterbath (Memmert, Germany)

Sonicator (Bendelin, Germany)

SpectraMax M5 Microplate Reader (Molecular Devices, USA)

จุฬาลงกรณ์มหาวิทยาลัย
CHULALONGKORN UNIVERSITY

Spectrophotometer (Eppendorf, Germany)

Syringe (Nipro Corporation Limited, Thailand)

Thin layer chromatographpy silica gel 60 F_{254} : sheets 20X20 cm (Merck, Germany)

Ultra-Low Temperature Freezer (- 80 °C) (New Brunswick Scientific, USA)

Vortex: Model K-550-GE (Sciencetific Industries Inc., USA)

2.2 Chemicals

5-Bromo-4-chloro-3-indolyl phosphate (BCIP) (Fermentas, Canada)

β-Mercaptoethanol (Fluka, Switzerland)

Acrylamide (GE Healthcare, England)

Agar (Merck, Germany)

Ammonium per sulfate (APS) (BIO-RAD, USA)

Ammonium sulphate (Sigma, USA)

Ampicillin (BIO BASIC INC., Canada)

Bovine serum albumin (BSA) (Sigma, USA)

ColorPlus prestained Protein Marker, P7709S, Lot: 0201203 (New England Biolabs Inc., USA)

จุฬาลงกรณ์มหาวิทยาลัย
CHULALONGKORN UNIVERSITY

Coomassie Brilliant Blue G-250 (Fluka, Switzerland)

Coomassie Brilliant Blue R-250 (BIO BASIC INC., Canada)

Cycloamylose (Wako, Japan)

D-Glucose (Ajax Finechem, Australia)

Dipotassium hydrogen phosphate (Ajax Finechem, Australia)

Ethidium bromide (Sigma, USA)

Ethylene diamine tetraacetic acid (EDTA) (Ajax Finechem, Australia)

Glacial acetic acid (Carlo Earba Reagenti, Italy)

Glucose liquicolor (Glucose oxidase kit) (HUMAN, Germany)

Glycerol (Ajax Finechem, Australia)

Glycine (Fisher Chemical, USA)

Hydrochloric acid (Carlo Erba Reagenti, Italy)

Iodine (Baker chemical, USA)

Isomaltose (Tokyo Chemical Inc., Japan)

Isomaltotriose (Tokyo Chemical Inc., Japan)

Isopanose (Hayashibara biomedical laboratories Inc., Japan)

Isopropyl β-D-1- thiogalactopyranoside (IPTG) (Thermo Fisher Scientific, USA)

Kojibiose (Hayashibara biomedical laboratories Inc., Japan)

Magnesium sulfate (Carlo Erba Reagenti, Italy)

Maltoheptaose (Hayashibara biomedical laboratories Inc., Japan)

Maltohexaose (Hayashibara biomedical laboratories Inc., Japan)

Maltopentaose (Hayashibara biomedical laboratories Inc., Japan)

Maltose (Conda, Spain)

จุฬาลงกรณ์มหาวิทยาลัย
CHULALONGKORN UNIVERSITY

Maltotetraose (Hayashibara biomedical laboratories Inc., Japan)

Maltotriose (Hayashibara biomedical laboratories Inc., Japan)

Methanol (Sigma, USA)

Nigerose (Hayashibara biomedical laboratories Inc., Japan)

Nitroblue tetrazolium chloride (NBT) (Fermentas, Canada)

Nitrocellulose Membrane (BIO-RAD, USA)

Panose (Hayashibara biomedical laboratories Inc., Japan)

Pea starch (Emsland-Stärke GmbH, Germany)

Potassium dihydrogen phosphate (Ajax Finechem, Australia)

Potassium iodide (Mallinckrodt, USA)

Protein Marker, P7702S, Lot: 0441201 (New England Biolabs Inc., USA)

Pullulan (Wako Pure Chemical Industries, Ltd. Japan)

Sodium acetate (LOBA Chemi, India)

Sodium azide (Ajax Finechem, Australia)

Sodium chloride (Ajax Finechem, Australia)

Sodium dodecyl sulfate (SDS) (Vivantis Technologies, Malaysia)

Sodium hydroxide (Carlo Erba Reagenti, Italy)

Sodium nitrate (Carlo Erba Reagenti, Italy)

Soluble starch (potato) (Scharlau microbiology, Spain)

Standard protein marker (Amersham Pharmacia Biotech Inc., USA)

Tetramethylethylenediamine (TEMED) (BIO-RAD, USA)

Trehalose (Wako Pure Chemical Industries, Ltd. Japan)

Tris-(hydroxyl methyl)-aminomethane (Carlo Erba Reagenti, Italy)

Tryptone (HIMEDIA, India)

Yeast extract (Affymetrix, USA)

จุฬาลงกรณ์มหาวิทยาลัย
CHULALONGKORN UNIVERSITY

2.3 Enzymes and restriction enzymes

Glucoamylase from *Rhizopus sp*. (Wako Pure Chemical Industries, Ltd. Japan)

2.4 Bacterial strains

Weissella confusa BBK-1 is a gram-positive bacteria with a short rod-shaped. Lyophilized stock of *W. confusa* BBK-1 isolated from Thai dessert was kindly given by Dr. Santhana Nakapong. *Wc*AG gene was cloned into modified pET28b vector. *Escherichia coli* BL21 (DE3) (Novagen, Germany) was used as an expression host.

METHODS

2.5 Analysis of *Wc*AG sequence

Bioinformatic tools were used to analyze the results from DNA sequencing. DNA sequence was translated into amino acid sequence by using ExPASy translated tool (http://web.expasy.org/translate/). Amino acid sequence alignment of *WcAG* gene was performed using ClustalW tool (http://www.ebi.ac.uk/Tools/).

2.6 Optimization of *Wc*AG expression

E. coli BL21(DE3) harboring *Wc*AG recombinant plasmid was cultured in 8 ml LB broth containing 30 µl/ml kanamycin at 37 ºC with 250 rpm shaking. Then, 1%(v/v) of cell culture was inoculated to 100 ml of LB medium containing 30 µl/ml kanamycin and continued cultured at 37ºC with 250 rpm shaking until the optical density at 600 nm reached 0.4-0.6. After that, isopropyl β-D-1-thiogalactopyranoside (IPTG) was added to the final concentration of 0.4 mM. Cells were harvested by centrifugation at 7000 xg for various time points at 0, 2, 4, 6, 20 and 24 h after IPTG induction. Cells were resuspended with 50 mM phosphate buffer pH 7.4 and 0.1% of tritonX-100 before disrupted by sonication with 30% power under alternating step of pulse-on 1 sec and pulse-off 4 sec for 1.30 min. After that, supernatant was collected by centrifugation at 12,000 rpm for 15 min. The expression pattern of *Wc*AG was observed by sodium dodecyl sulfate polyacrylamide gel electrophoresis (SDS-PAGE).

In case of low amount of *Wc*AG expressed in soluble form, the expression condition was improved by adding a final concentration of 1% (w/v) glucose in LB medium, lowering temperature, decreasing IPTG concentration, decreasing the round per minute (rpm) shaking during the expression or adding other chemical reagents.

When the concentration of *Wc*AG in soluble form was higher enough, the production of *Wc*AG was scaled up to 2.0 L.

2.7 Purification of *Wc*AG by His-Trap column chromatography

*Wc*AG was expressed as his-tagged proteins at the C-terminus so that it could be purified by Nickel (Ni^{2+}) Sepharose 6 Fast Flow column (GE Healthcare, England). Initially, His-Trap column was pre-equilibrated with 50 mM phosphate buffer pH 7.4 containing 50 mM NaCl at least 10 column volumes. Crude enzyme was applied onto the column column. Then the column was washed with at least 20 column volumes of the same equilibrating buffer until A_{280} reached baseline level. Bound protein was eluted by a stepwise elution of 50, 100 and 500 mM imidazole in 50 mM phosphate buffer pH 7.4. Fractions carrying *Wc*AG activity were pooled and dialyzed against 50 mM phosphate buffer, pH 7.4. Activity of *Wc*AG was followed as described in section 2.9.1.

2.8 Protein determination

2.8.1 Determination of protein concentration

Concentration of protein was estimated by Bradford's assay (Bradford, 1976). Two hundred microliters of Bradford's working reagent was mixed with 1 µl of protein sample for 2 min. The mixture was immediately measured at A_{595}. Standard curve for determining protein concentration was prepared using bovine serum albumin 1 mg/ml as a standard protein (Appendix 6).

2.8.2 Sodium dodecyl sulfate polyacrylamide gel electrophoresis (SDS-PAGE)

A denaturing gel with 10% (w/v) separating gel and 5% stacking gel comprising 0.1% (w/v) SDS was prepared (Appendix 1). Electrophoresis was carried out by Mini-Gel electrophoresis (Bio-Rad, Hercules, MA, USA). Protein sample was mixed with

5X SDS loading dye. The mixture was boiled for 10 min and then loaded into the gel. In the process of electrophoresis, a constant current of 25 mA (per gel slab) was set at a running time of 50 min. When the run was completed, the gel was stained with Coomassie blue staining solution in order to visualize the protein bands.

2.8.3 Coomassie blue staining

Coomassie blue staining was a common method used for investigating the protein bands. The gel was stained with Coomassie blue staining solution for 3 h at room temperature. Then, the gel was destained with destaining solution for many times until the bands of protein could be obviously seen on the gel without the disturbance from background.

2.9 Characterization of *Wc*AG

2.9.1 Enzyme assay by hydrolysis activity

Hydrolysis activity aimed to measure the amount of free glucose released as a by-product from catalyzing a substrate maltotriose (G3). The assay was performed by glucose oxidase method (Barham and Trinder, 1972). This reaction was described as follows.

จุฬาลงกรณ์มหาวิทยาลัย
CHULALONGKORN UNIVERSITY

$$\text{Glucose} + H_2O + O_2 \rightarrow \text{gluconic acid} + H_2O_2$$

$$2H_2O_2 + \text{4-aminophenazone} \rightarrow \text{quinoneimine} + 4H_2O$$

The reaction color became magenta when there were glucoses existed in the solution. Five microlitres of purified enzyme was incubated with 2.5 µl of 500 mM maltotriose (G3) at 50 ºC for 10 min and stopped by boiling for 10 min. Then, 475 µl of glucose oxidase reagent was added and incubated at 30 ºC for 10 min without light exposure. The reaction mixture was immediately measured at absorbance of 505 nm.

One unit of hydrolysis activity was defined as the amount of enzyme that produced 1 µmol of glucose per min under assayed condition.

2.9.2 Enzyme assay by transglycosylation activity

Transglycosylation activity was a transferring of glucose molecule from donor to accepter using maltose (G2) as a substrate. The different products formed were investigated by Thin-layer Chromatography (TLC). Enzyme carrying 0.4 U/ml hydrolysis activity in 50 mM phosphate buffer pH 6.0 was incubated with 50 mM maltose at 37 ºC for 10 min. Then, the reaction mixture of 0.5 µl was spotted on TLC plate. The solvent system (mobile phase) was prepared by mixing butanol, acetic acid and water in the ratio of 3:2:2. The TLC plate was placed into the solvent tank for 1 h (at least 3 times) to allow the solvent traveled up to 1 centimeter below the top of the TLC plate (Merck, Germany). The plate was then visualized by spray with mixing 10 ml of sulfuric acid, 29 ml of ethanol, 8 ml of distilled water and 0.1 g of orcinol before incubate at 110 ºC for 10 min. Maltooligosaccharide products were identified by comparison to the G1-G7 markers and other standard disaccharides.

จุฬาลงกรณ์มหาวิทยาลัย
CHULALONGKORN UNIVERSITY

2.9.3 Effect of temperature on *Wc*AG activity

The effect of temperature on *Wc*AG activity was observed on hydrolysis activity as described in section 2.9.1. Assay condition was performed in 50 mM phosphate buffer pH 6.0 at various temperatures from 20 to 70 °C for 10 min. The results were shown as a plot of relative activity (%) against temperature. The highest activity was set as 100%.

2.9.4 Temperature stability of *Wc*AG

Effect of temperature on *Wc*AG stability was determined at various temperatures. The enzyme was pre-incubated at each temperature for 1 h and then

withdrawn to assay hydrolysis activity. The mean of hydrolysis activity assay was described in section 2.9.1. The results were illustrated as a percentage of relative activity.

2.9.5 Effect of pH on *Wc*AG activity

The effect of pH on *Wc*AG activity was carried out on hydrolysis activity. The reaction was performed under optimum temperature from section 2.9.3 but varied in pH ranging from pH 3.0 to 9.0. Different buffer systems were used as follows; acetate buffer for pH 3.0 – pH 6.0, phosphate buffer for pH 6.0 – pH 8.0 and Tris-HCl for pH 7.0 – pH 10.0. The activities were examined as previously described in section 2.9.1. The pH at which *Wc*AG possessed maximum activity was set to be 100%.

2.9.6 pH stability of *Wc*AG

To observe pH stability of *Wc*AG, the assay aimed to detect the remaining hydrolysis activity after the purified enzyme was pre-incubated at different pHs ranging from 3.0 to 9.0. Incubation was performed at 50 ºC for 1 h before taken out to measure hydrolysis activity as described in section 2.9.1. The results were plotted as a percentage of relative activity over a period of time.

จุฬาลงกรณ์มหาวิทยาลัย
CHULALONGKORN UNIVERSITY

2.9.7 Ion effect on *Wc*AG

Different ions or chelating agent including Ca^{2+} ,Fe^{3+}, Zn^{2+}, Cu^{2+}, Fe^{2+}, Mn^{2+}, Ni^{2+}, Mg^{2+}, Co^{2+}, K^{+}, Na^{+} and EDTA were used to investigate their effects toward *Wc*AG hydrolysis activity. Purified enzyme was pre-incubated at optimum condition for 10 min. It was then incubated with each ion at a concentration of 5 mM at 50 ºC for 1 h. The reaction mixture was withdrawn to measure hydrolysis activity as mentioned in section 2.9.1. The results were shown as a relative activity against incubation time.

2.9.8 Half-life of *Wc*AG

To determine half-life of *Wc*AG, the enzyme was pre-incubated at 50 ºC under incubation time of 10, 20, 30, 40, 50, 60, 90 min and then terminated by boiling for 10 min. The remaining hydrolysis activity was measured as described in section 2.9.1. The results were illustrated as a percentage of relative activity.

2.9.9 Kinetic study of *Wc*AG on hydrolysis activity

In order to determine hydrolysis kinetic parameters, *Wc*AG of 0.5 U/ml hydrolysis activity in 50 mM phosphate buffer pH 6.0 was incubated with various concentrations of maltose and maltotriose from 0, 1, 2.5, 5, 7.5, 10, 20, 30, 40, 50, 100, 200 to 300 mM for 10 min at 50 ºC. After that, the reaction was stopped by boiling 10 min. The amount of free glucose was detected by glucose oxidase method as mentioned in section 2.9.1. The kinetic parameters, K_m and V_{max}, were calculated from Lineweaver-Burk plot. The turnover number of enzyme (k_{cat}) and catalytic efficiency (k_{cat}/K_m) of the enzyme were analyzed as well. Michaelis-Menten equation was calculated from the following equation: $V_i = (V_{max}[S])/(K_m+[S])$.

2.9.10 Substrate specificity of *Wc*AG

2.9.10.1 Substrate specificity on hydrolysis activity of *Wc*AG

An ability of *Wc*AG to catalyze different substrates including maltotriose (G3), maltotetraose (G4), maltopentaose (G5), maltohexaose (G6), pullulan, dextrin and para-nitrophenyl α-D-glucopyranoside (pNPG) was investigated on hydrolysis activity. Purified enzyme of 0.5 U/ml in 50 mM phosphate buffer pH 6.0 was incubated with 50 mM of substrate at optimum temperature for 10 min. The amount of free glucose was examined by glucose oxidase method as mentioned in section 2.9.1.

2.9.10.2 Substrate specificity on transglycosylation activity of *Wc*AG

Transglycosylation activity towards different substrates, G2– G7, was also analyzed by TLC analysis. Enzyme of 0.4 U/ml hydrolysis activity in 50 mM phosphate buffer pH 6.0 was incubated substrates at 50 ºC for 10 min. Aliquot of 0.5 µl was subjected to TLC analysis as described in section 2.9.2. Substrate specificity was then determined from TLC plate.

2.10 Optimization of transglycosylation activity

Initially, the production of maltooligosaccharide products was optimized aiming to obtain higher amount of products. Factors including temperature, concentration of enzyme, concentration of substrate and incubation time were investigated.

2.10.1 Effect of temperature

The reaction was performed by incubating *Wc*AG of 0.4 U/ml hydrolysis activity with 50 mM maltose at various temperatures including 18, 30 and 37 ºC for 24 h. The reaction was terminated by boiling for 10 min. Aliquot of 0.5 µl was subjected to TLC analysis as described in section 2.9.2. The optimum temperature was determined from spot size of products on TLC plate.

2.10.2 Effect of enzyme concentration

Fifty millimolar of maltose was incubated at optimum temperature from 2.10.1 for 24 h with various enzyme concentrations including 0.2, 0.4, 0.6, 0.8 and 1.0 U/ml hydrolysis activity of *Wc*AG. The reaction was terminated by boiling for 10 min. Aliquot of 0.5 µl was subjected to TLC analysis as described in section 2.9.2. The optimum enzyme concentration was then determined from TLC plate.

2.10.3 Effect of substrate concentration

Optimum *Wc*AG concentration obtained from section 2.10.2 was incubated with maltose varying in concentration including 50, 100, 150 and 200 mM at optimum temperature for 24 h and then stopped by boiling for 10 min. Aliquot of 0.5 µl was analyzed by TLC analysis as described in section 2.9.2. The optimum substrate concentration was identified from spot size of products on TLC plate.

2.10.4 Effect of incubation time

The activity was performed by varying incubation time of 0, 1, 3, 6, 9, 12, 15, 16, 18, 21 and 24 h under optimum temperature, enzyme concentration and substrate concentration obtained from previous section. The reaction was terminated by boiling for 10 min. Aliquot of 0.5 µl was analyzed by TLC analysis as described in section 2.9.2. The optimum incubation time was identified from spot size of products on TLC plate.

2.11 Large scale production of maltooligosaccharide products

Large scale production of maltooligosaccharide products was prepared in the total volume of 50 ml under optimum condition of transglycosylation activity obtained from section 2.10 with 50 rpm shaking. Any hardly dissolved components in the reaction were removed via centrifugation at 6000 xg for 20 min. Then, the products were lyophilized at -50 ºC, 0.7 mbar and 24 h or until it was completely dried.

2.12 Isolation of maltooligosaccharide products

Lyophilized products from section 2.11 was purified by Bio gel P2 column (BIO-RAD, USA), a size exclusion column chromatography. Bio gel P2 was first equilibrated with ultrapure water at least 2 column volumes. Two molars of products were applied onto the column and eluted by distilled water at a constant flow rate of 0.5

ml/ min. Fraction size of 5 ml was collected. All fractions were detected by TLC analysis as described in 2.9.2. Then, fractions containing maltooligosaccharide products were pooled before analyzed using High Performance Anion Exchange Chromatography with Pulse Amperometric Detection (HPAEC-PAD).

2.13 HPAEC-PAD analysis of maltooligosaccharide products

The products from 2.5.14 were analyzed by HPAEC- PAD. The model instrument ICS 3000 system (DIONEX, USA) was used with Carbopac- PA1 column (4 × 250 mm). Column was first equilibrated with 150 mM sodium hydroxide. A sample of 50 µl was injected into the column and then eluted with linear gradient elution of CH_3COONa with a flow rate of 1.0 ml/min at 30 °C. During the first 1–5 min, 150 mM NaOH was used. After that, from 6–43 min, the products were eluted by 150 mM NaOH with a gradient of 0 to 600 mM CH_3COONa. Finally, the last 2 min, 500 mM NaOH was used to backwash the column. The products were identified by comparing to the standard carbohydrates including G1-G7,panose, isopanose, isomaltose, isomaltotriose, kojibiose, nigerose and trehalose. Fractions carrying products of interest were pooled and then lyophilized at -50 ºC, 0.7 mbar and 24 h or until it was completely dried.

จุฬาลงกรณ์มหาวิทยาลัย
CHULALONGKORN UNIVERSITY

CHAPTER III

RESULTS

3.1 Sequence analysis of α–glucosidase from *Weissella confusa* BBK-1

The nucleotide sequence of *WcAG* gene was found to be 1,775 bps (Figure 3.1) which could be deduced into 593 amino acids (Figure 3.2). ProtParam tool program (http://web.expasy.org/protparam/) was used to calculate molecular weight and pI of protein. pI and molecular weight of *Wc*AG were 4.75 and 62 kDa, respectively. Amino acid sequence of *Wc*AG was blasted (https://www.ncbi.nlm.nih.gov/) and aligned using ClustalW program (http://www.ebi.ac.uk/Tools/). Blast results of *Wc*AG sequence showed 97% identity to α-glucosidase from *W. confusa* (WP_056973603.1), 96% identity to neopullulanase from *Streptococcus pneumonia* (COI29563.1) and 96% identity to neopullulanase from *W. confusa* (SJX69567.1). The results from structural sequence analysis revealed that *Wc*AG contained two domains including alpha amylase at N-terminal ig-like domain on amino acid residue 2-128 and alpha-amylase catalytic domain on amino acid residue 142-518, as indicated by Figure 3.3.

จุฬาลงกรณ์มหาวิทยาลัย
CHULALONGKORN UNIVERSITY

CC**ATG**GGCAACCTAGCAGGTATTATGCACCGTCCCGACAGTGAGATGGCGTACG
TCGTGAACGAGCAAACCGTTAATATTCGCCTGCGGACTGCCAAAGACGATATCG
TTAGCGTTGAATTATTAGCAGGTGATCCTTACAGTTTGCGGAGCTTGCCGACTG
ATGAAAAGTTCTACCAAGTGCCAAAGCAGATGACCAAGATTATGTCAGATGGGA
TTTCTGATTTCTGGCAGGTGACGGTGACCGAGCCGAAGCGGCGGTTAGCATATG
CCTTCCTAGTGACTGATATGCTCGGTATCCAGAAAATTTATAGTGACAAAGGCT
TCTTTAAAGTAGCTGATGCCGATTTAATGGATATGAACTTTTACTTTCGCATGC
CGTTTTTTCAAACGATTGATCAGTACAACGCCCCGGAATGGGTGACCGATACGG
TTTGGTATCAAATCTTTCCAGAGCGGTTTGCAAACGGGGATGTATCAAATGATC
CGGTAGGCACGAAGCCTTGGGATTCAACGGATCATCCGGGTCGTGAAGATTTTT
ATGGTGGTGACTTGCAAGGAATTTTGGACCATTTGGACCACTTGCAAGAACTTG
GGATTTCAGGTATCTATTTGAATCCAATCTTCCAAGCGCCATCGAATCACAAAT
ATGACACGCAAGATTATATGACGGTGGACCCACACTTCGGGGATGCCAAGTTGT
TTAAGCAACTTGTTCAAGCAGCGCATGAACGTGGCATTCGCGTCATGTTGGATG
CGGTCTTCAATCACATTGGTGACAAGTCAGTGCAGTGGCAGGATGTGTTAAAGA
ACGAGCAAGCATCACCATATGCGGACTGGTTCCACATTCATCAGTTCCCAGCAA
CGTACACACCAACCGACAACTTTGAATTTGCAGCTGATGCAACGTATGACACGT
TTGACTACACGCCACACATGCCAAAGCTGAATACAAGTAATCCGGAAGTGGTTG
ATTATTTGTTGAACATTGCGACGTATTGGGTTAAAGAATTTGATATTGATGCTT
GGCGTCTAGATGTTGCCAATGAAATTGATCATCATTTCTGGCGTAAATTCCACG
ATGCGATGATGGCATTGAAACCTGATTTTTACATTCTAGGTGAGATTTGGCACA
CATCGCAGAGCTGGTTGGTCGGCGATGAATTTACAGCCGTTATGAACTACAGTT
ACACCGGCGCCATTCTCCAATATTTCTTGGAAAATGAGTCAGCAGATGCATTAG
TTCAAAAGATGAGCCATCAATTGATGTTGTACCGTGATGCAACGAACCGCATGA
TGTTTAACACGGTGGATTCACACGATACGCCACGTTTGATGACCTTGGCGCATG
AAGATAAGCAACTAGCGAAAAGCATTCTCACATTTACCTTCATGCAACCAGGTG
TTCCATCAATCTACTATGGAACAGAATACGGTATGACCGGGGAGAATGATCCTG
ACGATCGCAAGCCGATGGTTTGGCAGCCAGAGTTACAAGACCATGATTTGTACG
ACTTTATGCAAAAATTAGTACAAGTCAGGCGCCAAGTCATTGCTAAGCTATCTG
ACGACAAAATTATCTTTGACGTGATTGGGGAACGTCAAATCCGATTGACGCGCG
AAGACAATCAAACGCGCATCGTTGGGGTATTCAACAATGGCACGACCGACTTAA
CAGTTGCGCAGCCAACAAGTATTTTGCTAAAAACAAATCAATCTGAGACGCAAC
TGGCACCAAACGACTTTATGATTTGGACCGAGCCAGTGCGC**TGA**CTCGAG

Figure 3. 1 Nucleotide sequence of *WcAG* gene with *Nco*I and *Xho*I restriction sites (underlined), respectively. Bold three codons of ATG and TGA indicated start and stop codon, respectively.

```
1   MGNLAGIMHRPDSEMAYVVNEQTVNIRLRTAKDDIVSVEL  40
41  LAGDPYSLRSLPTDEKFYQVPKQMTKIMSDGISDFWQVTV  80
81  TEPKRRLAYAFLVTDMLGIQKIYSDKGFFKVADADLMDMN  120
121 FYFRMPFFQTIDQYNAPEWVTDTVWYQIFPERFANGDVSN  160
161 DPVGTKPWDSTDHPGREDFYGGDLQGILDHLDHLQELGIS  200
201 GIYLNPIFQAPSNHKYDTQDYMTVDPHFGDAKLFKQLVQA  240
241 AHERGIRVMLDAVFNHIGDKSVQWQDVLKNEQASPYADWF  280
281 HIHQFPATYTPTDNFEFAADATYDTFDYTPHMPKLNTSNP  320
321 EVVDYLLNIATYWVKEFDIDAWRLDVANEIDHHFWRKFHD  360
361 AMMALKPDFYILGEIWHTSQSWLVGDEFTAVMNYSYTGAI  400
401 LQYFLENESADALVQKMSHQLMLYRDATNRMMFNTVDSHD  440
441 TPRLMTLAHEDKQLAKSILTFTFMQPGVPSIYYGTEYGMT  480
481 GENDPDDRKPMVWQPELQDHDLYDFMQKLVQVRRQVIAKL  520
521 SDDKIIFDVIGERQIRLTREDNQTRIVGVFNNGTTDLTVA  560
561 QPTSILLKTNQSETQLAPNDFMIWTEPVRLENH        593
```

Figure 3. 2 Deduced amino acid sequence of *Wc*AG.

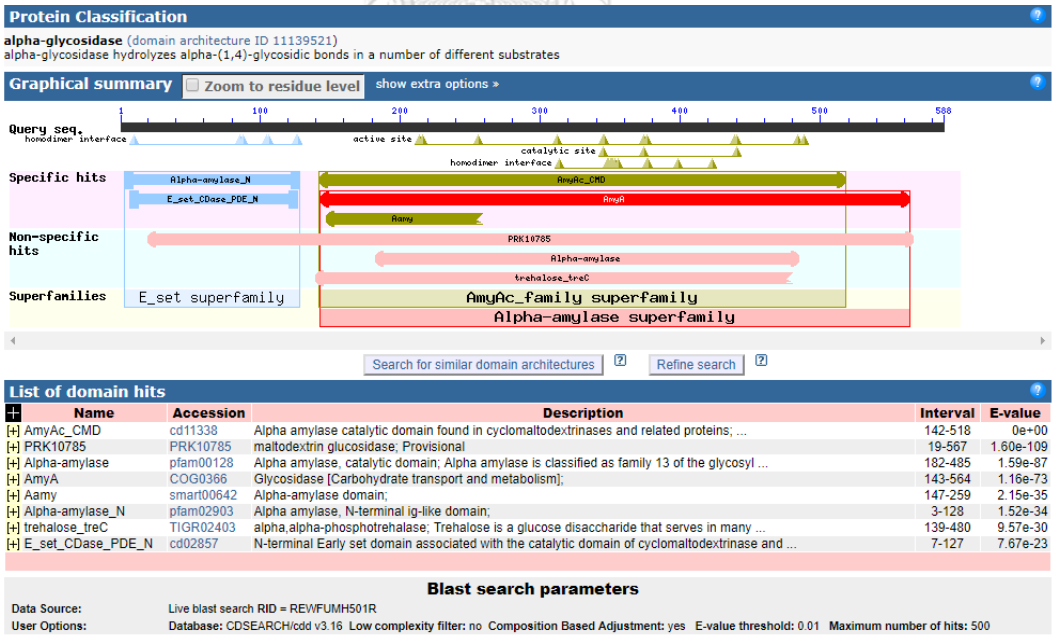

Figure 3. 3 Structural analysis of *Wc*AG sequence.

The result of multiple sequence alignment of *Wc*AG comparing to other α–glucosidase producing organisms in GH family 13 showed 4 short conserve regions and β→α loop 4 of α–glucosidase as indicated by Figure 3.4. In addition, phylogenetic tree constructed from multiple sequence alignment of *Wc*AG showed that *Wc*AG closely related to α- glucosidase from *Danaus plexippus* (EHJ74127.) , and α-glucosidase from *Anopheles darlingi* (ETN58833.1). However, *Wc*AG was far related to other α-glucosidases producing organisms such as *Hisliotis discus hannai* (BAN67474.1), *Homo sapiens* (ABI53718.1), *Kalmanozyma brasiliensis* GHG001 (XP_016294356.1), *Pseudozyma hubeiensis SY62* (GAC98011.1) and *Pyrobaculum arsenatieum* DSM 13514 (ABP51590.1). Region I, II, III and IV are conserved region of His, Arg, Glu and His residues, respectively.

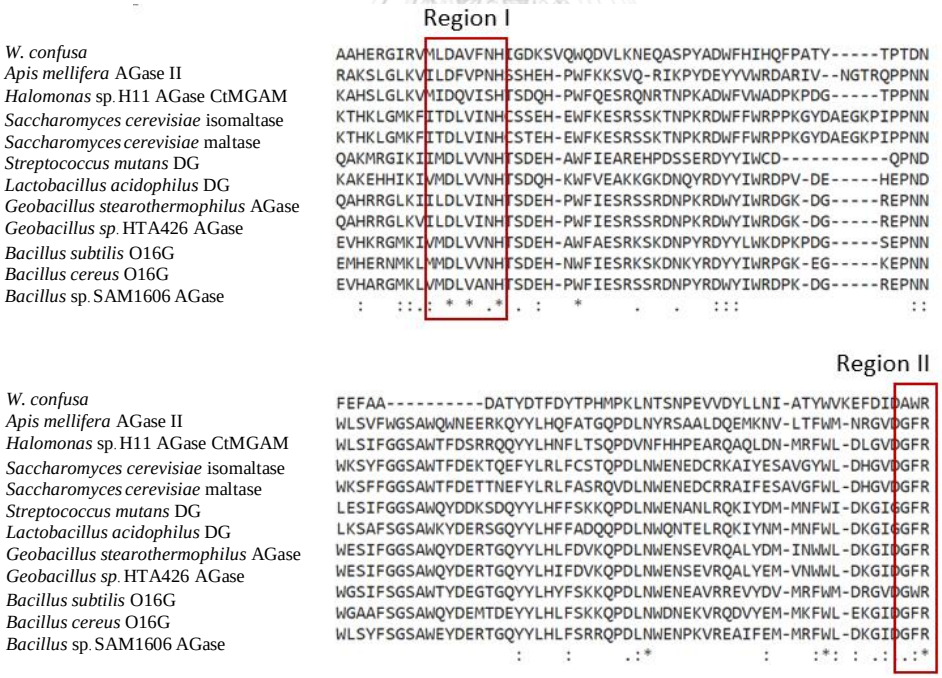

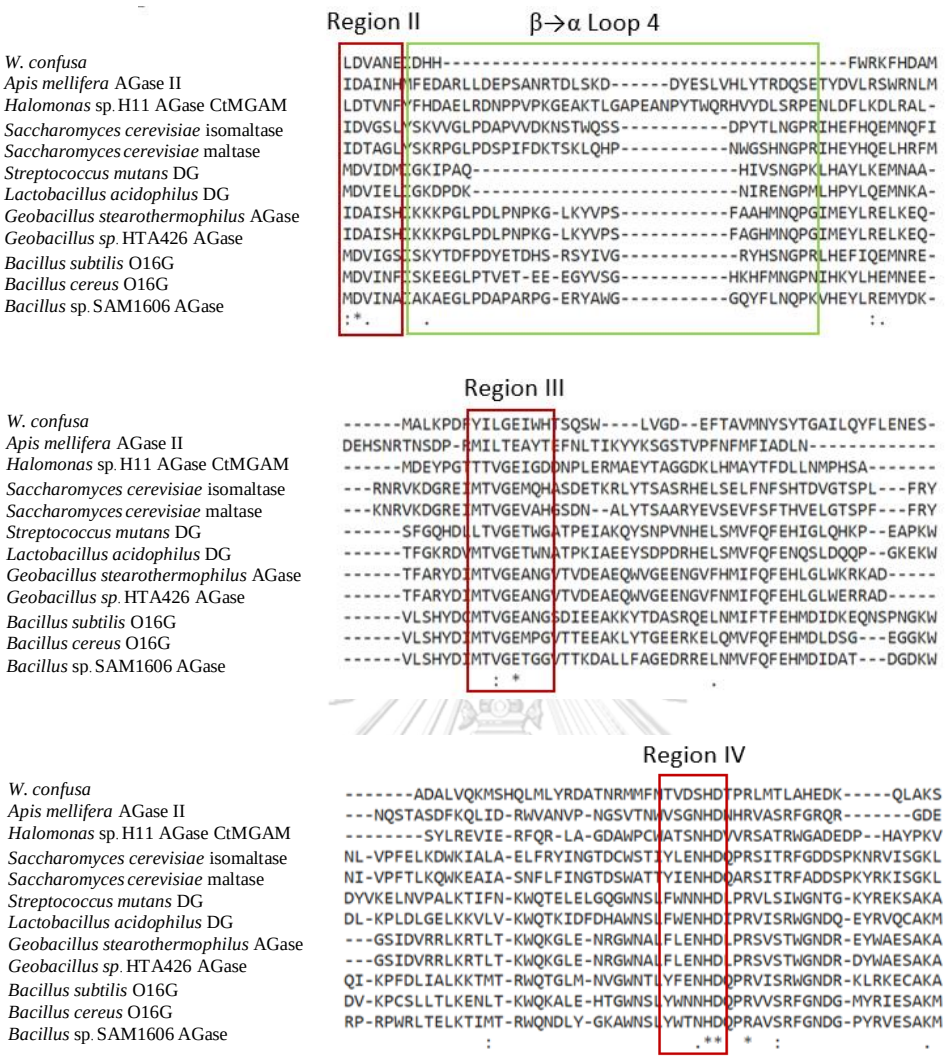

Figure 3. 4 Multiple sequence alignment of *Wc*AG comparing to α–glucosidases from other organisms

- HBGII, *Apis mellifera* AGase II (GenBank ID: BAE86927.1);
- HaG, *Halomonas* sp. H11 AGase CtMGAM (GenBank ID: BAL49684.1);
- ScO16G, *Saccharomyces cerevisiae* isomaltase (GenBank ID: BAA07818.1);
- ScaG, *S. cerevisiae* maltase (GenBank ID: CAA85264.1);
- SmDG, *Streptococcus mutans* DG (GenBank ID: BAE79634.1);
- LaDG, *Lactobacillus acidophilus* DG (GenBank ID: AAV42157.1);
- GstaG, *Geobacillus stearothermophilus* AGase (GenBank ID: BAA12704.1);

- GsaG, *Geobacillus sp*. HTA426 AGase (GenBank ID: BAE48285.1);
- BsO16G, *Bacillus subtilis* O16G (GenBank ID: CAB15461.1);
- BcO16G, *Bacillus cereus* O16G (GenBank ID: CAA37583.1);
- BSAMaG, *Bacillus* sp. SAM1606 AGase (GenBank ID: CAA54266.1).

An asterisk (*) indicates positions which have a single, fully conserved residue, (.) indicates some conservation and (:) indicates conservation between groups of strongly similar properties.

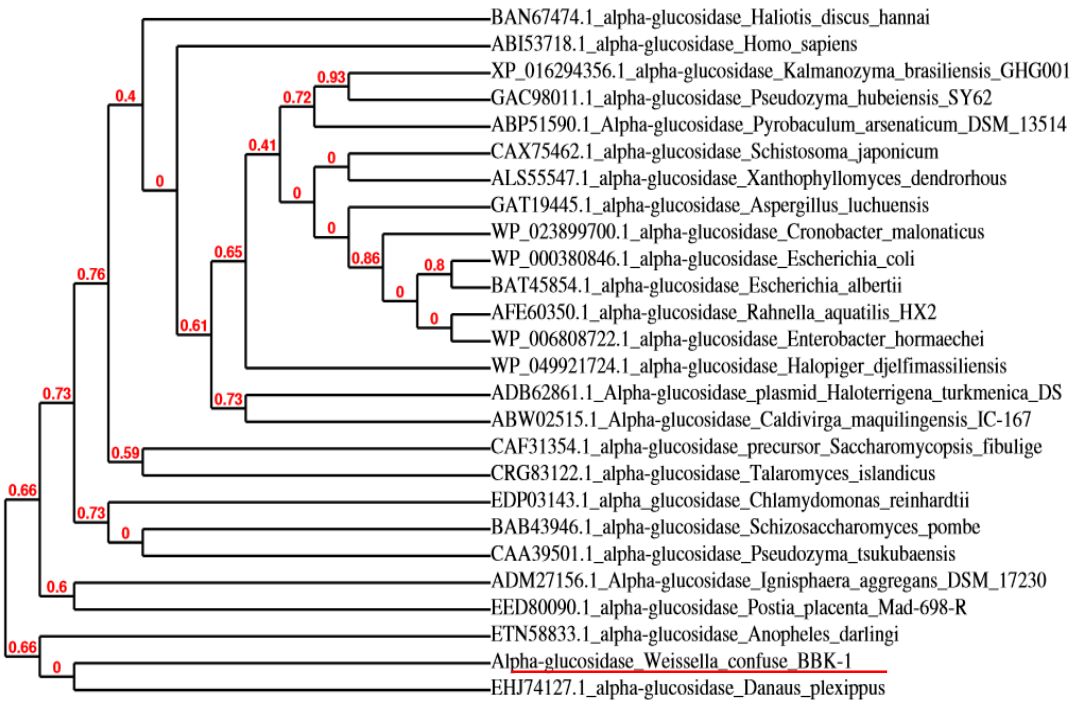

Figure 3. 5 Phylogenetic tree showed the relationship of *Wc*AG with others organisms. The number in red, represent evolutionary distance calculated from bootstrapping value. These are generally numbers between 0 and 1. A high value means that there is strong evidence indicated that the sequences are similar.

3.2 Expression of α–glucosidase from *Weissella confusa* BBK-1

3.2.1 Transformation of recombinant pET*28Wc*AG plasmid

The recombinant pET28*Wc*AG plasmid was transformed into expression host *E. coli* BL21(DE3) by $CaCl_2$ method. Recombinant plasmids harboring *WcAG* gene were extracted and digested with *Nco*I and *Xho*I, aiming to confirm the presence of gene in the expression host.

3.2.2 Optimization of *Wc*AG expression

*Wc*AG was expressed in *E. coli* BL21 (DE3). One percent (v/v) of cell culture was inoculated into 100 ml of LB medium containing 30 µl/ml kanamycin and continued cultured at 37 ºC with 250 rpm shaking until the optical density at 600 nm reached 0.4-0.6. To optimize the expression of *Wc*AG, the effects of major factors including temperature, concentration of IPTG and expression time, were varied. The results were shown as follows.

3.2.2.1 Expression of *W*cAG under 1 mM IPTG induction at 30 ºC and 37 ºC, 250 rpm.

The expression level of *Wc*AG was obviously higher in insoluble protein than soluble protein when induced with 1 mM IPTG both at 30 and 37 °C as shown in Figure 3.6 (A) and (B).

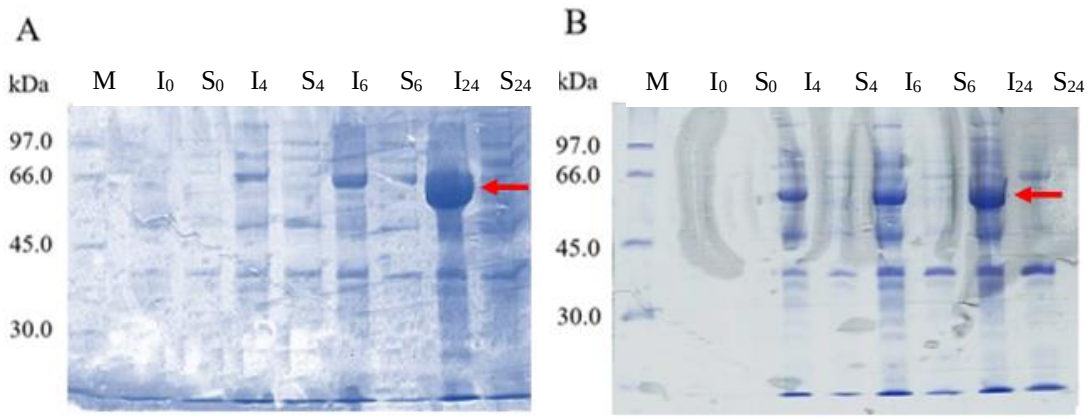

Figure 3. 6 (A) 10% SDS-PAGE of *Wc*AG expressed at 30 ºC, 1 mM IPTG induction at 0 to 24 h. (B) 10% SDS-PAGE of *Wc*AG expressed at 37 ºC, 1 mM IPTG induction at 0 to 24 h.

Lane M (A and B) = Protein molecular weight marker (Amershame Bioscience, USA), S = Soluble fraction, I = Insoluble protein and number = induction time (h)

*red arrow indicated the expected *Wc*AG size of 62.0 kDa.

3.2.2.2 Expression of *Wc*AG under 0.1, 0.5, 1 mM IPTG induction at 30 ºC, 250 rpm.

The result showed that the expression level of *Wc*AG was obviously higher in insoluble protein than soluble protein when the concentrations of IPTG was increased as shown in Figure 3.7 (A), (B) and (C).

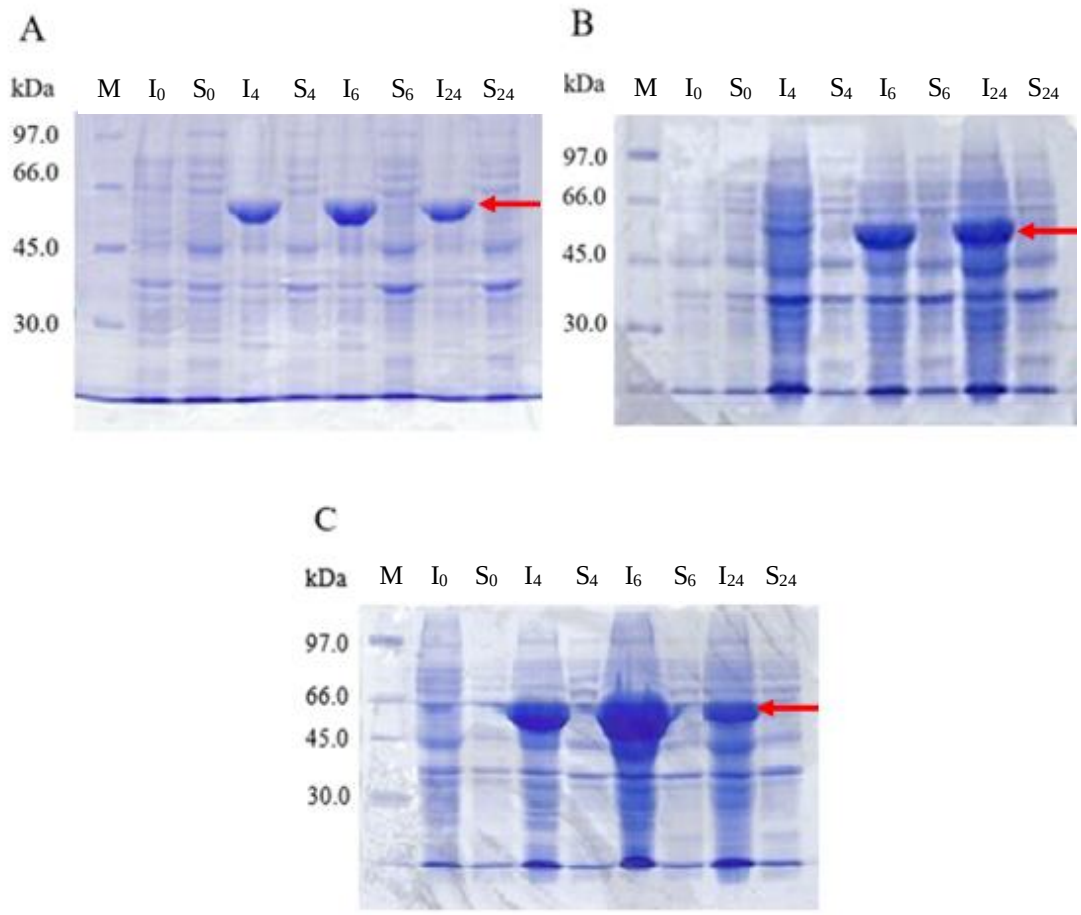

Figure 3. 7 (A) 10% SDS-PAGE of *Wc*AG expressed at 30 ºC, 0.1 mM IPTG induction at 0 to 24 h. (B) 10% SDS-PAGE of *Wc*AG expressed at 30 ºC, 0.5 mM IPTG induction at 0 to 24 h. (C) 10% SDS-PAGE of *Wc*AG expressed at 30 ºC, 1 mM IPTG induction at 0 to 24 h.

Lane M (A, B and C) = Protein molecular weight marker (Amershame Bioscience, USA),

S = Soluble fraction, I = Insoluble protein and number = induction time (h)

*red arrow indicated the expected *Wc*AG size of 62.0 kDa.

จุฬาลงกรณ์มหาวิทยาลัย
CHULALONGKORN UNIVERSITY

3.2.2.3 Expression of *Wc*AG under 0.1, 0.5, 1 mM IPTG induction at 16 ºC, 250 rpm.

*Wc*AG was expressed in insoluble form with no expression in soluble form when temperature was decreased to 16 ºC and the concentration of IPTG was at 0.1, 0.5 and 1 mM as shown in Figure 3.8 (A), (B) and (C).

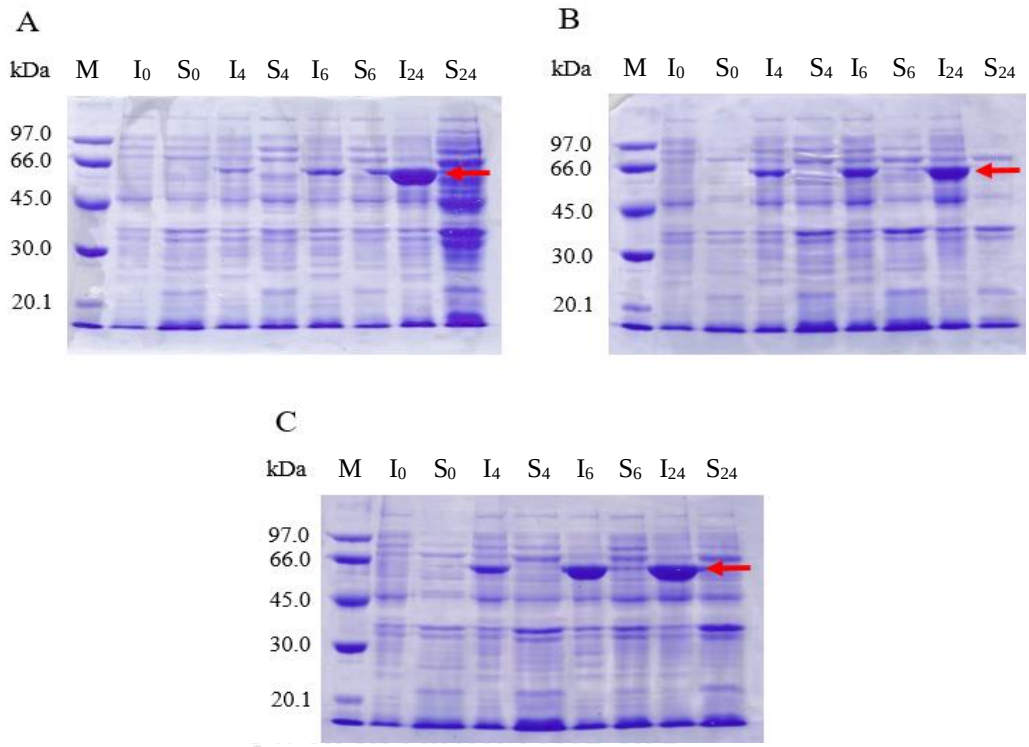

Figure 3. 8 (A) 10% SDS-PAGE of *Wc*AG expressed at 16 ºC, 0.1 mM IPTG induction at 0 to 24 h. (B) 10% SDS-PAGE of *Wc*AG expressed at 16 ºC, 0.5 mM IPTG induction at 0 to 24 h. (C) 10% SDS-PAGE of *Wc*AG expressed at 16 ºC, 1 mM IPTG induction at 0 to 24 h.

Lane M (A, B and C) = Protein molecular weight marker (Amershame Bioscience, USA),

S = Soluble fraction, I = Insoluble protein and number = induction time (h)

*red arrow indicated the expected *Wc*AG size of 62.0 kDa.

3.2.2.4 Expression of *Wc*AG with addition of 1% glucose under 1 mM IPTG induction at 16 ºC, 150 rpm.

To increase the expression level of *Wc*AG in soluble form, 1% (w/v) of glucose was added into LB medium. It was found that the expression of *Wc*AG in soluble form was increased as shown in Figure 3.9 (A) and (B).

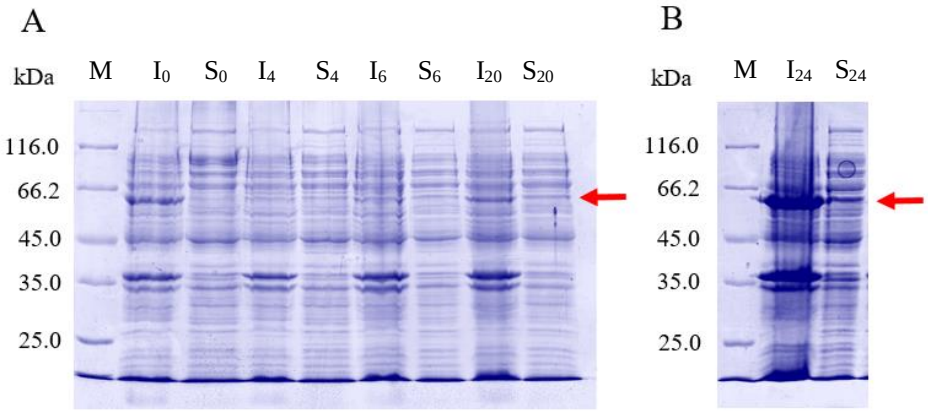

Figure 3. 9 (A) 10% SDS-PAGE of *Wc*AG expressed at 16 ºC, 1 mM IPTG induction at 0 to 20 h. (B) 10% SDS-PAGE of *Wc*AG expressed at 16 ºC, 1 mM IPTG induction at 24 h.

Lane M (A and B) = Protein molecular weight marker (Bio Basic, Canada),

S = Soluble fraction, I = Insoluble protein and number = induction time (h)

*red arrow indicated the expected *Wc*AG size of 62.0 kDa.

3.2.2.5 Expression of *Wc*AG with addition of 1% glucose under 0.4 mM IPTG induction at 12 ºC and 20 ºC, 150 rpm.

To increase the expression level of *Wc*AG in soluble form, 1% (w/v) of glucose was added into LB medium and temperatures were then varied at 12 ºC and 20 ºC with 150 rpm shaking. SDS-PAGE showed that the *Wc*AG was expressed as soluble protein when cultivating was at 20 ºC as shown in Figure 3.10 (B).

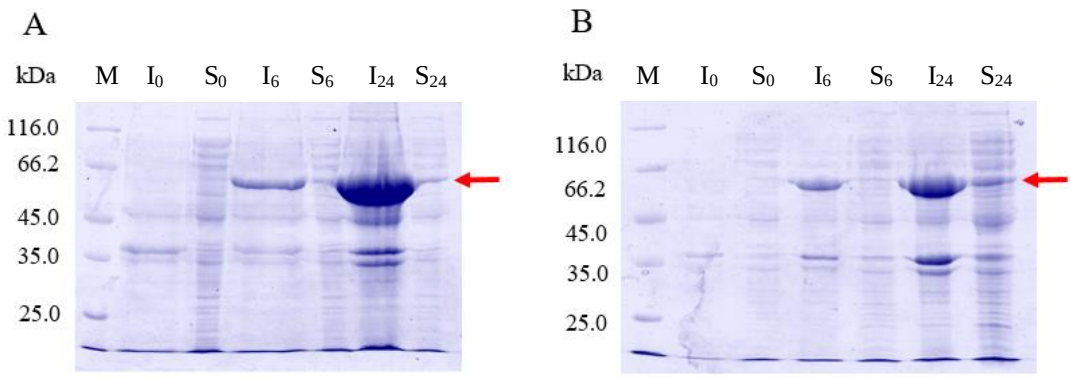

Figure 3. 10 (A) 10% SDS-PAGE of *Wc*AG expressed at 12 ºC, 0.4 mM IPTG induction at 0 to 24 h. (B) 10% SDS-PAGE of *Wc*AG expressed at 20 ºC , 0.4 mM IPTG induction at 0 to 24 h.

Lane M (A and B) = Protein molecular weight marker (Bio Basic, Canada),

S = Soluble fraction, I = Insoluble protein and number = induction time (h)

*red arrow indicated the expected *Wc*AG size of 62.0 kDa.

3.2.2.6 Expression of *Wc*AG with addition of 1% glucose under 0.1 and 0.4 mM IPTG induction at 25 ºC, 150 rpm.

The concentrations of IPTG were varied at 0.1 and 0.4 mM under *Wc*AG expression at 25 ºC, 150 rpm shaking with addition of 1%(w/v) glucose. SDS-PAGE showed that the expression of soluble *Wc*AG was increased after induced with 0.4 mM IPTG at 25 ºC as shown in Figure 3.11 (B).

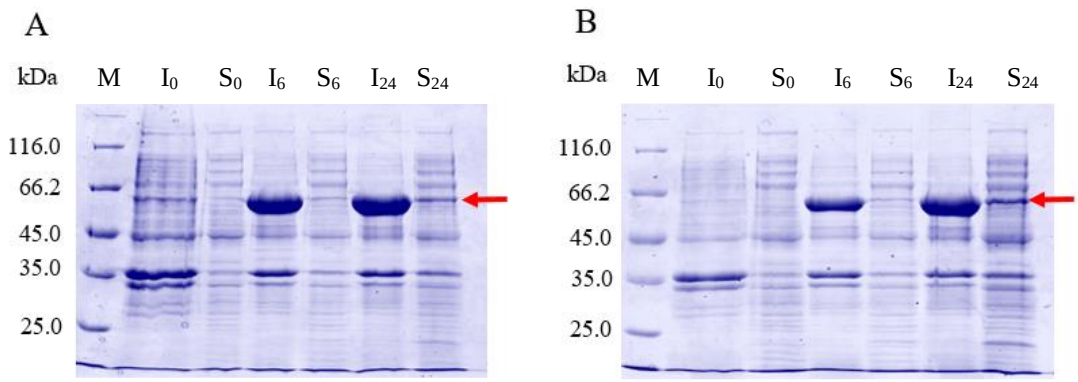

Figure 3. 11 (A) 10% SDS-PAGE of *Wc*AG expressed at 25 ºC, 0.1 mM IPTG induction at 0 to 24 h. (B) 10% SDS-PAGE of *Wc*AG expressed at 25 ºC, 0.4 mM IPTG induction at 0 to 24 h.

Lane M (A and B) = Protein molecular weight marker (Bio Basic, Canada),

S = Soluble fraction, I = Insoluble protein and number = induction time (h)

*red arrow indicated the expected *Wc*AG size of 62.0 kDa.

3.2.2.7 Expression of *Wc*AG with addition of 1% glucose under 0.1, 0.2 and 0.4 mM IPTG induction at 20 ºC, 150 rpm.

The expression of *Wc*AG was further improved by varying final IPTG concentrations of 0.1, 0.4 and 1 mM under cultivation at 20 ºC, 150 rpm, supplemented with 1% (w/v) glucose. Figure 3.12 (F) indicated that the expression of soluble *Wc*AG was successfully increased under the condition of 0.4 mM IPTG at 20 ºC for 20 h with 1% (w/v) glucose adding.

จุฬาลงกรณ์มหาวิทยาลัย
Chulalongkorn University

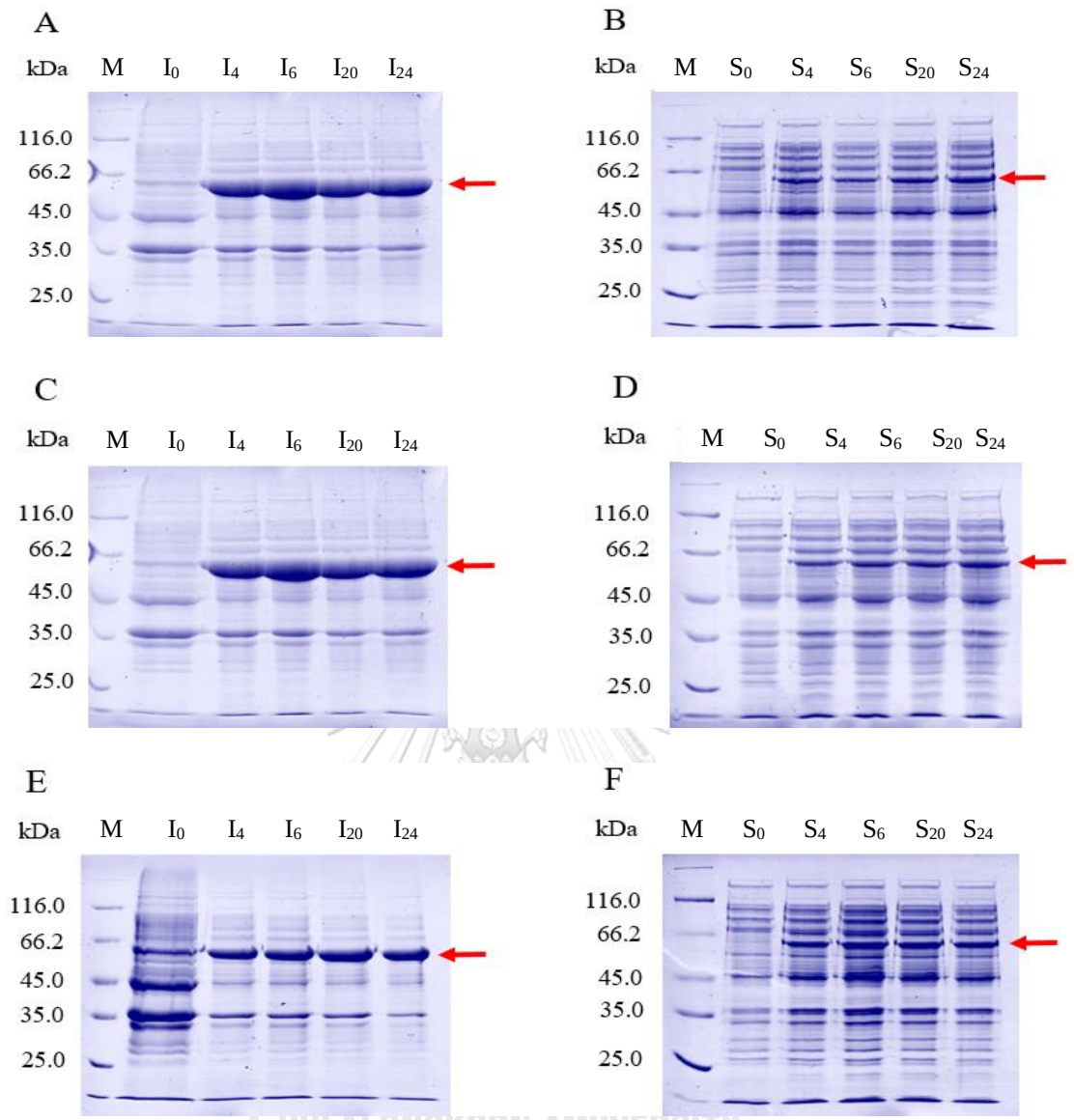

CHULALONGKORN UNIVERSITY

Figure 3. 12 (A and B) 10% SDS-PAGE of *Wc*AG expressed at 20 ºC , 0.1 mM IPTG induction at 0 to 24 h. (C and D) 10% SDS-PAGE of *Wc*AG expressed at 20 ºC, 0.2 mM IPTG induction at 0 to 24 h. (E and F) 10% SDS-PAGE of *WcAG* expressed at 20 ºC, 0.4 mM IPTG induction at 0 to 24 h.

Lane M (A, B, C, D, E and F) = Protein molecular weightmarker (Bio Basic, Canada), S = Soluble fraction, I = Insoluble protein and number = induction time (h)

*red arrow indicated the expected *Wc*AG size of 62.0 kDa.

3.2.3 Optimization of *WcAG* gene expression using chemicals

In order to obtain the highest amount of soluble *Wc*AG, effects of chemical agents including L-arginine, D-sorbitol, TritonX-100 and Tween-20 were investigated.

3.2.3.1 Expression of *Wc*AG with addition of 0.1 and 0.25 mM L-arginine, 0.1 and 0.5 mM D-sorbitol, 0.5 mM TritonX-100 and 0.1 mM Tween-20 under 0.4 M IPTG induction at 20 ºC, 150 rpm

The results showed that the expression level of *Wc*AG was obviously higher in insoluble protein than soluble protein at 20 h when any chemical agents including L-arginine, D-sorbitol, TritonX-100 and Tween-20 were added. Figure 3.13 (A) - (F) show that using chemicals for *Wc*AG expression can not increase solubility in soluble fraction compare with optimum expression condition at 20 ºC, 0.4 mM IPTG as shown in Figure 3.12 (E and F).

จุฬาลงกรณ์มหาวิทยาลัย
CHULALONGKORN UNIVERSITY

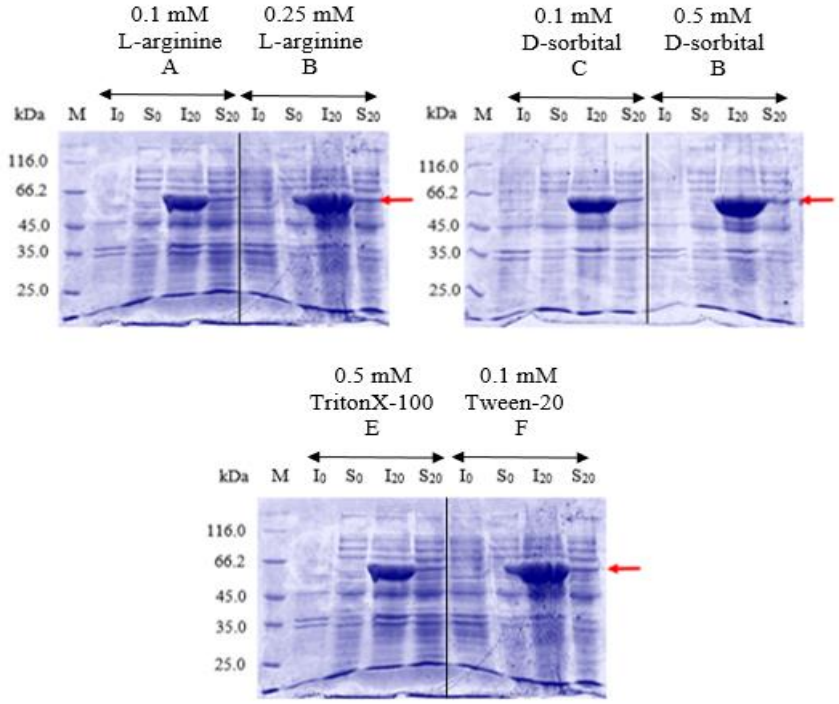

Figure 3. 13 (A) 10% SDS-PAGE of *Wc*AG expressed at 20 ºC with 0.1 mM L-arginine, 0.4 mM IPTG induction at 0 to 24 h. (B) 10% SDS-PAGE of *Wc*AG expressed at 20 ºC with 0.25 mM L-arginine, 0.4 mM IPTG induction at 0 to 24 h. (C) 10% SDS-PAGE of *Wc*AG expressed at 20 ºC cultivation with 0.1 mM D-sorbitol, 0.4 mM IPTG induction at 0 to 24 h. (D) 10% SDS-PAGE of *Wc*AG expressed at 20 ºC cultivation with 0.5 mM D-sorbitol, 0.4 mM IPTG induction at 0 to 24 h. (E) 10% SDS-PAGE of *Wc*AG expressed at 16 ºC with 0.5 mM TritonX-100, 0.4 mM IPTG induction at 0 to 24 h. (F) 10% SDS-PAGE of *Wc*AG expressed at 16 ºC with 0.1 mM Tween-20, 0.4 mM IPTG induction at 0 to 24 h.

Lane M (A, B, C, D, E and F) = Protein molecular weight marker (Bio Basic, Canada), S = Soluble fraction, I = Insoluble protein and number = induction time (h)

*red arrow indicated the expected *Wc*AG size of 62.0 kDa.

3.2.4 Scale-up of *Wc*AG expression and crude extract preparation

E. coli BL21 (DE3) carrying recombinant *Wc*AG plasmid was cultured in 2 L of LB medium containing 30 µg/ml of kanamycin. One percent (w/v) of glucose was added to the medium. The cultivation was at 20 °C using 0.4 mM IPTG for 20 h with 150 rpm shaking. Cells were then harvested and resuspended in extraction buffer before they were disrupted by sonication. In this step, volume of phosphate buffer pH 7.4 and concentration of Triton-X100 in extraction buffer were varied. Then supernatant was assayed by hydrolytic activity as described in section 2.9.1.

3.2.4.1 Expression of *Wc*AG with addition of 1%(w/v) glucose under 0.4 mM IPTG induction at 20 ºC, 150 rpm. Varying volume of 50 mM phosphate buffer pH 7.4.

SDS-PAGE showed that *Wc*AG was expressed as insoluble protein higher than the soluble protein as indicated by Figure 3.14. To increase expression level of *Wc*AG in soluble fraction, volume of 50 mM phosphate buffer pH 7.4 was varied for resuspened *Wc*AG before sonication. However, the optimum condition for stabilizing *Wc*AG was at using 200 ml of 50 mM phosphate buffer pH 7.4 per cell culture in 1 L of LB medium.

จุฬาลงกรณ์มหาวิทยาลัย
CHULALONGKORN UNIVERSITY

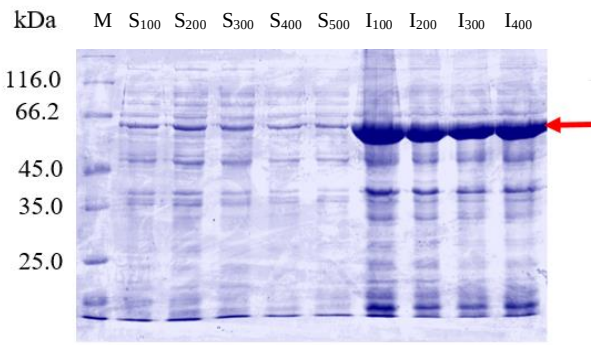

Figure 3. 14 10% SDS-PAGE of *Wc*AG expressed at 20 ºC, 0.4 mM IPTG induction at 20 h and resuspended in 50-500 ml of 50 mM phosphate buffer pH 7.4/cell culture in 1 L of LB medium.

Lane M = Protein molecular weight marker (Bio Basic, Canada),

S = Soluble fraction, I = Insoluble protein and number = volume of 50 mM phosphate buffer pH 7.4 (ml)

*red arrow indicated the expected *Wc*AG size of 62.0 kDa.

3.2.4.2 Expression of *Wc*AG with addition of 1 % glucose under 0.4 mM IPTG induction at 20 ºC, 150 rpm. Varying concentration of Triton-X100 in extraction buffer.

The optimum condition for *Wc*AG expression as soluble form was using 0.1% Triton-X100 in 200 ml of 50 mM phosphate buffer pH 7.4 per cell culture in 1 L of LB medium.

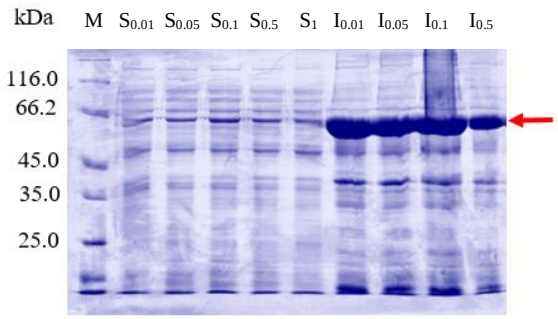

Figure 3. 15 10% SDS-PAGE of *Wc*AG expressed at 20 ºC, 0.4 mM IPTG induction at 20 h and resuspended in 0.01-1% of Triton-X100. Red arrow indicated the expected *Wc*AG size of 62.0 kDa.

Lane M: Protein molecular weight marker (Bio Basic, Canada)

(S; Soluble fraction, I; Insoluble protein and number; concentration of Triton-X100 (%v/v))

3.3 Purification of *Wc*AG

3.3.1 Purification of *Wc*AG by His-Trap column chromatography

The optimum expression of *Wc*AG was carried out by cultivating at 20 ºC for 20 h with 0.4 mM IPTG and 1% (w/v) of glucose at 20 ºC. In this research, Ni Sepharose^{TM} 6 Fast Flow column, an affinity column that has specificity toward Histidine tag (His-tag) protein, was used to purify this protein. *Wc*AG was purified by stepwise purification at 100 mM imidazole (Figure 3.16A) and 50 mM phosphate buffer pH 7.4 as described in section 2.7. The results from SDS-PAGE revealed that a single band of *Wc*AG was obtained with estimated size of 62 kDa when the protein was eluted by 100 mM imidazole (Fugure 3.16). Then, the purified *Wc*AG was confirmed by Western blot to detect a C-terminal polyhistidine (6xHis) of *Wc*AG fusion protein, using 6x anti-His antibody and alkaline phosphatse-conjugate goat anti-rabbit IgG as primary and secondary antibody, respectively. The size of *Wc*AG was detected by color

development using NBT and BCIP (Fermentus). In Figure 3.17 B, although *Wc*AG was present as a single band in Lane 2, it was disappeared in crude extract (Lane 1). *Wc*AG was successfully purified by 2.93-fold with a specific activity of 45.29 U/mg (Table 3.1). Molecular weight of *Wc*AG analysed by SDS-PAGE was present in Appendix 8.

A

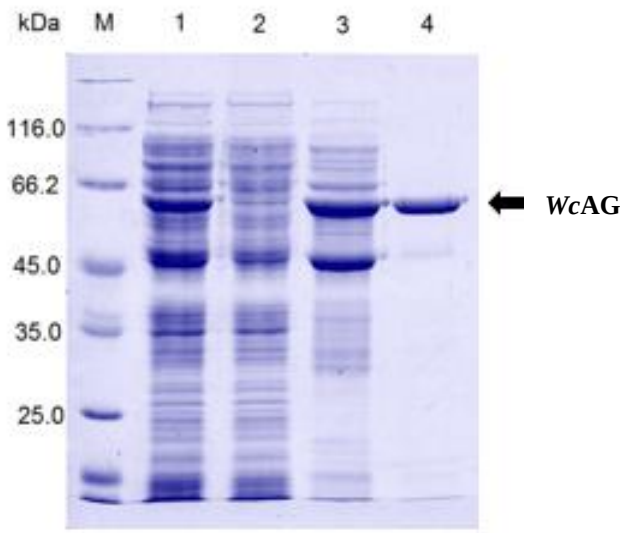

Figure 3.16 A 10% SDS-PAGE analysis of *Wc*AG purified by His-Trap column.

Lane M: protein molecular weight marker (Bio Basic, Canada)

Lane 1: crude extract (15 µg)

Lane 2: flowthrough fraction (15 µg)

Lane 3: fraction eluted with 50 mM imidazole (5 µg)

Lane 4: fraction eluted with 100 mM imidazole (5 µg)

จุฬาลงกรณ์มหาวิทยาลัย
Chulalongkorn University

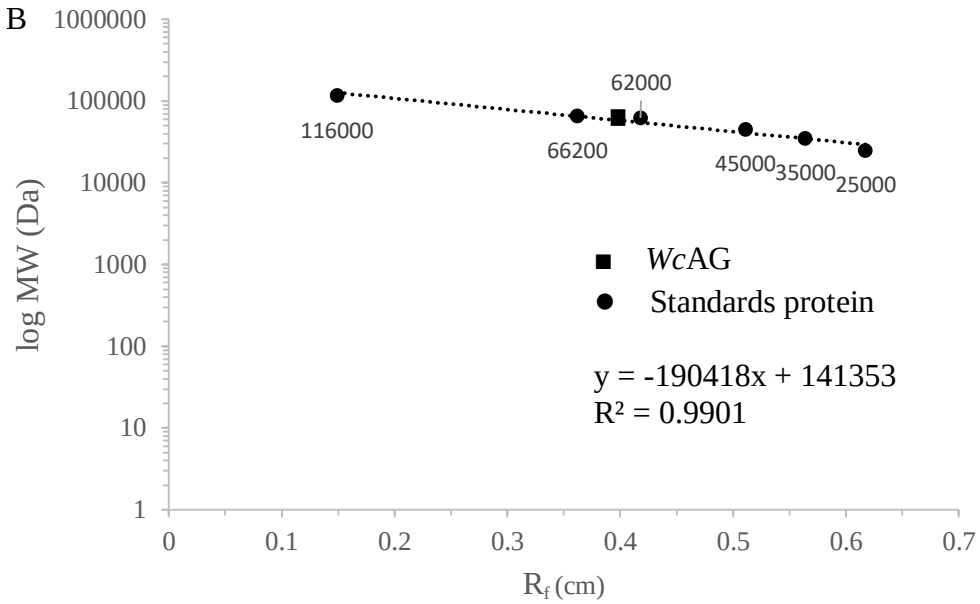

Figure 3.16 B Determining the molecular weight of *Wc*AG by SDS-PAGE.

จุฬาลงกรณ์มหาวิทยาลัย
CHULALONGKORN UNIVERSITY

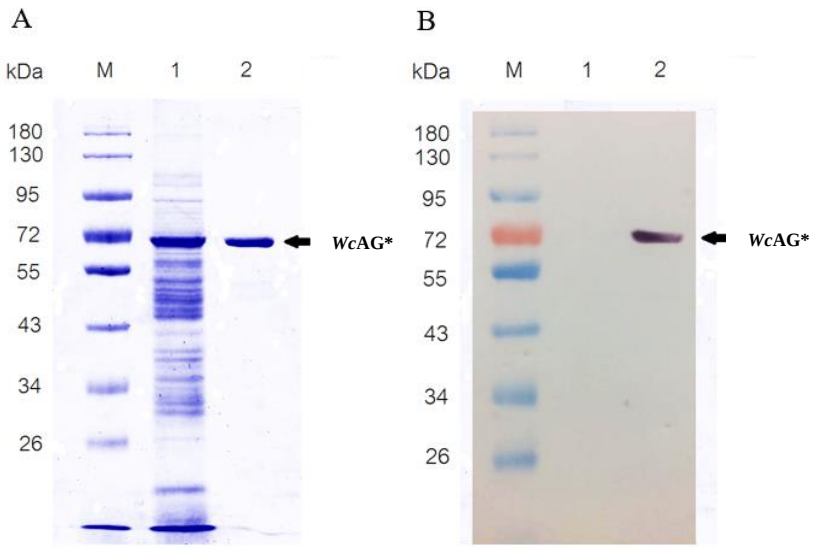

Figure 3. 17 10% SDS-PAGE (A) and Western blot (B) analysis of *Wc*AG.

Lane M: prestained protein molecular weight marker (Bio Basic, Canada)

Lane 1: crude extract (15 µg)

Lane 2: purified *Wc*AG (5 µg)

*black arrow indicated purified *Wc*AG with a size of 62 kDa.

*Wc*AG was successfully purified by 2.93 fold with a specific activity of 45.29 U/mg. Calculation molecular weight of *Wc*AG by SDS-PAGE was presented in Appendix 9. The specific activity of *Wc*AG crude extract was 15.45 U/mg as shown in Table 3.1.

Table 3. 1 Purification table of *Wc*AG by His-Trap column.

Purification steps	Total protein (mg)	Total activity (U)	Specific activity (U/mg)	Yield (%)	Purification fold
Crude enzyme	130.0	2008.00	15.45	100.00	1.00
His-Trap column	9.6	434.80	45.29	21.65	2.93

3.4 Characterization of *Wc*AG

3.4.1 Enzyme assay by hydrolysis activity

Purified *Wc*AG was used to determine hydrolysis activity as described in section 2.9.1. The specific activities of hydrolytic of *Wc*AG was 45.29 U/mg as shown in Table 3.1.

จุฬาลงกรณ์มหาวิทยาลัย
Chulalongkorn University

3.4.2 Effect of temperature on hydrolysis activity

To determine the optimum temperature on *Wc*AG activity, purified *Wc*AG was tested for hydrolysis activity assay at various temperatures (20, 25, 30, 35, 40, 45, 48, 50, 55, 60, 65 and 70 °C). Hydrolysis activity was measured by glucose oxidase method. As illustrated by Figure 3.18, the optimum temperature of *Wc*AG was at 50 °C.

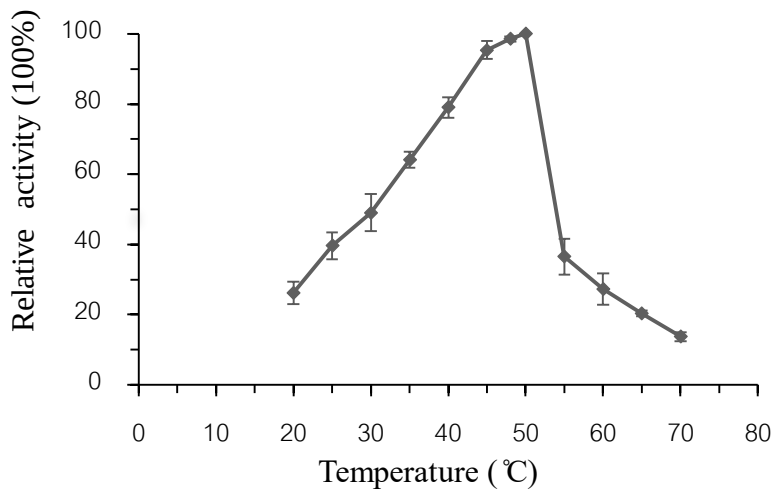

Figure 3. 18 Effect of temperature on hydrolysis activity. Purified *Wc*AG was incubated with 50 mM maltotriose in phosphate buffer pH 6.0 for 10 min at various temperatures. Free glucose, by-product of the reaction, was detected by glucose oxidase method, measuring at A_{505}

3.4.3 Effect of temperature on *Wc*AG stability

To determine the effect of temperature on *Wc*AG stability, purified enzyme was pre-incubated at different temperatures (4, 30, 35, 40, 45, 50, 60, 70 and 80 °C) for 1 h before examining residual hydrolysis activity by glucose oxidase method as described in section 2.9.1. The results showed that the enzyme maintained 80% of its activity in range of 4 to 40 °C. At higher temperature than 40 °C, the activity of *Wc*AG was dramatically dropped as shown in Figure 3.19.

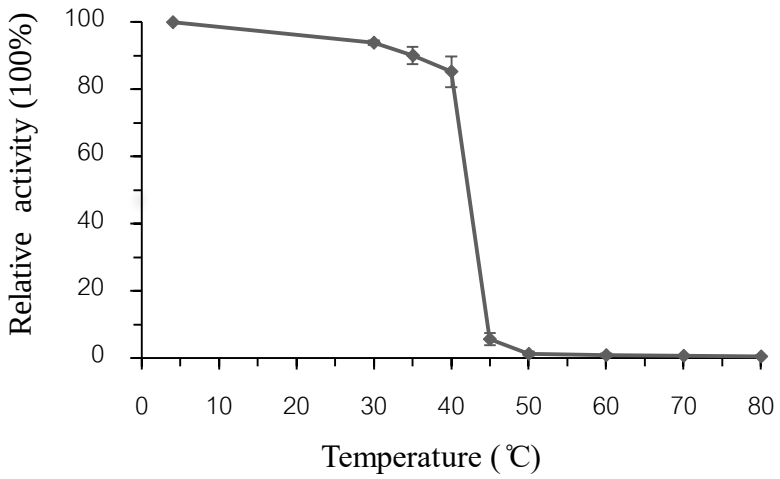

Figure 3. 19 Effect of temperature on *Wc*AG stability assayed by hydrolysis method. *Wc*AG was pre- incubated at different temperatures for 1 h. Purified *WcAG* was incubated with 50 mM maltotriose in phosphate buffer pH 6.0 for 10 min at 50 ºC. Free glucose, by- product of the reaction, was detected by glucose oxidase method, measuring at A_{505}

3.4.4 Effect of pH on hydrolysis activity

The effect of pH on enzyme activity was investigated at different pHs of three separate buffer systems as described in section 2. 9.5. Hydrolysis activity was determined by glucose oxidase method as described in section 2. 9.1. *Wc*AG showed the optimum pH at pH 6.0 of phosphate buffer as presented in Figure 3.20.

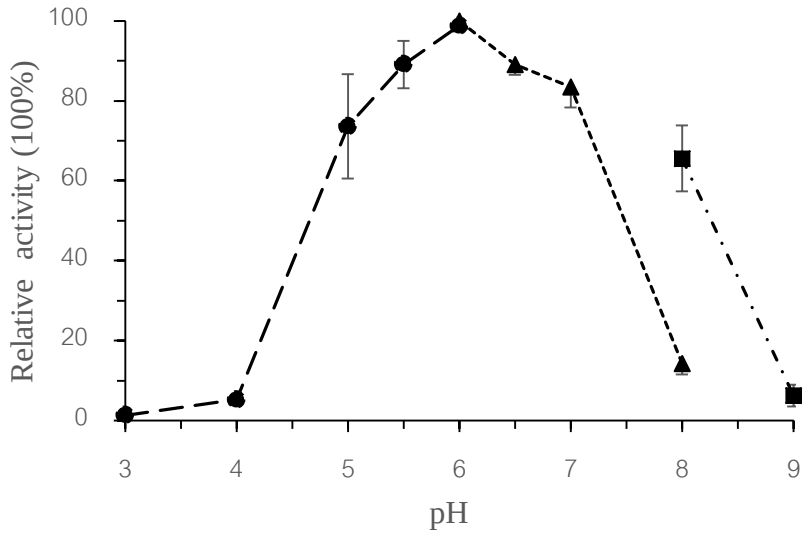

Figure 3. 20 Effect of pH on hydrolytic activity. Purified *Wc*AG was incubated with 50 mM maltotriose in buffers with various pHs for 10 min at 50 ºC. Free glucose, by-product of the reaction, was detected by glucose oxidase method, measuring at A_{505}. A —●— indicates acetate buffer pH 3-6 , a ---▲--- indicates phosphate buffer pH 6-8 and – · ■· – · indicates Tris-HCl pH 8-9.

3.4.5 Effect of pH on *Wc*AG stability

In order to determine the effect of pH on *Wc*AG stability, purified *Wc*AG was pre-incubated in different buffers, pH ranging from 3.0 to 9.0, for 1 h before examining residual hydrolytic activity by glucose oxidase method at 50 ºC as described in section 2.9.1. The results revealed that *Wc*AG can maintain 100% of its activity in phosphate buffer pH range 7.0 to 8.0 while *Wc*AG can keep approximately 80 % of its activity in phosphate buffer pH range 6.0 to 7.0 and Tris-HCl pH 8-9. At phosphate buffer pH range 5.0 to 6.0, activity of *Wc*AG was dramatically reduced to 20-40 % of its activity and continually decreased until lose of all activity at pH 3.0 as shown in Figure 3.21.

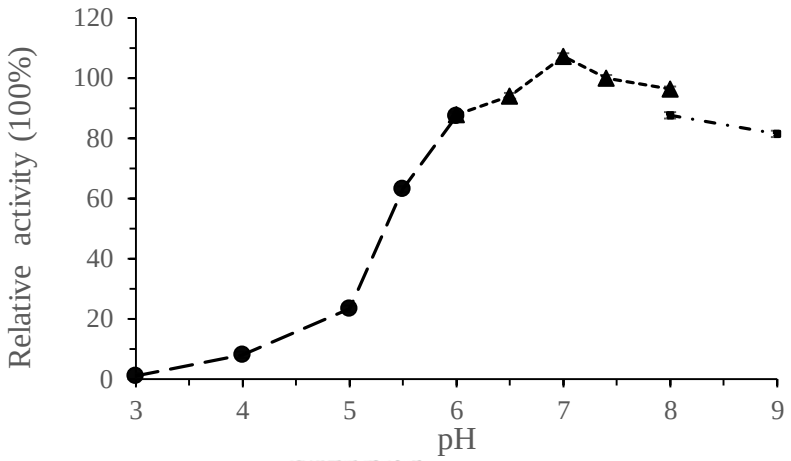

Figure 3. 21 Effect of pH on *Wc*AG stability assayed by hydrolytic method. *Wc*AG was pre-incubated at different temperatures for 60 min. Purified *Wc*AG was incubated with 50 mM maltotriose in 50 mM phosphate buffer pH 6.0 for 10 min at 50 ºC. Free glucose, by-product of the reaction, was detected by glucose oxidase method, measuring at A_{505}. A —●— indicates acetate buffer pH 3-6 , a ----▲---- indicates phosphate buffer pH 6-8 and – · ■· – · indicates Tris-HCl pH 8-9.

3.4.6 Ion effect on *Wc*AG hydrolysis activity

To determine the effect of ion on *Wc*AG activity, purified *Wc*AG was incubated with different ions before it was measured for hydrolysis activity by glucose oxidase method as described in section 2.9.1. In this research, SPSS statistic program version 17.0 (https://en.freedownloadmanager.org/userschoice/Spss_Statistics17.0_Free.html) was used for data analysis. Statistic significant difference at *p*-value of 0.01 was used. The results revealed that Ca^{2+}(A), Mg^{2+}(G), K^{+} and Na^{+}(I) were group of ions which had slightly positive effect with activity of *Wc*AG (110-120% as compared to *Wc*AG activity without ions). Effect of K^{+} and Na^{+}(I) for *Wc*AG activity was not significantly different. In contrast, Zn^{2+}(C), Cu^{2+}(D) and Ni^{2+}(F) were group of ions which had negative effect on *Wc*AG activity resulting in activity of 5-15% of the control. EDTA

(J) did not affect the acticity of *Wc*AG. Besides, Co^{2+}(H), Mn^{2+} and Fe^{2+}(E) were group of ions which decreased *Wc*AG activity to 40% relative activity while Fe^{3+} (V) displayed 80% relative activity. Effect of Mn^{2+} and Fe^{2+}(E) for *Wc*AG activity was not significantly different as shown in Figure 3.22.

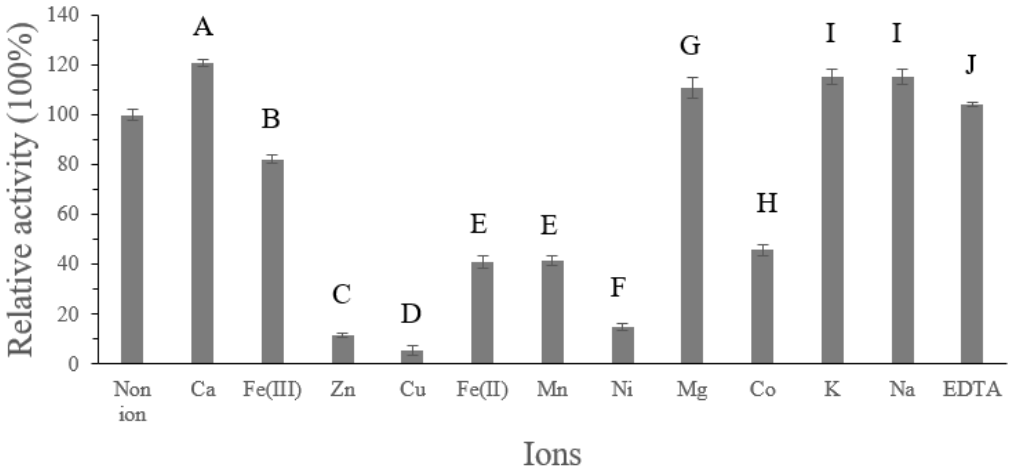

Figure 3. 22 Effect of ions towards hydrolysis activity of *Wc*AG. Bar graph calculated from mean ± S.D. of three replicates of hydrolysis activity. Activity of *Wc*AG without ion was set as 100%. The letters indicated significant differences accepted at *p*-value = 0.01.

จุฬาลงกรณ์มหาวิทยาลัย
Chulalongkorn University

3.4.7 Molecular weight determination of *Wc*AG

Purified *Wc*AG was sent off for molecular weight determination by gel filtration. Hiprep 16/60 sephacryl S-200 High Resolution (GE Healthcare, England) column was equilibrated with 50 mM Tris-HCl buffer (pH 7.4) and 50 mM NaCl for at least 2 column volumes. Purified *Wc*AG of 10 mg/ml was loaded onto the column and eluted with ultrapure water at a flow rate of 0.5 ml/min. The molecular weight of the enzyme was identified from molecular weight calibration curve derived from gel filtration chromatographic profile as presented in Figure 3.23 (A). Purification profile

of *Wc*AG showed that *Wc*AG was eluted at an elution time of 58 min. The molecular weight of *Wc*AG was 124 kDa as determined from standard curve (Figure 3.23 (B). So, *Wc*AG existed in soluntion as dimer protein. Calculation molecular weight of *Wc*AG by gel filtration was presented in Appendix 10.

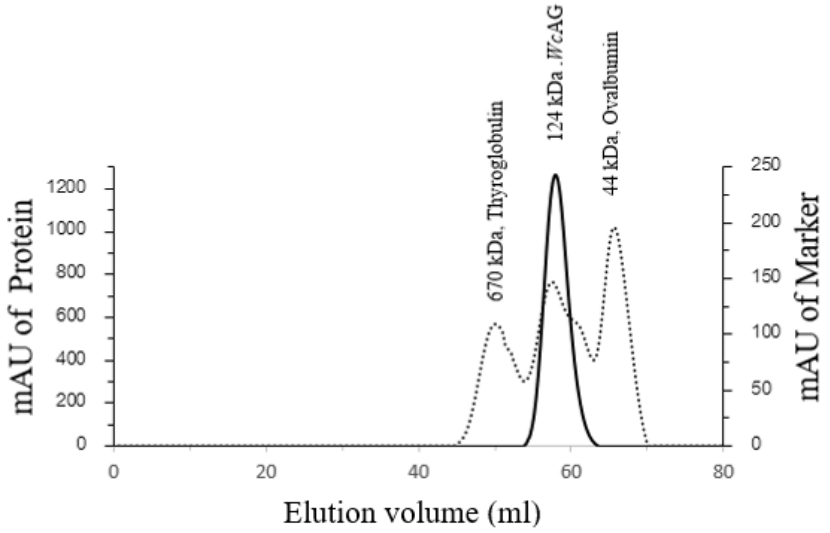

Figure 3.23 A Purification profile of *Wc*AG by gel filtration. The x-axis indicated elution time.

The y-axis indicated absorbance at 280 nm. A bold line (·····) indicated *Wc*AG and a round dot (————) line indicated protein marker. Thyroglobulin (bovine)(670 kDa) , γ- globulin (bovine) (158 kDa) , *Wc*AG (124 kDa) Ovalbumin (chicken)(44 kDa)were eluted at 50.64, 57.84, 58,14 and 65.86 ml, respectively.

จุฬาลงกรณ์มหาวิทยาลัย
CHULALONGKORN UNIVERSITY

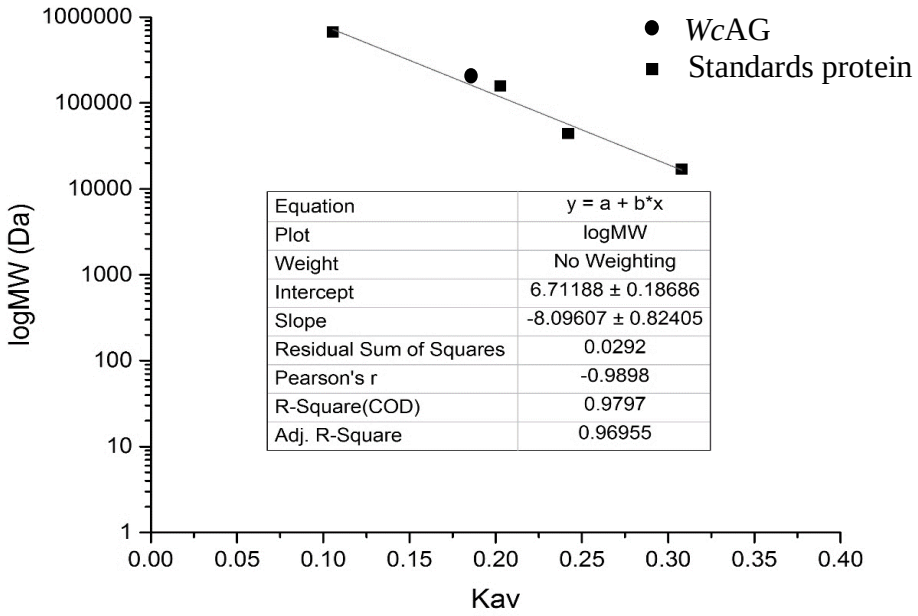

Figure 3.23 B Calibration curve for determining molecular weight of *Wc*AG by gel filtration chromatography. X-axis represented $K_{average}$ and Y-axis represented the log molecular weight. Marker proteins; Thyroglobulin (bovine) (670 kDa), γ-globulin (bovine) (158 kDa), Ovalbumin (chicken) (44 kDa), Myoglobin (horse) (17 kDa) and Vitamin B12(1.35 kDa).

3.4.8 Half- life of *Wc*AG

To identify half-life of *Wc*AG, purified *Wc*AG was pre-incubated in 50 mM phosphate buffer pH 6.0 at 50 ºC under varying times from 0-90 min before determining residual hydrolysis activity by glucose oxidase method as described in section 2.9.2. Half-life of *Wc*AG was an incubation time that the enzyme contains 50% of its activity. The results revealed that half-life of *Wc*AG was at 15 min under 50 ºC as presented in Figure 3.24.

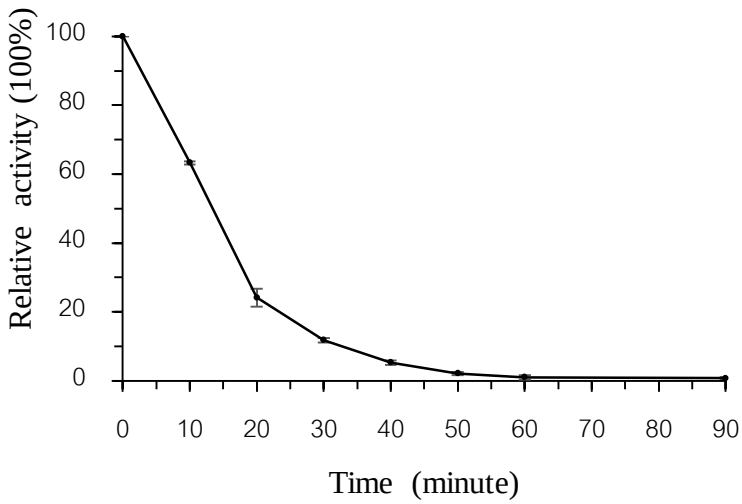

Figure 3. 24 Half-life of *Wc*AG assayed by hydrolytic method. *Wc*AG was pre-incubated at 50 ºC for 10 min. Purified *Wc*AG was incubated with 50 mM maltotriose in phosphate buffer pH 6.0 at various times. Free glucose, by-product of the reaction, was detected by glucose oxidase method, measuring at A_{505}

3.4.9 Substrate specificity of *Wc*AG

3.4.9.1 Substrate specificity by hydrolytic activity of *Wc*AG

Activity of *Wc*AG was examined toward maltotriose (G3), maltotetraose (G4), maltopentaose (G5), maltohexaose (G6), pullulan, dextrin and para-nitrophenyl α-D-glucopyranoside (pNPG). All substrates were assayed by hydrolysis activity. As shown in Table 3.2, G3 was the best substrate for *Wc*AG. The order of substrate specificity was in order of G3>> G4>G5~G6>G2. *Wc*AG displayed no activity on pullulan, dextrin and pNPG. Calculation of substrate specificity was presented in Appendix 8.

Table 3. 2 Substrate preference of *Wc*AG[a].

Substrate	Relative activity (%)
50 mM Maltose (G2)	2.80 ± 0.00
50 mM Maltotriose (G3)	100.00 ± 0.04
50 mM Maltotetraose (G4)	26.25 ± 0.01
50 mM Maltopentaose (G5)	13.47 ± 0.01
50 mM Maltohexaose (G6)	15.20 ± 0.00
50 mM Maltoheptaose (G7)	0.45 ± 0.00
1% Pullulan	0.00 ± 0.00
1% Dextrin	0.12 ± 0.00
1% Amylopectin	0.12 ± 0.00
0.5 mM pNPG	0.25 ± 0.00
50 mM Isomaltotriose	0.49 ± 0.00
50 mM Isomaltose	0.45 ± 0.00
2.5% Raffinose	0.29 ± 0.00
2.5% Cellobiose	0.21 ± 0.00
2.5% Melibiose	0.12 ± 0.00
2.5% Palatinose	0.45 ± 0.00

[a] The α-glucosidase activity was assayed by measuring glucose released under reported condition (section 2.9.1).

3.4.9.2 Substrate specificity by TLC analysis.

Purified *Wc*AG was incubated with 50 mM phosphate buffer pH 6.0 at different times before investigating products hydrolysis activity reaction by TLC analysis as described in section 2.9.2. The results showed that glucose and maltose were obtained from the reaction. Maltotriose (G3) was the best substrate because it gave the highest amount of glucose and maltose at every incubation time as shown in Figure 3.25 and 3.26.

จุฬาลงกรณ์มหาวิทยาลัย
CHULALONGKORN UNIVERSITY

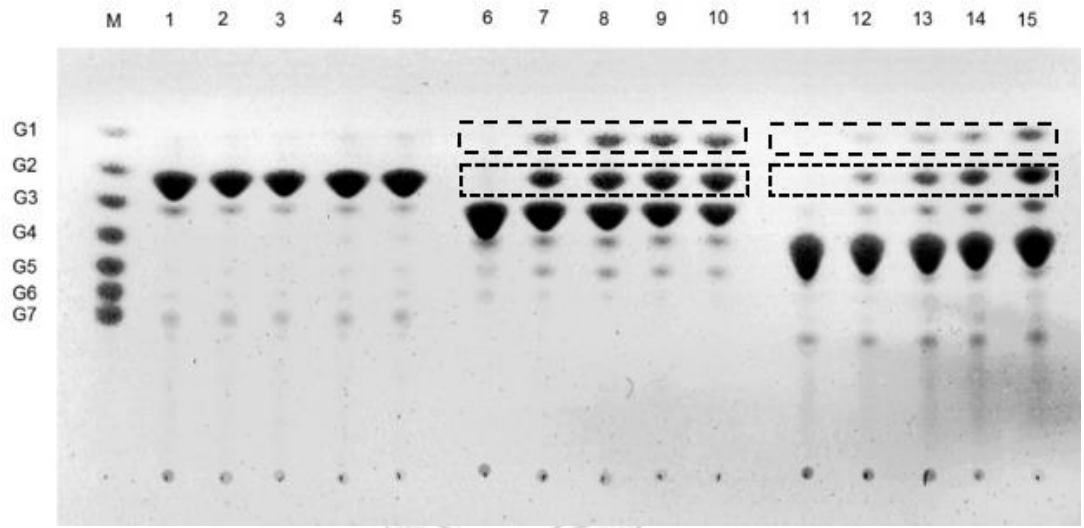

Figure 3. 25 TLC chromatogram of reaction product of *Wc*AG incubated with maltose (G2), maltotriose (G3) and maltotetraose (G4) as substrate. Solvent system was butanol : acetic acid : water (3:3:2, v/v). Dash box indicated glucose, the product from hydrolysis activity and square dot box indicated maltose, the product from hydrolysis activity.

Lane M : Marker G1-G7

Lane 1-5 : 0 min (Control), 15 min, 30 min, 45 min and 60 min incubation time of G2, respectively.

Lane 6-10 : 0 min (Control), 15 min, 30 min, 45 min and 60 min incubation time of G3, respectively.

Lane 11-15 : 0 min (Control), 15 min, 30 min, 45 min and 60 min incubation time of G4, respectively.

จุฬาลงกรณ์มหาวิทยาลัย
CHULALONGKORN UNIVERSITY

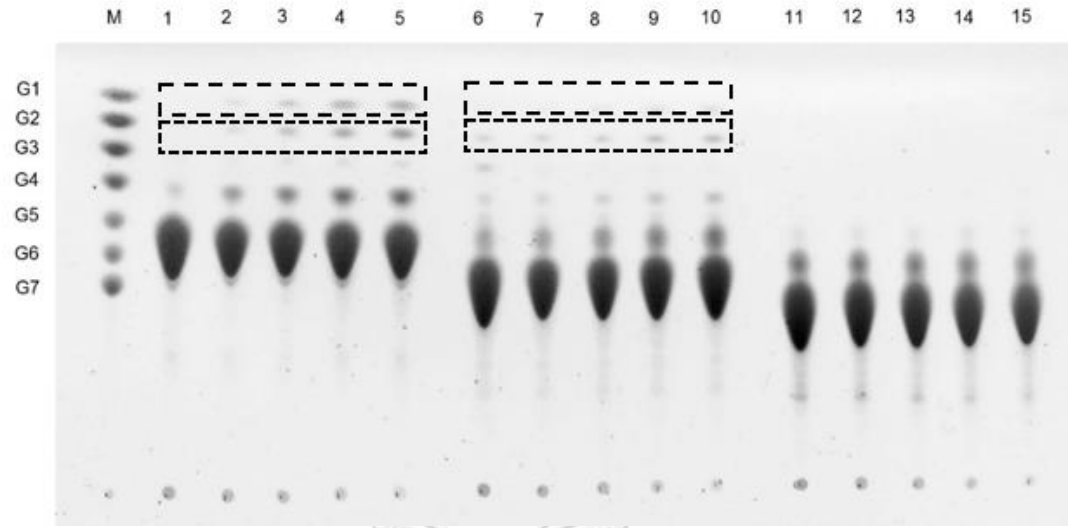

Figure 3. 26 TLC chromatogram of reaction product of *Wc*AG incubated with maltopentaose (G5), maltohexaose (G6) and maltoheptaose (G7) as substrate. Solvent system was butanol : acetic acid : water (3:3:2, v/v). Dash box indicated glucose, the product from hydrolytic activity and square dot box indicated maltose, the product from hydrolytic activity.

Lane M : Marker G1-G7

Lane 1-5 : 0 min (Control), 15 min, 30 min, 45 min and 60 min incubation time of G5, respectively.

Lane 6-10 : 0 min (Control), 15 min, 30 min, 45 min and 60 min incubation time of G6, respectively.

Lane 11-15 : 0 min (Control), 15 min, 30 min, 45 min and 60 min incubation time of G7, respectively.

จุฬาลงกรณ์มหาวิทยาลัย
CHULALONGKORN UNIVERSITY

3.4.10 Kinetic study of hydrolytic activity

In this research, kinetic parameters of *Wc*AG were identified from hydrolysis activity towards G2 and G3 as substrates. K_m and V_{max} values were calculated from Lineweaver-Burk plot. Line-weaver-burk plots of *Wc*AG hydrolysis activity were illustrated in Figure 3.27 (B) and 3.28 (B). All kinetic parameters were summarized in Table 3.3. The K_m values of *Wc*AG for G2 and G3 as substrate were 16.22 and 2.67 mM, respectively. The V_{max} values of *Wc*AG toward G2 and G3 were 0.357 and 6.821 mM, respectively. The k_{cat} of maltotriose was 19 time greater than maltose's while k_{cat}/K_m of maltotriose was 115 time greater than maltose's as presented in Table 3.3.

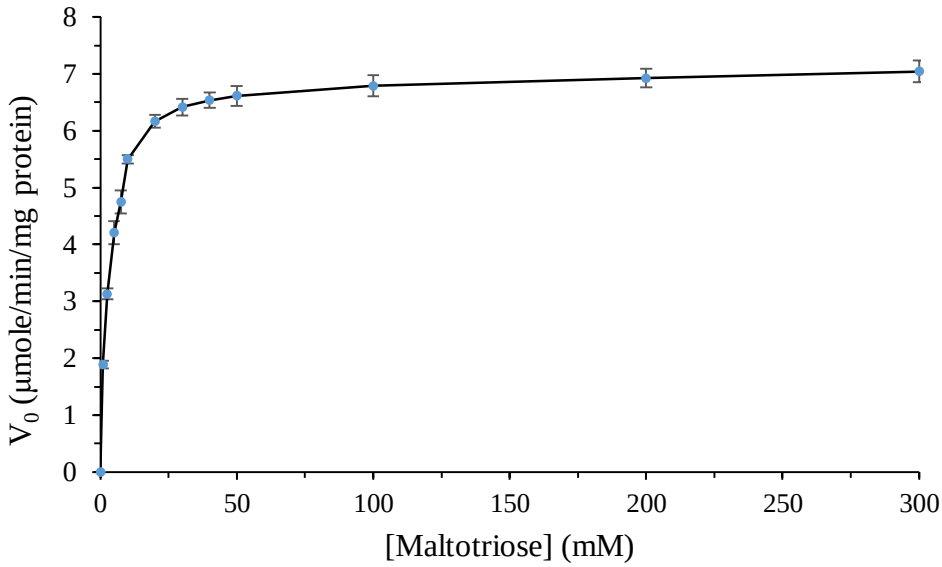

Figure 3.27 A Michealis-Menten plot of *Wc*AG hydrolysis activity using maltotriose as substrate. The K_m and V_{max} values of *Wc*AG for G3 as substrate were 2.67 mM and 6.821 mM, respectively.

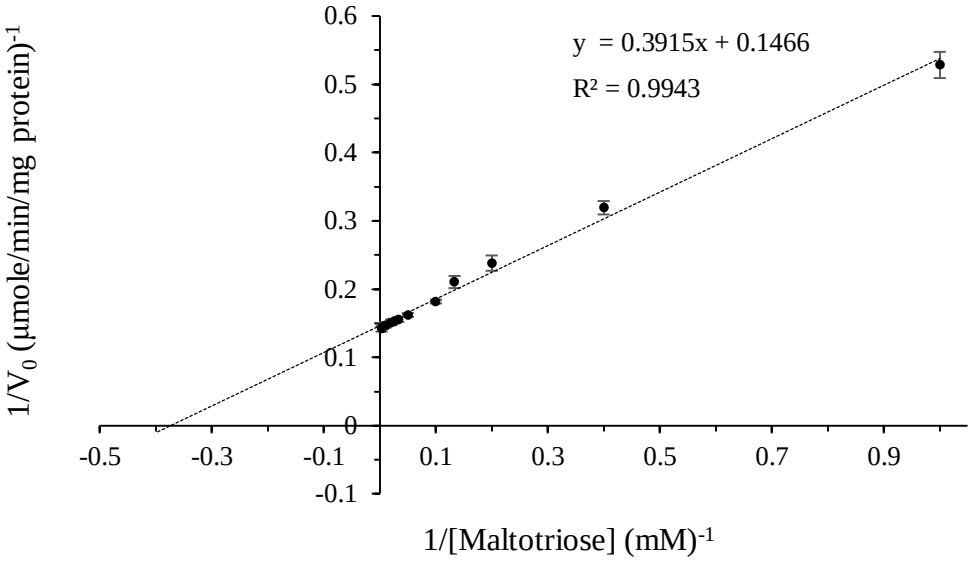

Figure 3.27 B Lineweaver-Burk plot of *Wc*AG hydrolysis activity using maltotriose as substrate.

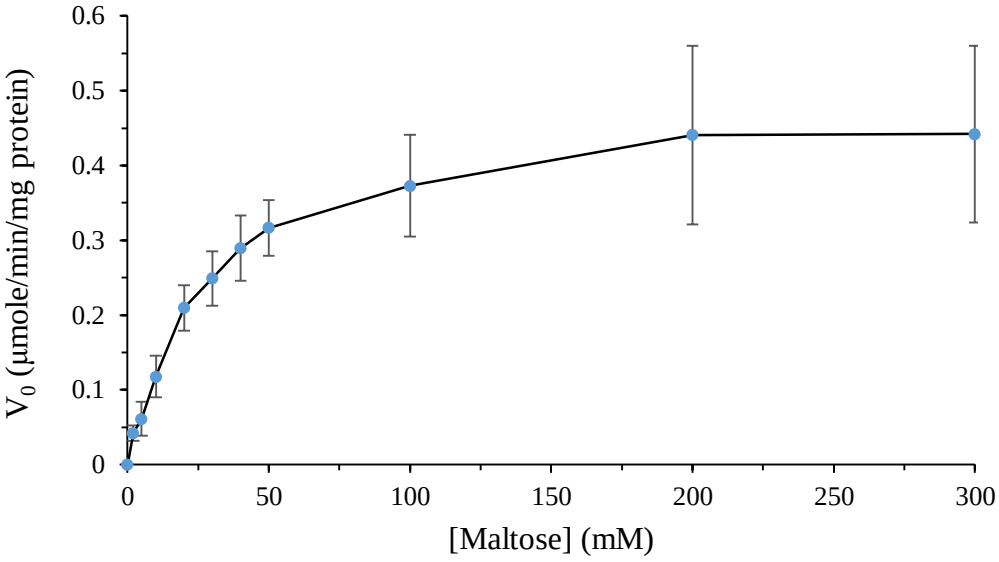

Figure 3.28 A Michealis-Menten plot of *Wc*AG activity using maltose as substrate. The K_m and V_{max} values of *Wc*AG for G2 as substrate were 16. 22 and 0. 357 mM, respectively.

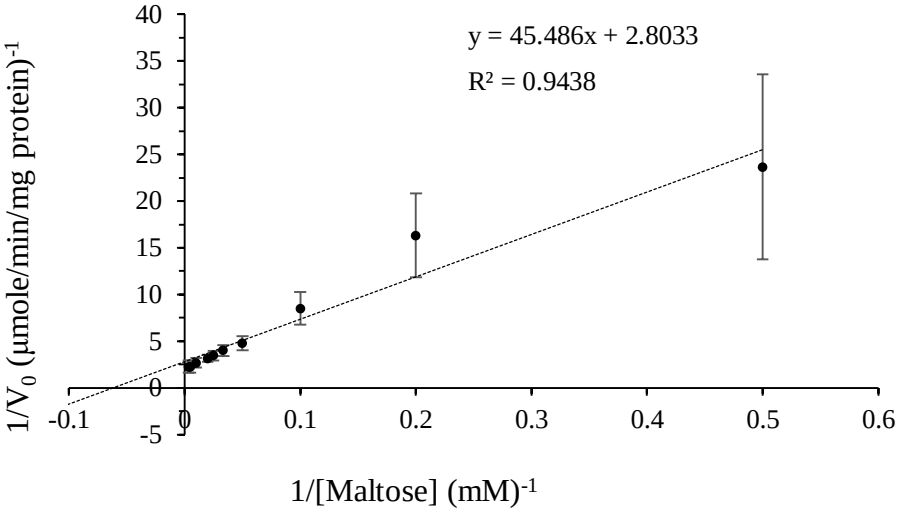

Figure 3.28 B Lineweaver-Burk plot of *Wc*AG activity using maltose as substrate.

Table 3. 3 Summary of kinetic parameters of *Wc*AG hydrolysis activity using maltose and maltotriose as substrates.

Kinetic parameter	Substrate	
	Maltose	Maltotriose
K_m (mM)	16.22	2.67
V_{max} (µmole/min/mg protein)	0.357	6.821
$k_{cat} = V_{max}/[E]$ (s^{-1})	0.738	14.096
k_{cat}/K_m $(s \cdot mM)^{-1}$	0.046	5.279
Unit of enzyme from batch 1 (Unit)	11.856	10.061
Unit of enzyme from batch 2 (Unit)	12.163	11.530
[E] from batch 1 (mg protein/ml)	0.453	0.349
[E] from batch 2 (mg protein/ml)	0.603	0.331

3.5 Optimization of transglycosylation reaction

In this work, enzyme concentration, temperature, substrate concentration, and incubation times were optimized for transglycosylation reaction. The optimum condition for the production of maltooligosaccharide was determined using maltose as glucosyl donor and acceptor. The yield of products was considered from spot areas of products at each condition. The optimum conditions were suggested from the spots size on TLC plates.

3.5.1 Effect of temperature

Under condition described in section 2.10.1, the result indicated that yield of product was increased when incubation temperature was increased from 18-37 ºC. The optimum temperature was at 37 ºC as shown in Figure 3.29 (A), Lane 6 and Figure 3.29 (B), Lane 1.

จุฬาลงกรณ์มหาวิทยาลัย
CHULALONGKORN UNIVERSITY

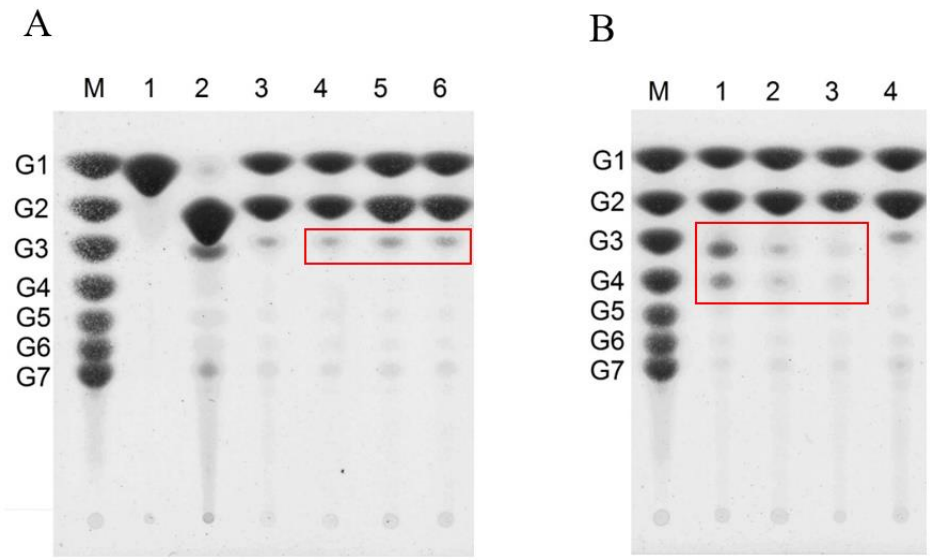

Figure 3. 29 (A and B) TLC of transglycosylated products for 0.04 U/ml and 0.4 U/ml of *Wc*AG incubated with 100 mM maltose for 16 h.

Lane M (A and B) : Marker G1-G7

Lane 1A : 0.5 µl of 100 mM glucose (2 times)

Lane 2A : 0.5 µl of 100 mM maltose (2 times)

Lane 3A : Control for 0.04 U/ml of *Wc*AG

Lane 4A, 5A, 6A : transglycosylated products of 0.04 U/ml of *Wc*AG incubated at 18, 30, 37 ºC, respectively.

Lane 1B, 2B, 3B : transglycosylated products of 0.4 U/ml of *Wc*AG incubated at 37, 30, 18 ºC, respectively.

Lane 4B : Control for 0.4 U/ml of *Wc*AG

*red boxs indicated products of interest from transglycosylation reaction.

จุฬาลงกรณ์มหาวิทยาลัย
Chulalongkorn University

3.5.2 Effect of enzyme concentration

Effect of enzyme concentration on transglycosylation reaction was carried out as mentioned in section 2.10.2. Transglycosylation reactions which contained 0.4 to 1.0 U/ml of *Wc*AG give highest amount of product at the same level. Figure 3.30, Lane 3-5 was not shown significantly different level of products. So, the optimum enzyme concentration for transglycosylation of *Wc*AG was 0.4 U/ml because enzyme concentration enough for catalyze the reaction (Figure 3.30, Lane 3).

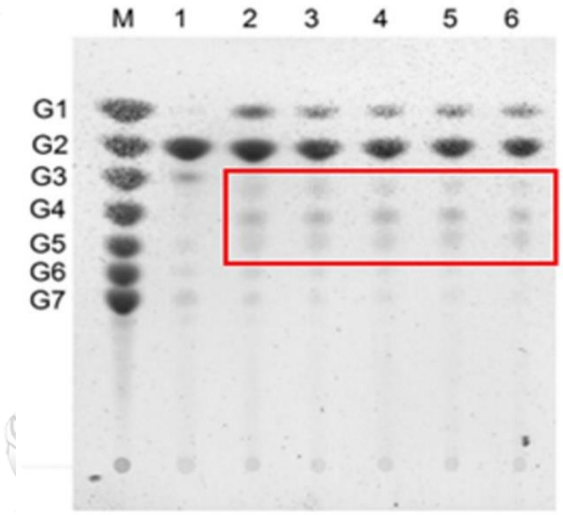

จุฬาลงกรณ์มหาวิทยาลัย
CHULALONGKORN UNIVERSITY

Figure 3. 30 TLC of transglycosylated products for various *Wc*AG concentrations incubated with 100 mM maltose at 37 ºC for 16 h.

Lane M : Marker G1-G7

Lane 1, 2, 3, 4, 5, 6: transglycosylated products obtained from 0, 0.2, 0.4, 0.6, 0.8, 1.0 U/ml *Wc*AG, respectively.

*red box indicated products of interest from transglycosylation reaction.

3.5.3 Effect of substrate concentration

Effect of substrate concentration on transglycosylation reaction was investigated as mentioned in section 2.10.3.The result showed that the yield of product was increased when concentration of maltose was increased from 50 – 200 mM. The maximum yield was obtained when 0.4 U/ml of *Wc*AG was used to incubate with 200 mM maltose as shown in Figure 3.31 (A), Lane 8. When compared with different enzyme concentration, maltotriose was a major product from incubating 200 mM maltose with 0.04 U/ml *Wc*AG. Meanwhile, maltotetraose was a major product from incubating 200 mM maltose with 0.4 U/ml *Wc*AG. The maximum product was obtained from 200 mM of maltose incubated with 0.4 U/ml *Wc*AG at 37 ºC for 24 h as shown in Figure 3.31 (B), Lane 8.

จุฬาลงกรณ์มหาวิทยาลัย
CHULALONGKORN UNIVERSITY

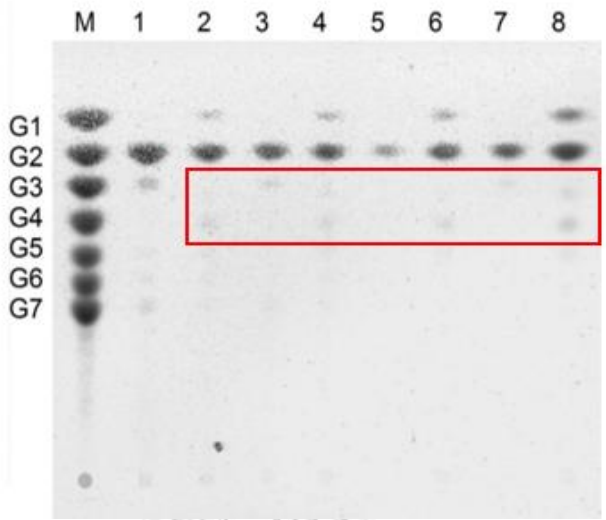

Figure 3.31 A TLC of transglycosylated products for *Wc*AG 0.4 U/ml incubated with various maltose concentrations at 37 ºC for 16 h.

Lane M : Marker G1-G7

Lane 1, 3, 5, 7 : Control for 50, 100, 150, 200 mM maltose, respectively.

Lane 2, 4, 6, 8 : transglycosylated products obtained from using 50, 100, 150, 200 mM maltose, respectively.

*red box indicated products of interest from transglycosylation reaction.

จุฬาลงกรณ์มหาวิทยาลัย
CHULALONGKORN UNIVERSITY

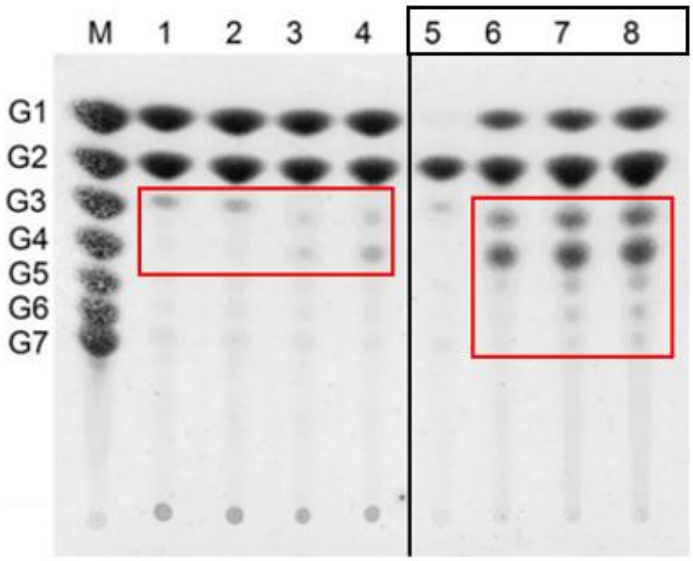

Figure 3.31 B TLC of transglycosylated products for 0.04 and 0.4 U/ ml *Wc*AG incubated at 18, 30 and 37 ºC for 24 h.

Lane M : Marker G1-G7

Lane 1 and 2 : transglycosylated products obtained from 100 mM glucose and 100 mM maltose incubated with 0.04 U/ml *Wc*AG at 18 and 37 ºC, respectively.

Lane 3 and 4 : transglycosylated products obtained from 100 mM glucose and 100 mM maltose incubated with 0.4 U/ml *Wc*AG at 30 and 37 ºC, respectively.

Lane 5 : 0.5 µl of 50 mM maltose (2 times)

Lane 6, 7, 8 : transglycosylated products obtained from 0.4 U/ml *Wc*AG incubated with 50, 100, 200 mM maltose at 37 ºC, respectively.

*red boxs indicated products of interest from transglycosylation reaction.

*black boxs indicated effect of substrate concentration

3.5.4 Effect of incubation time

Incubation times were varied to optimize the amount of transglycosylated products as mentioned in section 2.10.4. The result showed that the yield of product was significantly increased when incubation time was increased from 0-24 h. The optimum incubation time was at 24 h as shown in Figure 3.32, Lane 11.

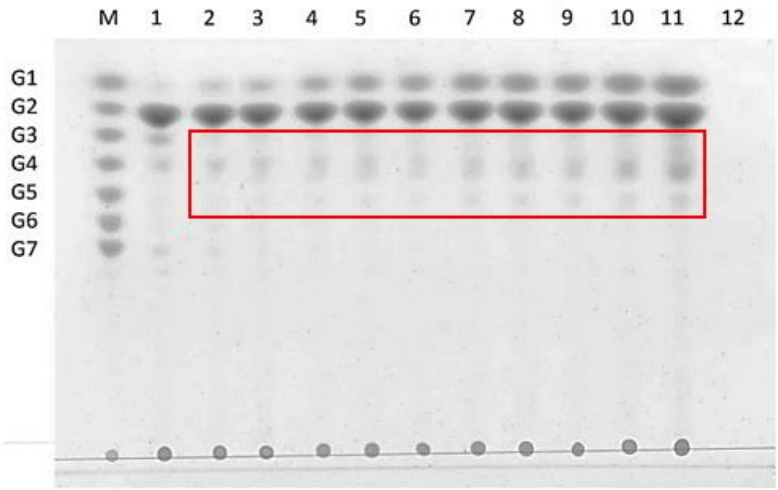

Figure 3. 32 TLC of transglycosylated products for 0.4 U/ml *Wc*AG incubated with 200 mM maltose at 37 ºC at various times.

Lane M : Marker G1-G7

Lane 1 - 11 : transglycosylated products obtained from 0, 1, 3, 6, 9, 12, 15, 16, 18, 21 and 24 h, respectively.

Lane 12 : 0.4 U/ml *Wc*AG with no substrate

*red boxs indicateg products of interest from transglycosylation reaction.

3.6 Large scale production and isolation of maltooligosaccharide products

Aiming for higher amounts of maltooligosaccharide products, the larger scale production was prepared in 50 ml using optimum condition for transglycosylation obtained from section 3.5. The products were analyzed by HPAEC-PAD. Profile of crude products was shown in Figure 3.33 Four main peaks including I, II, III and IV were observed at retention time (R_t) of 6.50, 11.30, 14.10 and 16.30 min, respectively.

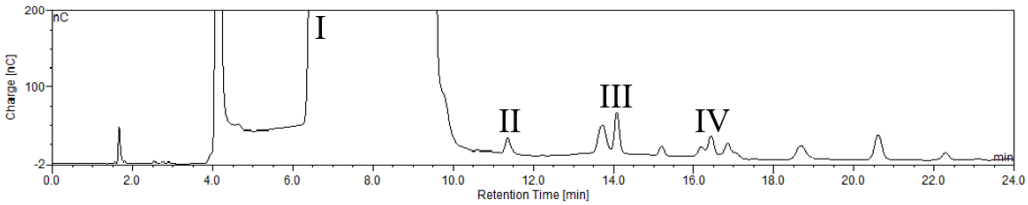

Figure 3. 33 HPAEC-PAD chromatogram of crude maltooligosaccharide products.

3.7 Characterization of maltooligosaccharide products

The transglycosylated products were purified by Biogel P2 column. The products were successfully eluted with distilled water. Each fraction was detected by transglycosylation activity of *Wc*AG. Fractions containing maltooligosaccharide were then analyzed by TLC technique. The results showed that the products might be maltose (G2), maltotriose (G3), maltotetraose (G4) and maltopentaose (G5) as shown in Figure 3.34.

จุฬาลงกรณ์มหาวิทยาลัย
Chulalongkorn University

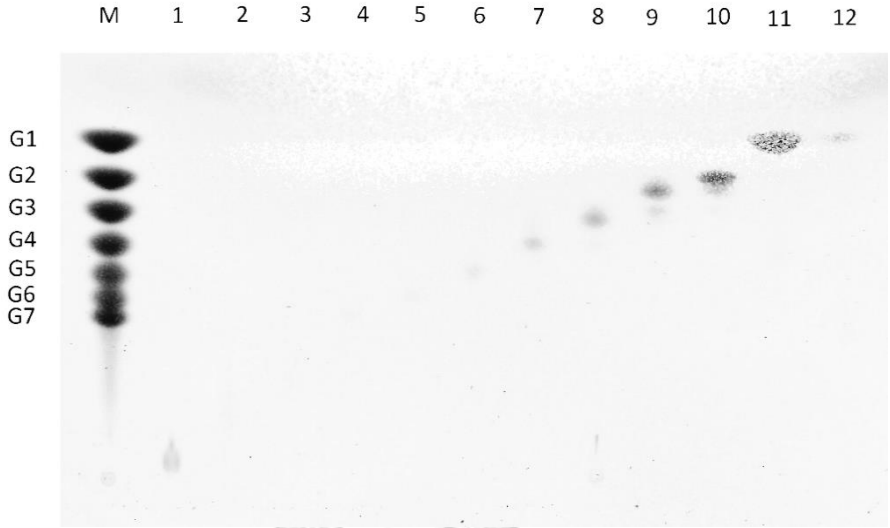

Figure 3. 34 TLC of purified transglycosylated products by Biogel P2 column

Lane M : Marker G1-G7

Lane 1-12 : Fractions number 27, 33, 36, 40, 38, 47, 50, 54, 56, 63, 69, 72, respectively

However, purified products were further analyzed by HPAEC. The results showed that there were four main peaks observed on the HPAEC profile. Each peak was identified by comparing to standard. It was found that peak I, eluted at a retention time (R_t) of 6.50 min, was identified as isomaltose as shown in Figure 3.35. Next, peak II was a panose eluted at R_t of 11.30 min as shown in Figure 3.36. Peak III was unable to be identified with our standard; therefore, glucoamylase was used to cleave α-(1,4)-glycosidic linkage of peak III product (R_t = 14.10 min). The results after treated with glucoamylase revealed that glucose, isomaltose and isopanose were found at R_t of 4.00, 6.50 and 10.80 min, respectively as shown in Figure 3.37. Finally, peak IV (R_t = 16.30 min) was unable to identify with our standard so it was incubated with glucoamylase. The results after treated with glucoamylase revealed that glucose, isomaltose and isopanose were found at R_t of 4.00, 6.50 and 10.80 min, respectively as shown in Figure 3.38.

จุฬาลงกรณ์มหาวิทยาลัย
Chulalongkorn University

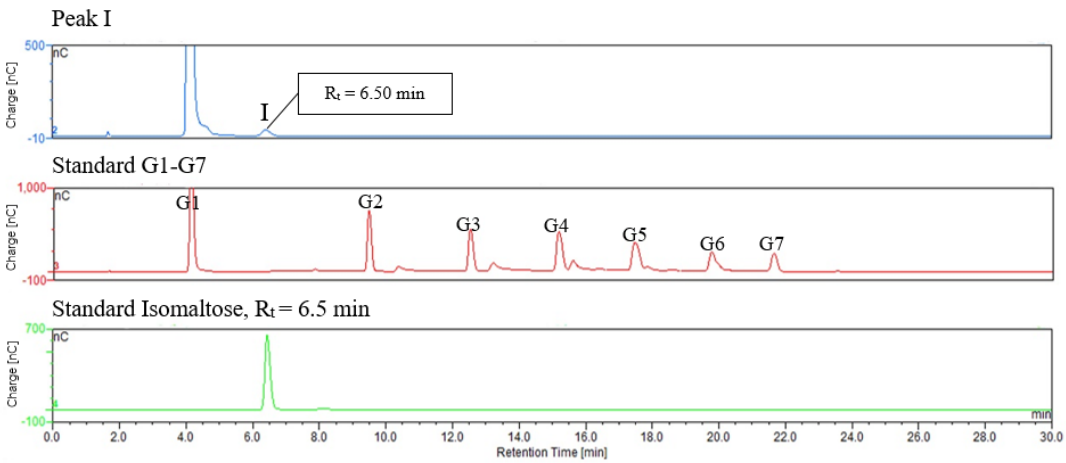

Figure 3. 35 HPAEC-PAD analysis of peak I compared with standard isomaltose from CarboPac® PA1 analytical column.

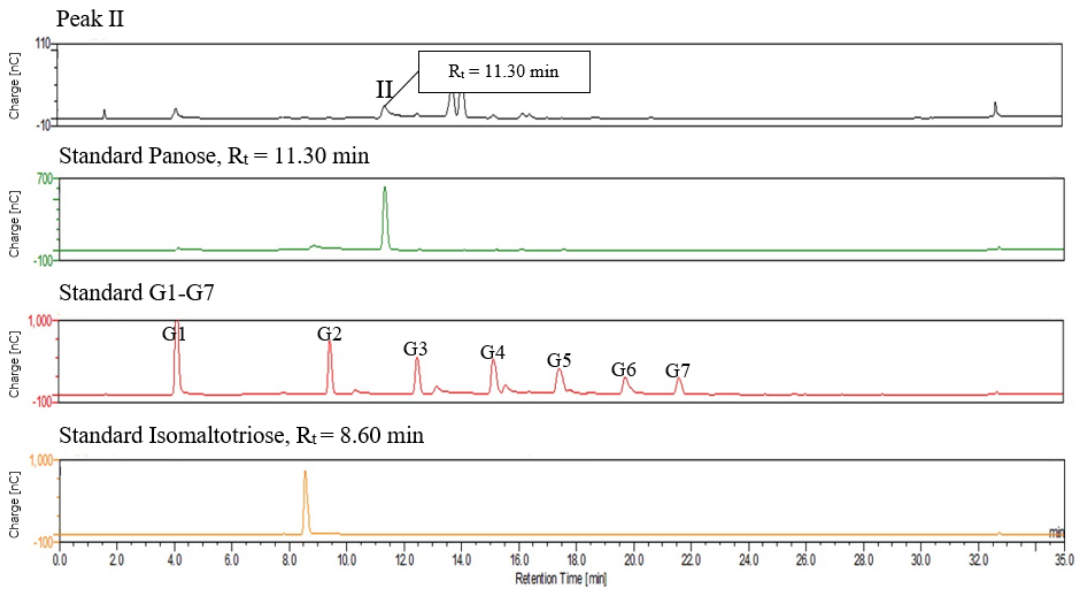

Figure 3. 36 HPAEC-PAD analysis of peak II compared with standard panose from CarboPac® PA1 analytical column.

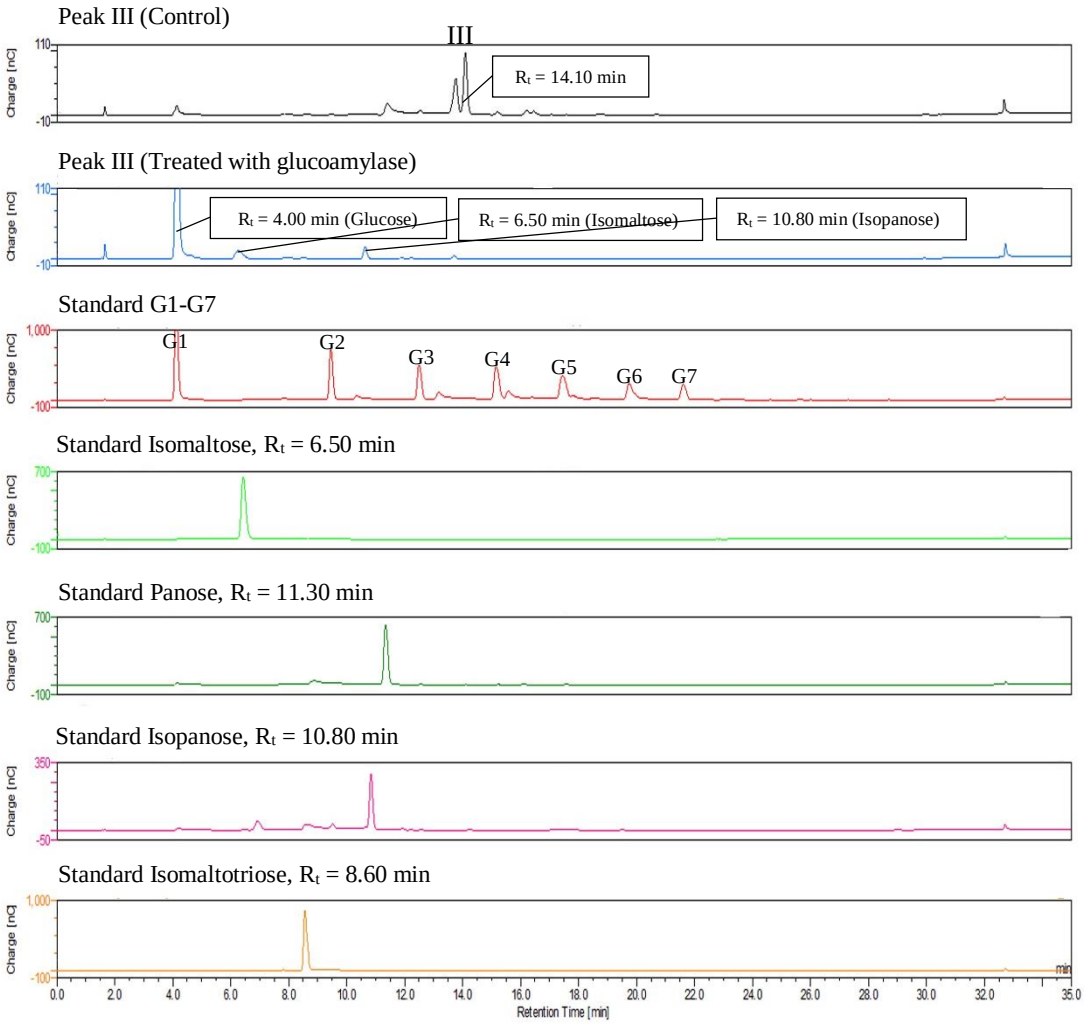

จุฬาลงกรณ์มหาวิทยาลัย
CHULALONGKORN UNIVERSITY

Figure 3. 37 HPAEC-PAD analysis of peak III from CarboPac® PA1 analytical column.

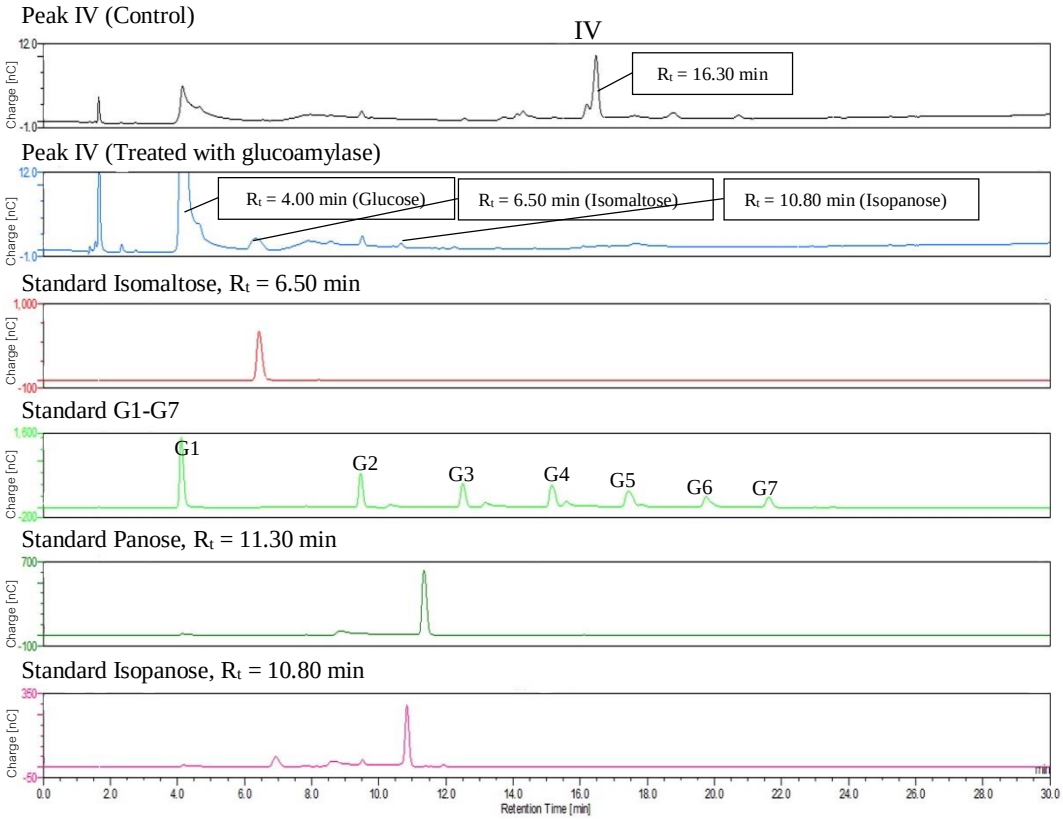

Figure 3. 38 HPAEC-PAD analysis of peak IV from CarboPac® PA1 analytical column.

To elucidate the structure of product III and IV, ^{1}H- NMR and ^{13}C- NMR techniques were sent to Department of Chemistry, Faculty of Science, Chulalongkorn University. It was still unable to determine structure of product III and IV because they had 2 isoforms from 2 peaks as shown on Figure 3.37 and 3.38.

CHAPTER IV

DISCUSSION

Nowaday, α-glucosidases have considerably interested to be applied in both the food and the pharmaceutical industries. Activity of the α- glucosidases are used to produce isomaltooligosaccharides and modify health-relevant sugar conjugates with various types of α-(1,2)-, α-(1,3)-, or α-(1,6) linkages by improve and increase their chemical properties and physiological functions (Ravaud et al., 2007; Yoshinaga et al., 1999). Furthermore, α- glucosidase is used to produce variety of glycoconjugated products such as complex carbohydrates and glycoconjugated vitamins and drugs which provide benefits to human health (Fernández et al., 2007; Hung et al., 2005). Currently research studies on mechanism, structural and the activity of α-glucosidases in order to have a deep knowledge about this enzyme.

The result from sequence analysis confirmed that this gene was α-glucosidase from *W. confusa* (*Wc*AG) (E.C. 3.2.1.20). Percent identity of this gene was described as follows: α-glucosidase from *W. confusa* (GenBank code, WP_056973603.1), 97.0%; neopullulanase from *Streptococcus pneumonia* (GenBank code, COI29563. 1), 96.0%; neopullulanase from *W. confusa* (GenBank code, SJX69567. 1), 96.0% and α-glucosidase from *Lactobacillus panis* (GenBank code, WP_047767241.1), 62.0%. The resulted from multiple sequence alignment showed that *Wc*AG had high sequence identity as compared to AG from *Bacillus* sp. AHU 2001 (BspAG31A) (Saburi et al., 2015) and AG from *Aspergillus nidulans* (AgdB) (Kato et al., 2002).

Sequence structural analysis revealed that *Wc*AG consisted of two domains including alpha amylase at N-terminal ig-like domain on amino acid residue 2-128 and alpha amylase catalytic domain on anino acid residue 142-518 as shown in Figure 3.3.

Previous research reported that alpha amylase catalytic domain was found in cyclomaltodextrinases (CDase; EC3.2.1.54), neopullulanase (NPase; EC 3.2.1.135) and maltogenic amylase (MA; EC 3.2.1.133). This domain function is to hydrolyze alpha-1,4 glycosidic linkage. However, *Wc*AG hydrolyzes only maltotriose, maltotetraose, maltopentaose and maltohexaose by cleavage of α-1,4 glycosidic bonds whereas it lacks activity on oligosaccharide more than 6 units and other oligosaccharides such as pullulan, dextrin, amylopectin, pNPG, isomaltotriose, isomaltose, raffinose, cellobiose, melibiose and palatinose as shown in Table 3.2. Furthermore, *Wc*AG also catalyzes transglycosylation of maltose to synthesize maltooligosaccharide products as shown in Figure 3.29-3.32. Therefore, this enzyme is indistinguishable from another AG.

*Wc*AG is classified as alpha amylase family. The alpha amylase family contains the largest family of glycoside hydrolases (GH), with the majority of enzymes acting on starch, glycogen, and related oligo- or polysaccharides. These enzymes catalyze the transformation of α-1,4 and α-1,6 glycosidic linkages with retention of anomeric center. According to published 3D structure of AG, crystal structure of AG mutant E271Q in complex with maltose (Protein Data Bank (PDB) entry code 3WY4) suggested that AG had 3 domains including A, B and C (Shen et al., 2015). A was beta/alpha 8-barrel. B was a loop between beta 3 strands and alpha 3 helix of A and C was C-terminal extension characterized by a Greek key as indicated in Figure 4.1 (Yang et al., 2012). The essential structure of enzyme was an active site cleft between domains A and B where a triad of catalytic residues including Asp, Glu and Asp, located as shown in Figure 4.2 (Buisson et al., 1987).

จุฬาลงกรณ์มหาวิทยาลัย
CHULALONGKORN UNIVERSITY

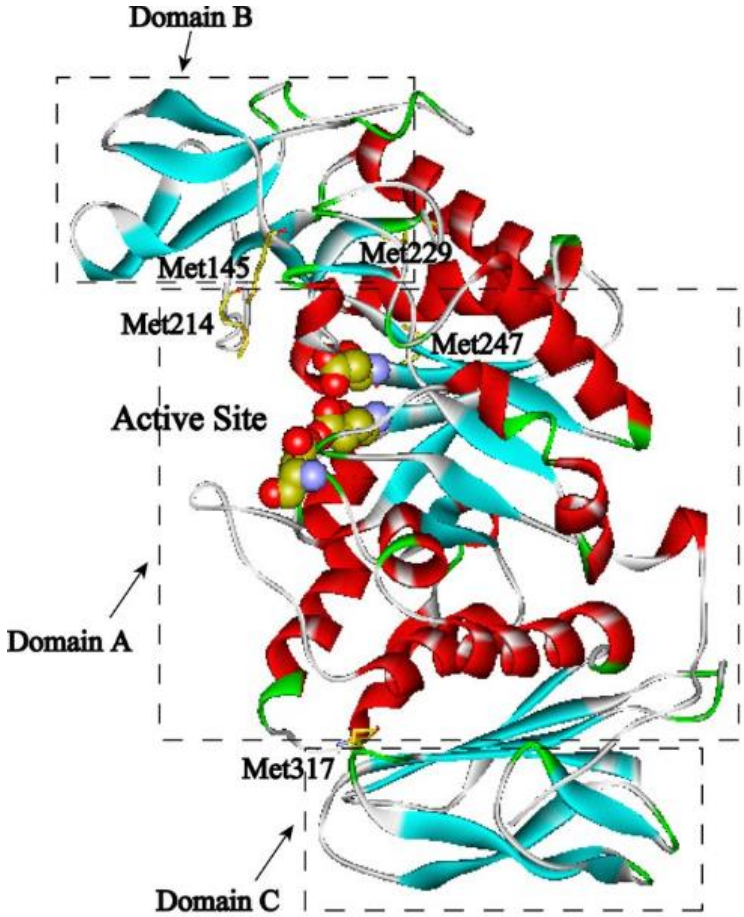

Figure 4. 1 Structural modeling of alpha amylase. The α-helices and β-sheets are presented in red and cyan, respectively. The oxygen atoms are in red, the nitrogen atoms are in light blue, the carbon atoms are in yellow-green, and the sulfur atoms are in yellow (Figure from Yang et al., 2012).

จุฬาลงกรณ์มหาวิทยาลัย
CHULALONGKORN UNIVERSITY

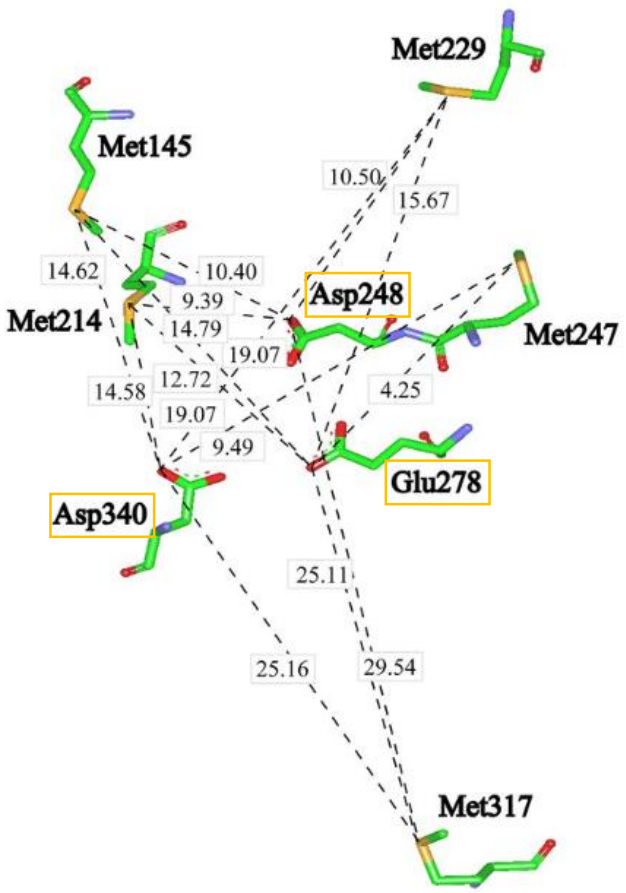

Figure 4. 2 Structural modeling of alpha amylase. The catalytic residues Asp 248, Glu 278, and Asp 340 are shown in a "CPK" (Corey-Pauling-Koltun) representation. ---- indicated distances from the respective catalytic residues to Met 145, Met 214, Met 229, Met 247, and Met 317. The oxygen atoms are in red for Met and dark purple for catalytic residues, the nitrogen atoms are in purple for Met and dark purple for catalytic residues, the carbon atoms are in green, and the sulfur atoms are in yellow. (Figure from Yang et al., 2012).

Phylogenetic analysis of AGs revealed that *Wc*AG was closely related to AGs from *Danaus plexippus* and *Anopheles darlingi*, clustered in insect type while it was phylogenetically distant from those AGs from *Haliotis discus*, *Homo sapien*, classified as mammalian and plant type. The phylogenic location of *Wc*AG as shown in Figure

3.5, being independent from those of other AGs, indicated that *Wc*AG was a novel AG that appeared to have diverged from the other AGs at an early stage of bacterial evolution (Jeon et al., 2015).

In this research, *E. coli* BL21(DE3) which contained recombinant pET28*Wc*AG gene was cultivated in LB medium containing 30 µg/ml of kanamycin at 1 mM IPTG both at 30 and 37 °C with 250 rpm shaking. Initially, *Wc*AG was expressed as inclusion body in higher amount than in soluble protein. To achieve an expression as soluble protein, reduction of temperature, concentration of IPTG and speed of shaking incubator were done. The results showed that there was little expression of *Wc*AG in soluble form as shown in Figure 3.8 (A)-(C). Thus, the experiment was further improved by adding 1% (w/v) of glucose. Generally, glucose affects the amount of cyclic adenosine monophosphate (cAMP). When the cell has high concentration of glucose, the cAMP concentration is low. On the other hand, when glucose concentration decreases, the concentration of cAMP increases proportionally. The high concentration of cAMP is required for stimulating *lac* operon. CAP forms complex with cAMP to form CAP-cAMP complex. The complex binds to CAP site of the operon and help RNA polymerase initiate gene transcription. Meanwhile, glucose inhibits formation of the CAP-cAMP complex which leads to decrease in the expression of gene as shown in Figure 4.3. Therefore, the presence of glucose in the cell can control the expression level of gene (Paigen and Williams, 1969). The result showed that addition of 1% (w/v) glucose successfully increased the expression of soluble *Wc*AG. Finally, the optimum expression of soluble *Wc*AG was successfully increased under the condition of 0.4 mM IPTG at 20 ˚C for 20 h with 1% (w/v) glucose adding.

จุฬาลงกรณ์มหาวิทยาลัย
CHULALONGKORN UNIVERSITY

Inserted into pET28b, *WcAG* was expressed as his-tagged proteins at the C-terminus. In this research, Ni Sepharose^{TM} 6 Fast Flow column or His-Trap column, an affinity column that has specificity towards histidine tag (His-tag) protein, was used to purify *Wc*AG. Bound *Wc*AG can be eluted with high concentration of imidazole. Recombinant *Wc*AG was successfully purified using Ni-NTA affinity column chromatography in one-step process as shown in Figure 3.16 (A). *Wc*AG was purified by stepwise purification at 100 mM imidazole in 50 mM phosphate buffer pH 7.4. Purified *Wc*AG displayed a single band on SDS-PAGE of 62 kDa. In addition, Western blot analysis showed a single band of *Wc*AG which also confirm that this protein band was *Wc*AG as shown in Figure 3.17 (B), Lane 2. However, *Wc*AG disappeared in Figure 3.17 (B) , Lane 1. This result can be occurred from the amount of *Wc*AG expression was one-third of total protein as shown in Figure 3.17 (A) Lane 1 and 2. So, others protein in crude fraction interfere the interraction between *Wc*AG and antibody. Therefore, Western blot analysis can not deteced *Wc*AG band in crude fraction as showed in Figure 3.17 (B) , Lane 1. Another reason is this experiment was done only one time so this negative result might be occur from experiment error such as *Wc*AG spread out of well in loading step.

จุฬาลงกรณ์มหาวิทยาลัย
CHULALONGKORN UNIVERSITY

From purification table (Table 3.1), the purified protein showed specific activity (hydrolysis) of 45.29 U/mg. The purification fold of *Wc*AG was 2.93 with 21.65% yield. Comparing of *Wc*AG among mesophilic bacterium including *Aspergillus nidulans* (AgdB) (Kato et al., 2002) and *Pyrobaculum aerophilum* Strain IM2 (PAE1968) AGs (Jeon et al., 2015). AgdB were purified by DEAE-Toyopearl 650 M column, Phenyl Sepharose CL-4B column and RESOURCE Q column, respectively. This enzyme was purified 52-fold with a specific activity of 9.6 U/mg and the overall

yield was 22% using pNPG as a substrate. Whlie PAE1968 was purified using Ni-NTA affinity chromatography which increase 496.2 fold with specific activity of 2.25 U/mg and the overall yield were 11.4% using maltose as a substrate.

To study hydrolysis activity, the hydrolysis pattern was investigated using maltotriose as substrate as described in section 2.9.1. It was found that *Wc*AG cleaved α-1,4 glucosidic linkage of maltotriose, releasing glucose and maltose as by product. In case of transglycosylation activity, *Wc*AG can transfer maltose to acceptor, producing maltooligasaccharide products as shown in Figure 3.31 (B), Lane 8. The results suggested that *Wc*AG had an ability to elongate maltooligosacchareide with α-1,6 glycosidic linkage. *Wc*AG had similar transglycosylation activity with AG from *Bacillus stearothermophilus* (Malá et al., 1999), *Bacillus* sp. AHU 2001 (Saburi et al., 2015), *Acremonium implicatum* (Yamamoto et al., 2004), *Aspergillus nidulans* (Kato et al., 2002) and *Pyrobaculum aerophilum* IM2 (Jeon et al., 2015).

The reaction of *Wc*AG may occur in two-way reaction. First, direct reaction is to transfer of glucose or maltose to acceptor to form maltooligosaccharide products. In another way, when transglycosylation reaction proceed at equilibrium state, it has a couple reaction of hydrolysis and transglycosylation activity simultaneously or sequentially, depending on many factors such as time, temperature, concentration of enzyme and concentration of substrate. When transglycosylated products present in excess amount, it may act as substrate for further hydrolysis reaction as shown in Figure 4.3. This is similar to transglycosylation of previous report on *Bacillus stearothermophilus* AG (Malá et al., 1999).

The substrate specificity of *Wc*AG was analyzed using different substrates as described in 3.4.9. The result showed that *Wc*AG can hydrolyze maltooligosaccharides,

จุฬาลงกรณ์มหาวิทยาลัย
CHULALONGKORN UNIVERSITY

di- and oligosaccharides, such as maltose (G2), maltotriose (G3), maltotretraose (G4), maltopentaose (G5) and maltohexaose (G6). *Wc*AG showed lower affinity towards maltose, longer-chain substrates (G5-G7) and substrates with α-1,6 glucosidic linkage (isomaltose). Therefore, *Wc*AG hydrolyzed specific type of substrate that contained α-1,4-glucosidic linkages with appropriate chain length. Thus, G3 was the most suitable substrate for on hydrolysis activity. G3 was the best substrate for *Wc*AG which was similar to novel AG from *Aspergillus nidulans* (Kato et al., 2002). No hydrolysis activity was detected with pullulan substrate as shown in Table 3.2. The order of preferable substrate of *Wc*AG was G3 > G4 > G5 > G6 > G7 ~ G2 as shown in Table 3.2. However, AGs from other organism like *Pyrobaculum aerophilum* Strain IM2 (PAE1968) had a difference pattern of G2> G3 ~ pNPG > G4 > G5 > IsoG2 > G7 > G6 (Jeon et al., 2015). The result from TLC analysis also confirmed this result as indicated from the amount of product. For transglycosylation activity, the most preferable substrates was G2. Under optimum condition, transglycosylated products might contain higher amount of maltooligosaccharide with 3-4 glucose units and little amount of maltooligosaccharide 5 glucose units as compared to standard sugar (Figure 3.34). In addition, using G2 was promising alternative substrate for producing transglycosylated products. G2 is an inexpensive substrate which can produce high value products such as isomaltose and panose as shown in Figure 3.35 and 3.36.

The optimum temperature of *Wc*AG was at 50 ºC for hydrolysis reaction as shown in Figure 3.18. The activity decreased about 80 % at 45 ºC. Properties parameters for hydrolysis activity of α-glucosidase from various strains was compared in Table 4.1. The optimum temperature of *Wc*AG was similar to *Acremonium implicatum* (Yamamoto et al., 2004). However, it was distinct from other AGs such as *Aspergillus*

nidulans (AgdB) (Kato et al., 2002), *Bacillus licheniformis* TH4-2 (Nimpiboon et al., 2011) and *Bacillus* sp. AHU 2001 (Saburi et al., 2015) which report optimum temperature were at 45 ºC as shown in Table 4.1. Interestingly, *Wc* BBK-1 is mesophilic bacteria which has optimum growth temperature at 20 to 45 ºC but optimum temperature for catalyzing activity is at 50 ºC. This indicated that *Wc*AG required higher temperature to maximize its activity. *Wc*AG maintained 80% activity in range of 4 to 40 ºC. When temperature increased from 45 °C to 80 °C, its activity decreased and finally lost all activity as shown in Figure 3.19. In general, proteins are denatured when the temperature is increased. Thus, high temperature affects bonds between amino acid residues of the enzyme resulting in changing its structure. In contrast, at low temperature, enzyme works slowly because substrate molecules have lower energy to move into the active site (Tombs, 1985).

The optimum pH for hydrolysis activity of *Wc*AG was pH 6.0 of phosphate buffer. The optimum pH of *Wc*AG was similar to previous report from *Pyrobaculum aerophilum* strain IM2 (Jeon et al., 2015) and *Bacillus licheniformis* TH4-2 (Nimpiboon et al., 2011). Furthermore, *Wc*AG was stable and maintained its activity (90 to 100 % relative activity) in range of pH 6.0 to 8.0 in phosphate buffer.

จุฬาลงกรณ์มหาวิทยาลัย
CHULALONGKORN UNIVERSITY

Table 4. 1 Properties parameters for hydrolysis activity of α-glucosidase from various strains.

Strains	Optimum temperature (ºC)	Optimum pH	Molecular weight (kDa)	Specific substrate
Weissella confusa BBK-1 (*Wc*AG)	50.0	6.0	124.0 (Dimer)	Maltotriose
Acremonium implicatum (Yamamoto et al., 2004)	50.0	7.0	103.0 (Momomer)	Maltotriose
Aspergillus nidulans (Kato et al., 2002)	45.0	5.5	130.0 (Dimer)	Maltose
Bacillus licheniformis TH4-2 (Nimpiboon et al., 2011)	45.0	6.0	64.0 (Momomer)	pNPG
Bacillus sp. AHU 2001 (Saburi et al., 2015)	45.0	6.8	91.3 (Momomer)	Maltotriose
Geobacillus sp. strain HTA-462 (Hung et al., 2005)	60.0	9.0	130.0 (Dimer)	pNPG
Pyrobaculum aerophilum strain IM2 (Jeon et al., 2015)	90.0	6.0	76.0 (Momomer)	pNPG

จุฬาลงกรณ์มหาวิทยาลัย
Chulalongkorn University

To study the effect of metal ions and chemical reagents on activity of *Wc*AG, the reaction was performed as described in section 2.9.7. Previous research reported that metal ions and chemical reagents had important functions in biological properties of enzymes. Some of them have ability to increase or decrease the activity of enzymes (Riordan, 1977). Figure 3.22 showed that metal ions were not necessary for *Wc*AG activity. The enzyme was not inhibited by EDTA that it was usually reduced metaloenzyme activity. The enzyme could be almost inhibited by Zn^{2+}, Cu^{2+}, Ni^{2+}, and partially inhibited (20~60% of activity) by Fe^{3+}, Mn^{2+}, Fe^{2+}, Co^{2+}. The results also revealed that, Ca^{2+}, Mg^{2+}, K^{+} and Na^{+} had slightly positive effect on *Wc*AG activity. Positive effect of K^{+} and Na^{+} for *Wc*AG activity was not significantly different. Zn^{2+}, $Cu^{2+}$and Ni^{2+} had negative effect on *Wc*AG activity resulting in activity of 5-15% of the control. EDTA did not affect the acticity of *Wc*AG. Besides, Co^{2+}, Mn^{2+} and Fe^{2+} decreased *Wc*AG activity to 40% relative activity while Fe^{3+} displayed 80% relative activity. Negative effect of Mn^{2+} and Fe^{2+} for *Wc*AG activity was not significantly different as shown in Figure 3.22. Similar to the activity of α-glucosidase from *Geobacillus* sp. strain HTA-462 was enhanced by 10 mM $MgCl_2$ and $CaCl_2$ by 144 and 139%, respectively. Heavy metal ions including Zn^{2+}, Cu^{2+} and Ni^{2+} generally inhibited the activity of most enzymes. In this case, *Wc*AG contains 25 methionine residues and dose not has cysteine. Interaction between heavy metal ion and sulfer atom of methionine affects on folding step which form disulfide bond in tertiary structure (Hung et al., 2005). When structure of active site was changed, *Wc*AG will lose catalytic activity.

Molecular weight of *Wc*AG was determined by gel filtration chromatography and SDS-PAGE analysis. Gel filtration chromatography, or called molecular exclusion,

is a separation technique based on the size of molecules. In gel filtration, the stationary phase consists of porous beads with well-defined range of pore sizes. Proteins that are small enough can fit inside all the pores in the beads. These small proteins have access to the mobile phase inside the beads as well as the mobile phase between beads. Proteins that are too large to fit inside any of the pores are excluded. They have access only to the mobile phase between the beads. During the separation, proteins with larger size are therefore eluted first before those small proteins are then eluted.

As previously mentioned, the molecular weight of *Wc*AG was 62 kDa on SDS-PAGE. For gel filtration, the molecular mass of *Wc*AG was estimated to be 124 kDa as shown in Figure 3.23 (A) and (B). It suggested that *Wc*AG existed in native form as a dimer. In comparison to previous report, the molecular mass of AGs from *Aspergillus nidulans* (Kato et al., 2002), *Geobacillus* sp. strain HTA-462 (Hung et al., 2005) and *Saccharomyces cerevisiae* (Dušan et al., 2014) were similar to *Wc*AG and also existed in native form as homodimer as shown in Table 4.1.

All kinetic parameters of *Wc*AG were investigated on hydrolysis activity using maltose (G2) and maltotriose (G3) as substrates. K_m or Michaelis-Menten constant represents the concentration of the substrate when the reaction velocity is equal to one half of the maximum velocity whlie V_{max} is the maximum rate of the reaction. Lowering in K_m value indicates more binding affinity to specific substrate whereas higher K_m indicates the enzyme does not bind efficiently with that substrate. Besides, k_{cat} value describes the turnover rate of changing enzyme-substrate complex into product and enzyme. This can be called the rate of catalyst with a particular substrate. k_{cat}/K_m is the catalytic efficiency of the enzyme.

จุฬาลงกรณ์มหาวิทยาลัย
CHULALONGKORN UNIVERSITY

α-Glucisidase (AG) are classified into three types (I, II and III) according to substrate specificity. Type I AG prefer to hydrolyzes heteroside linkage such as aryl-glucosides and sucrose, more efficiently than holoside linkage. Type II AG shows high activity on G2 and isomaltose and low activity towards aryl-glucosides. Type III AG can hydrolyzes substrates as type II AG does but its activity extends to polysaccharides such as amylose and starch (Nimpiboon et al., 2011; Yamamoto et al., 2004). From kinetic analysis showed that the K_m values of G2 and G3 were 16.22 and 2.67 mM. This indicated that G3 was better substrate for *Wc*AG. Besides, the k_{cat}/K_m ratio towards G3 was higher than G2 estimated 115 time, indicating that *Wc*AG might be Type-II AG because it prefer to hydrolyze G3 and G4 which are a short chain homogeneous substrate. Moreover, *Wc*AG can not hydrolyze long chain substrate such as amylopectin.

Kinetic parameters of hydrolysis activity from various strains using maltose as substrate was showed in Table 4.2. This suggested that *Wc*AG had lowest affinity towards G2 among other reported AGs. k_{cat} and k_{cat}/K_m of *Wc*AG showed the lowest value when compared with AGs from other strains. Comparison of kinetic parameters of α–glucosidase from several strains was presented in Table 4.2 (for maltose) and 4.3 (for maltotriose), respectively. K_m of *Wc*AG using G2 as a substrate (16.22 mM) was higher than AGs from *Aspergillus nidulans* (0.51 mM) (Kato et al., 2002), *Ferroplasma acidiphilum* strain Y (0.64 mM) (Ferrer et al., 2005), *Geobacillus* sp. strain HTA-46 (7.58 mM) (Hung et al., 2005), *Pyrobaculum aerophilum* strain IM2 (1.00 mM) (Jeon et al., 2015), *Acremonium implicatum* (0.28 mM) (Yamamoto et al., 2004) and *Bacillus* sp. AHU 2001 (0.75) (Saburi et al., 2015). So, *Wc*AG had lowest affinity towards G2 among other reported AGs. Moreover, k_{cat} and k_{cat}/K_m of *Wc*AG showed the lowest

จุฬาลงกรณ์มหาวิทยาลัย
CHULALONGKORN UNIVERSITY

value when compared with AGs from other strains. For G3 substrate, K_m of *Wc*AG (2.67 mM) was lower than AG from *Geobacillus* sp. strain HTA-46 (12.73) (Hung et al., 2005). So, *Wc*AG had higher affinity towards G3 than *Geobacillus* sp. strain HTA-46 AG. However, K_m of *Wc*AG was higher than AGs from *Aspergillus nidulans* (0.26 mM) (Kato et al., 2002), *Ferroplasma acidiphilum* strain Y (0.69 mM) (Ferrer et al., 2005), *Pyrobaculum aerophilum* strain IM2 (1.00 mM) (Jeon et al., 2015), *Acremonium implicatum* (0.01 mM) (Yamamoto et al., 2004) and *Bacillus* sp. AHU 2001 (0.46) (Saburi et al., 2015). Moreover, k_{cat}/K_m of *Wc*AG showed the lowest value when compared with AGs from other strains. To summarize, G3 was the best substrate for hydrolysis activity of *Wc*AG while G2 was the most favorable substrate for type II AG. This made *Wc*AG distinct from other type II AGs.

จุฬาลงกรณ์มหาวิทยาลัย
CHULALONGKORN UNIVERSITY

Table 4. 2 Kinetic parameters of hydrolysis activity from various strains using maltose as substrate.

Strains	K_m (mM)	k_{cat} (s^{-1})	k_{cat}/K_m ($s \cdot mM^{-1}$)
Weissella confusa BBK-1 (*Wc*AG)	16.22	0.738	0.046
Aspergillus nidulans (Kato et al., 2002)	0.51	21.00	41.00
Ferroplasma acidiphilum strain Y (Ferrer et al., 2005)	0.64	126.00	197.00
Geobacillus sp. strain HTA-46 (Hung et al., 2005)	7.58	283.30	37.40
Pyrobaculum aerophilum strain IM2 (Jeon et al., 2015)	1.00	16.00	15.40
Acremonium implicatum (Yamamoto et al., 2004)	0.28	80.00	286.00
Bacillus sp. AHU 2001 (Saburi et al., 2015)	0.75	53.80	71.90

จุฬาลงกรณ์มหาวิทยาลัย
CHULALONGKORN UNIVERSITY

Table 4. 3 Kinetic parameters of hydrolysis activity from various strains using maltotriose as substrate.

Strains	K_m (mM)	k_{cat} (s^{-1})	k_{cat}/K_m ($s \cdot mM^{-1}$)
Weissella confusa BBK-1 (*Wc*AG)	2.67	14.096	5.279
Aspergillus nidulans (Kato et al., 2002)	0.26	30.00	120.00
Ferroplasma acidiphilum strain Y (Ferrer et al., 2005)	0.69	13.00	18.80
Geobacillus sp. strain HTA-46 (Hung et al., 2005)	12.73	2500.00	196.40
Pyrobaculum aerophilum strain IM2 (Jeon et al., 2015)	1.00	14.40	13.70
Acremonium implicatum (Yamamoto et al., 2004)	0.01	33.00	2540.00
Bacillus sp. AHU 2001 (Saburi et al., 2015)	0.46	50.70	111.00

จุฬาลงกรณ์มหาวิทยาลัย
CHULALONGKORN UNIVERSITY

Transglycosylation activity of various AGs has been apply in biotechnology to synthesize conjugated compounds with biologically active materials and produce foodstuffs, oligosaccharides and drugs as well. Therefore, optimization for higher amount of transglycosylated products was important to use in industrial or medical applications (Hung et al., 2005; Yamamoto et al., 2004). In order to produce the highest amount of maltooligasaccharide products, the conditions for production were optimized and analyzed by Thin-layer chromatography (TLC).

The optimum temperature for transglycosylation activity of *Wc*AG was at 37 ºC which it was different from hydrolysis activity (50 ºC). Half-life of hydrolysis activity of *Wc*AG was 15 min at 50 ºC while incubation time for transglycosylation activity was 24 h which was longer than incubation time for hydrolysis activity as shown in Figure 3.24. At higher temperature, *Wc*AG lost its activity and the products might be further hydrolysed. This resulted in lower amount of products. The optimum temperature of transglycosylation activity was varied among different sources; for example, AGs from *Bacillus licheniformis* TH4-2, *Acremonium implicatum* (Yamamoto et al., 2004) displayed optimum temperature at 45 ºC (Nimpiboon et al., 2011) and *Geobacillus* sp. strain HTA-46 optimum temperature at 50 ºC (Hung et al., 2005).

The optimum enzyme concentration for transglycosylation activity was 0.4 U/ml as shown in Figure 3.30. Increase of enzyme concentration was related to the reaction rate. The amount of product was directly proportional to the level of enzyme concentration. However, the concentration higher than 0.4 U/ml did not increase the amount of products when compare with lower concentration at 0.2-0.4 U/ml of *Wc*AC as shown in Figure 3.30.

จุฬาลงกรณ์มหาวิทยาลัย
CHULALONGKORN UNIVERSITY

The optimum substrate concentration was 200 mM G2. Previous research reported that transglycosylation reaction of AGs from *B. stearothermophilus* (15%w/w) (Malá et al., 1999), *Acremonium implicatum* (200g/L) (Yamamoto et al., 2004), *Geobacillus* sp. strain HTA-462 (30 mM) (Hung et al., 2005), *Thermoplasma acidophilum* (20 mM) (Park et al., 2014), *Xantophyllomyces dendrorhous* (200g/L) (Fernández et al., 2007), *Thermus thermophilus* TC11 (300 mM) (Zhou et al., 2015) also used G2 as substrate but concentration was varied among strains.

Finally, the optimum incubation time of *Wc*AG was at 24 h, which was similar to AGs from *Bacillus licheniformis* TH4-2 (Ammar et al., 2002) but different from *Thermus thermophilus* TC11 (Zhou et al., 2015) (3 h). It can be concluded that the optimum condition was using 200 mM of G2 with 0.4 unit/ml *Wc*AG at 37 ºC for 24 h.

In order to obtain higher amount of maltooligosaccharide products, 50 ml of reaction mixture was prepared. The maltooligasaccharide products were isolated from the mixture using Bio-gel P2 column. Bio-Gel P2 gels are extremely hydrophilic and provide efficiently purification of various compounds (Ammar et al., 2002). Products with different size and polarity can be separated. Fractions which eluted with DI water, were detected for maltooligasaccharide products by TLC analysis. Fraction carrying the products were then analysed by HPAEC. The result of TLC analysis showed four major interesting products - peak I, II, III and IV which sizes were in range of G2 to G5.

Purified products obtained by Bio-gel P2 column were analyzed by HPAEC-PAD. Peak I and II were identified as isomaltose and panose, respectively while peak III and IV could not be identified with standard sugar as shown in Figure 3.35 – 3.38. As mentioned, *Wc*AG used G2 as donor and acceptor for transglycosylation activity (Figure 3.34). This indicated that *Wc*AG can transfer glucose or maltose unit to form α-1,6-glucosidic bonds to G2 acceptor, resulting in formation of isomaltose and panose. The structure of possible transglycosylated products were shown in Figure 4.3. The patterns for synthesis of each transglycosylation product were described as follows. Hydrolysis and transglycosylation activity occur simultaneously; therefore, free glucose, by-product of hydrolysis activity, is also in the reaction along with G2 substrate. For isomaltose, it is initially produced by transferring free glucose to C6-OH of another glucose by forming α-1,6-glucosidic linkage. Next, panose is produced by

จุฬาลงกรณ์มหาวิทยาลัย
CHULALONGKORN UNIVERSITY

transferring glucose moiety to C6-OH of G2, forming α-1,6-glucosidic linkage. The α-1,6-transglycosylation occurs further on G2 and panose to generate tetrasaccharides, which can then be the acceptor for producing pentasaccharides. In order to identify peak III, glucoamylase from *Rhizopus sp*. (Wako Pure Chemical Industries, Ltd. Japan) was used to specifically hydrolyze α-1,4-glycosidic bond to compare released structures between hydrolyzed and non-hydrolyzed products. This result help identify possible glycosidic linkage of peak III. If product contains α-1,4-glycosidic bond, it will be hydrolyzed after treated with glucoamylase. The result from HPAEC-PAD can imply that peak III contained α-1,4-glicosidic linkage because the profile show peaks of glucose, isomaltose and isopanose at R_t of 4.00, 6.50 and 10.80 min, respectively as shown in Figure 3.37. From this result can be indicated possible structures of peak III include Glc(α1-6)Glc(α1-4)Glc(α1-4)Glc and Glc(α1-4)Glc(α1-6)Glc(α1-4)Glc. Finally, peak IV (R_t = 16.30 min) was unable to identify with our standard so it was incubated with glucoamylase. The results after treated with glucoamylase revealed that glucose, isomaltose and isopanose were found at R_t of 4.00, 6.50 and 10.80 min, respectively as shown in Figure 3.38. The result revealed that the possible structures of peak IV include Glc(α1-6)Glc(α1-4)Glc(α1-4)Glc(α1-4)Glc, Glc(α1-4)Glc(α1-4)Glc(α1-6)Glc(α1-4)Glc, Glc(α1-4)Glc(α1-6)Glc(α1-4)Glc(α1-4)Glc and Glc(α1-4)Glc(α1-4)Glc(α1-4)Glc(α1-6)Glc. Although the linkages were successfully identified, it was difficult to identify this product from standard sugar. The results indicated that *Wc*AG had two main activities including formation of α-1,4 and α-1,6-glycosidic linkage and hydrolyzing of α-1,4-glucosidic linkage, resulting in various transglycosylated products as described. Transglycosylated products including

จุฬาลงกรณ์มหาวิทยาลัย
CHULALONGKORN UNIVERSITY

isomaltose, panose and other minor transglycosylation of *Wc*AG was similar to products from *Aspergillus nidulans* AG (AgdB) (Kato et al., 2002).

In conclusion, *Wc*AG contained an open reading frame of 1,775 bps which can be deduced into 593 amino acids. It was successfully expressed at 20 °C for 20 h, 150 rpm, in LB medium containing 1% (w/v) glucose with 0.4 mM IPTG and purified by His-Trap column with 21.65% yield. The enzyme had molecular mass of 124 kDa and existed as dimer in native form. The optimum temperature and pH were at 50 °C and pH 6.0 while temperature and pH stability were in range of 4 to 40 °C, and pH 6.0-8.0 in phosphate buffer, respectively. Substrate specificity for hydrolysis activity of *Wc*AG was G3 while G2 was for transglycosylation activity. The order of preferable substrate was G3>> G4>G5~G6>G2. Four products were obtained from transglycosylation activity was obtained from incubating 200 mM of G2 with 0.4 unit/ml of *Wc*AG at 37 ºC for 24 h. The structural identification of all products using HPAEC-PAD revealed that peak I was isomaltose, peak II was panose while peak III and IV still cannot be identified.

จุฬาลงกรณ์มหาวิทยาลัย
CHULALONGKORN UNIVERSITY

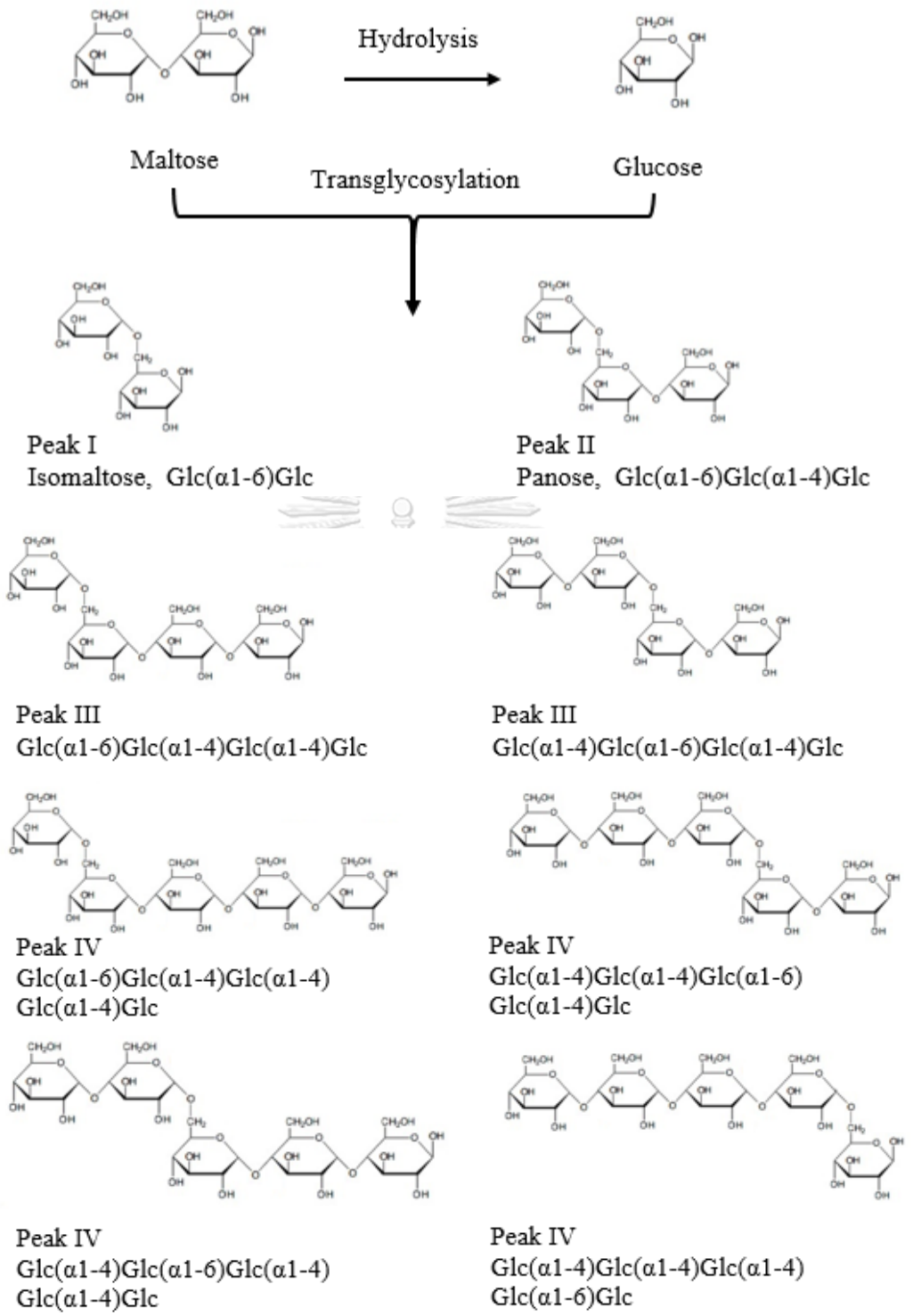

Figure 4. 3 Possible transglycosylated products of *Wc*AG using maltose as substrate

CHAPTER V

CONCLUSIONS

1. Alpha-glucosidase (*Wc*AG) from *Weissella confusa* BBK-1 in modified pET28b vector contained an open reading frame of 1,775 bps which can be deduced into 593 amino acids.
2. Optimum expression condition of *Wc*AG was to culture at 20 °C for 20 h, 150 rpm, in LB medium containing 1% (w/v) glucose with 0.4 mM IPTG.
3. *Wc*AG was successfully purified 2.93 fold by His-Trap column with 21.65% yield.
4. The enzyme had molecular mass of 124 kDa and existed as dimer in native form.
5. The optimum temperature and pH were at 50 °C and pH 6.0 while temperature and pH stability were in range of 4-40 °C, and pH 6.0-8.0 in phosphate buffer, respectively.
6. The most suitable substrate for hydrolysis activity of *Wc*AG was G3 while G2 was for transglycosylation activity. For hydrolysis activity, the order of preferable substrate was G3>> G4>G5~G6>G2.
7. The apparent K_m, k_{cat} and k_{cat}/K_m values for G3 substrate were 2.67 mM, 14.096 s^{-1} and 5.279 $(s \cdot mM)^{-1}$, respectively. Comparison with the apparent K_m, k_{cat} and k_{cat}/K_m values for G2 substrate were 16.22 mM, 0.738 s^{-1} and 0.046 $(s \cdot mM)^{-1}$, respectively.
8. The maximum maltooligasacharide product was obtained from incubating 200 mM of G2 with 0.4 unit/ml of *Wc*AG at 37 ºC for 24 h.
9. Four products were obtained from transglycosylation activity including product I, II III nd IV. The structural identification of all products using HPAEC-PAD

revealed that product I was isomaltose, product II was panose while product III and IV still cannot be identified

จุฬาลงกรณ์มหาวิทยาลัย
CHULALONGKORN UNIVERSITY

REFERENCES

Ammar, Y. B., Matsubara, T., Ito, K., Iizuka, M., Limpaseni, T., Pongsawasdi, P., and Minamiura, N. (2002). Characterization of a thermostable levansucrase from *Bacillus* sp. TH4-2 capable of producing high molecular weight levan at high temperature. *Journal of Biotechnology* **99**, 111-119.

Barham, D., and Trinder, P. (1972). Analyst. **72**.

Beyer, T. A., Sadler, J. E., Rearick, J. I., Paulson, J. C., and Hill, R. L. (1981). Glycosyltransferases and their use in assessing oligosaccharide structure and structure-function relationships. *Advances in Enzymology and Related Areas of Molecular Biology* **52**, 23-175.

Björkroth, J., Schillinger, U., Geisen, R., Weiss, N., Hoste, B., Holzapfel, W., Korkeala, H., and Vandamme, P. (2002). Taxonomic study of *Weissella confusa* and description of *Weissella cibaria* sp. novel detected in food and clinical samples. *Systematic and Evolutionary Microbiology* **52**, 141-148.

Bojsen, K., Yu, S., Kragh, K. M., and Marcussen, J. (1999). A group of α-1, 4-glucan lyases and their genes from the red alga *Gracilariopsis lemaneiformis*: purification, cloning, and heterologous expression. *Biochimica et Biophysica Acta (BBA)-Protein Structure and Molecular Enzymology* **1430**, 396-402.

Bradford, M. M. (1976). A rapid and sensitive method for the quantitation of microgram quantities of protein utilizing the principle of protein-dye binding. *Analytical Biochemistry* **72**, 248-254.

Breton, C., Šnajdrová, L., Jeanneau, C., Koča, J., and Imberty, A. (2006). Structures and mechanisms of glycosyltransferases. *Glycobiology* **16**, 29R-37R.

Buisson, G., Duée, E., Haser, R., and Payan, F. (1987). Three dimensional structure of porcine pancreatic alpha-amylase at 2.9 Å resolution. Role of calcium in structure and activity. *The EMBO Journal* **6**, 3909-3916.

Cihan, C., Benli, M., and Cokmus, C. (2012). Purification and characterization of intracellular and extracellular α-glucosidases from *Geobacillus toebii* strain E134. *Cell Biochemistry and Function* **30**, 69-81.

Cockburn, D. W., Vandenende, C., and Clarke, A. J. (2010). Modulating the pH−activity profile of cellulase by substitution: replacing the general base

catalyst aspartate with cysteinesulfinate in cellulase A from *Cellulomonas fimi*. *Biochemistry* **49**, 2042-2050.

Drickamer, K., and Taylor, M. E. (1998). Evolving views of protein glycosylation. *Trends in Biochemical Sciences* **23**, 321-324.

Drzewińska, J., Appelhans, D., Voit, B., Bryszewska, M., and Klajnert, B. (2012). Poly (propylene imine) dendrimers modified with maltose or maltotriose protect phosphorothioate oligodeoxynucleotides against nuclease activity. *Biochemical and Biophysical Research Communications* **427**, 197-201.

Dušan, V., Nenad, M., Dejan, B., Filip, B., Segal, M., Dejan, Š., Jovana, T., and Aleksandra, D. (2014). The specificity of α-glucosidase from *Saccharomyces cerevisiae* differs depending on the type of reaction: hydrolysis versus transglycosylation. *Applied Microbiology and Biotechnology* **98**, 6317-6328.

Fernández, L., Marin, D., De Segura, G., Linde, D., Alcalde, M., Gutiérrez, P., Ghazi, I., Plou, F., Fernández, M., and Ballesteros, A. (2007). Transformation of maltose into prebiotic isomaltooligosaccharides by a novel α-glucosidase from *Xantophyllomyces dendrorhous*. *Process Biochemistry* **42**, 1530-1536.

Ferrer, M., Golyshina, O. V., Plou, F. J., Timmis, K. N., and Golyshin, P. N. (2005). A novel α-glucosidase from the acidophilic archaeon *Ferroplasma acidiphilum* strain Y with high transglycosylation activity and an unusual catalytic nucleophile. *Biochemical Journal* **391**, 269-276.

Fierobe, H.-P., Mirgorodskaya, E., McGuire, K. A., Roepstorff, P., Svensson, B., and Clarke, A. J. (1998). Restoration of catalytic activity beyond wild-type level in glucoamylase from *Aspergillus awamori* by oxidation of the Glu400→ Cys catalytic-base mutant to cysteinesulfinic acid. *Biochemistry* **37**, 3743-3752.

Hers, H. (1963). α-Glucosidase deficiency in generalized glycogen-storage disease (Pompe's disease). *Biochemical Journal* **86**, 11.

Hondoh, H., Kuriki, T., and Matsuura, Y. (2003). Three-dimensional structure and substrate binding of *Bacillus stearothermophilus* neopullulanase. *Journal of molecular biology* **326**, 177-188.

Hondoh, H., Saburi, W., Mori, H., Okuyama, M., Nakada, T., Matsuura, Y., and Kimura, A. (2008). Substrate recognition mechanism of α-1, 6-glucosidic

จุฬาลงกรณ์มหาวิทยาลัย
Chulalongkorn University

linkage hydrolyzing enzyme, dextran glucosidase from *Streptococcus mutans*. *Journal of molecular biology* **378**, 913-922.

Hung, S., Hatada, Y., Goda, S., Lu, J., Hidaka, Y., Li, Z., Akita, M., Ohta, Y., Watanabe, K., and Matsui, H. (2005). α-Glucosidase from a strain of deep-sea *Geobacillus*: a potential enzyme for the biosynthesis of complex carbohydrates. *Applied Microbiology and Biotechnology* **68**, 757-765.

Iijima, H., and Ogawa, T. (1988). Total synthesis of 3-O-[2-acetamido-6-O-(N-acetyl-α-d-neuraminyl)-2-deoxy-α-d-galactosyl]-l-serine and a stereoisomer. *Carbohydrate research* **172**, 183-193.

Jeon, H., Lee, H., Byun, D., Choi, H., and Shim, H. (2015). Molecular cloning, characterization, and application of a novel thermostable α-glucosidase from the hyperthermophilic archaeon *Pyrobaculum aerophilum* strain IM2. *Food Science and Biotechnology* **24**, 175-182.

Jones, J. B., and Francis, C. J. (1984). Enzymes in organic synthesis 32. Stereospecific horse liver alcohol dehydrogenase-catalyzed oxidations of exo- and endo-oxabicyclic meso diols. *Canadian journal of chemistry* **62**, 2578-2582.

Kadziola, A., Abe, J., Svensson, B., and Haser, R. (1994). Crystal and molecular structure of barley α-amylase. *Journal of molecular biology* **239**, 104-121.

Kaewmuangmoon, J., Yoshiyama, M., Kimura, K., Okuyama, M., Mori, H., Kimura, A., and Chanchao, C. (2012). Characterization of some enzymatic properties of recombinant α-glucosidase III from the Thai honeybee, *Apis cerana indica* Fabricus. *African Journal of Biotechnology* **11**, 16220-16232.

Kato, N., Suyama, S., Shirokane, M., Kato, M., Kobayashi, T., and Tsukagoshi, N. (2002). Novel α-glucosidase from *Aspergillus nidulans* with strong transglycosylation activity. *Applied and Environmental Microbiology* **68**, 1250-1256.

Kimura, A., Takewaki, S., Matsui, H., Kubota, M., and Chiba, S. (1990). Allosteric properties, substrate specificity, and subsite affinities of honeybee α-glucosidase I. *The Journal of Biochemistry* **107**, 762-768.

Kobata, A. (2013). Exo- and endoglycosidases revisited. *Proceedings of the Japan Academy. Series B, Physical and Biological Sciences* **89**, 97-117.

จุฬาลงกรณ์มหาวิทยาลัย
Chulalongkorn University

Kobayashi, M., Hondoh, H., Mori, H., Saburi, W., Okuyama, M., and Kimura, A. (2011). Calcium ion-dependent increase in thermostability of dextran glucosidase from *Streptococcus mutans*. *Bioscience, biotechnology, and biochemistry* **75**, 1557-1563.

Koropatkin, N. M., and Smith, T. J. (2010). SusG: a unique cell-membrane-associated α-amylase from a prominent human gut symbiont targets complex starch molecules. *Structure* **18**, 200-215.

Kubo, T., Sasaki, M., Nakamura, J., Sasagawa, H., Ohashi, K., Takeuchi, H., and Natori, S. (1996). Change in the expression of hypopharyngeal-gland proteins of the worker honeybees (*Apis mellifera* L.) with age and/or role. *The Journal of Biochemistry* **119**, 291-295.

Kubota, M., Tsuji, M., Nishimoto, M., Wongchawalit, J., Okuyama, M., Mori, H., Matsui, H., Surarit, R., Svasti, J., and Kimura, A. (2004). Localization of α-glucosidases I, II, and III in organs of European honeybees, *Apis mellifera* L., and the origin of α-glucosidase in honey. *Bioscience, biotechnology, and biochemistry* **68**, 2346-2352.

Kurosu, J., Sato, T., Yoshida, K., Tsugane, T., Shimura, S., Kirimura, K., Kino, K., and Usami, S. (2002). Enzymatic synthesis of α-arbutin by α-anomer-selective glucosylation of hydroquinone using lyophilized cells of *Xanthomonas campestris* WU-9701. *Journal of bioscience and bioengineering* **93**, 328-330.

Lawson, C. L., van Montfort, R., Strokopytov, B., Rozeboom, H. J., Kalk, K. H., de Vries, G. E., Penninga, D., Dijkhuizen, L., and Dijkstra, B. W. (1994). Nucleotide sequence and X-ray structure of cyclodextrin glycosyltransferase from *Bacillus circulans* strain 251 in a maltose-dependent crystal form. *Journal of molecular biology* **236**, 590-600.

Lee, J., Heo, G., Lee, J., Oh, Y., Park, J., Park, Y., Pyun, Y., and Ahn, J. (2005). Analysis of kimchi microflora using denaturing gradient gel electrophoresis. *Food Microbiology* **102**, 143-150.

Li, W., Xue, Y., Li, J., Yuan, J., Wang, X., Fang, W., Fang, Z., and Xiao, Y. (2016). A cold-adapted and glucose-stimulated type II α-glucosidase from a deep-sea bacterium *Pseudoalteromonas* sp. K8. *Biotechnology Letters* **38**, 345-349.

จุฬาลงกรณ์มหาวิทยาลัย
Chulalongkorn University

Lombard, V., Golaconda Ramulu, H., Drula, E., Coutinho, P. M., and Henrissat, B. (2013). The carbohydrate-active enzymes database (CAZy) in 2013. *Nucleic acids research* **42**, D490-D495.

MacGregor, E. A., Janeček, Š., and Svensson, B. (2001). Relationship of sequence and structure to specificity in the α-amylase family of enzymes. *Biochimica et Biophysica Acta (BBA)-Protein Structure and Molecular Enzymology* **1546**, 1-20.

Machius, M., Declerck, N., Huber, R., and Wiegand, G. (1998). Activation of *Bacillus licheniformis* α-amylase through a disorder→ order transition of the substrate-binding site mediated by a calcium–sodium–calcium metal triad. *Structure* **6**, 281-292.

Malá, Š., Dvořáková, H., Hrabal, R., and Králová, B. (1999). Towards regioselective synthesis of oligosaccharides by use of α-glucosidases with different substrate specificity. *Carbohydrate Research* **322**, 209-218.

Malik, A., Radji, M., Kralj, S., and Dijkhuizen, L. (2009). Screening of lactic acid bacteria from Indonesia reveals glucansucrase and fructansucrase genes in two different *Weissella confusa* strains from soya. *FEMS Microbiology Letters* **300**, 131-138.

Martín, R., Heilig, H., Zoetendal, E., Jiménez, E., Fernández, L., Smidt, H., and Rodríguez, J. (2007). Cultivation-independent assessment of the bacterial diversity of breast milk among healthy women. *Research in Microbiology* **158**, 31-37.

Matsuura, Y., Kusunoki, M., Haurda, W., and Kakudo, M. (1984). Structure and possible catalytic residues of Taka-amylase A. *The Journal of Biochemistry* **95**, 697-702.

Mirza, O., Skov, L. K., Remaud Simeon, M., Potocki de Montalk, G., Albenne, C., Monsan, P., and Gajhede, M. (2001). Crystal structures of amylosucrase from *Neisseria polysaccharea* in complex with D-glucose and the active site mutant Glu328Gln in complex with the natural substrate sucrose. *Biochemistry* **40**, 9032-9039.

Møller, M. S., Fredslund, F., Majumder, A., Nakai, H., Poulsen, J. C. N., Leggio, L. L., Svensson, B., and Hachem, M. A. (2012). Enzymology and structure of the

จุฬาลงกรณ์มหาวิทยาลัย
CHULALONGKORN UNIVERSITY

GH13_31 glucan 1, 6-α-glucosidase that confers isomaltooligosaccharide utilization in the probiotic *Lactobacillus acidophilus* NCFM. *Journal of bacteriology* **194**, 4249-4259.

Mori, T., Fukusho, s., Kojima, J., and Okahata, Y. (1999). Enzymatic syntheses of glycolipids catalyzed by a lipid-coated glycoside hydrolase in the organic-aqueous two phase system. *Polymer Journal* **31**, 1105-1108.

Nakagawa, H., Dobashi, Y., Sato, T., Yoshida, K., Tsugane, T., Shimura, S., Kirimura, K., Kino, K., and Usami, S. (2000). α-Anomer-selective glucosylation of menthol with high yield through a crystal accumulation reaction using lyophilized cells of *Xanthomonas campestris* WU-9701. *Journal of bioscience and bioengineering* **89**, 138-144.

Nakai, H., Okuyama, M., Kim, Y.-M., Saburi, W., Wongchawalit, J., Mori, H., Chiba, S., and Kimura, A. (2005). Molecular analysis of α-glucosidase belonging to GH-family 31.

Nam, H., Ha, M., Bae, O., and Lee, Y. (2002). Effect of *Weissella confusa* strain PL9001 on the adherence and growth of *Helicobacter pylori*. *Applied and Environmental Microbiology* **68**, 4642-4645.

Nichols, B. L., Avery, S., Sen, P., Swallow, D. M., Hahn, D., and Sterchi, E. (2003). The maltase-glucoamylase gene: common ancestry to sucrase-isomaltase with complementary starch digestion activities. *Proceedings of the National Academy of Sciences* **100**, 1432-1437.

Nilsson, K. G. (1988). Enzymatic synthesis of oligosaccharides. *Trends in Biotechnology* **6**, 256-264.

Nimpiboon, P., Nakapong, S., Pichyangkura, R., Ito, K., and Pongsawasdi, P. (2011). Synthesis of a novel prebiotic trisaccharide by a type I α-glucosidase from *Bacillus licheniformis* strain TH4-2. *Process Biochemistry* **46**, 448-457.

Nishimoto, M., Kubota, M., Tsuji, M., Mori, H., Kimura, A., Matsui, H., and Chiba, S. (2001). Purification and substrate specificity of honeybee, *Apis mellifera L.*, α-glucosidase III. *Bioscience, Biotechnology and Biochemistry* **65**, 1610-1616.

Ojima, T., Saburi, W., Yamamoto, T., and Kudo, T. (2012). Characterization of *Halomonas* sp. Strain H11 α-Glucosidase activated by monovalent cations and

จุฬาลงกรณ์มหาวิทยาลัย
Chulalongkorn University

its application for efficient synthesis of α-D-Glucosylglycerol. *Applied and environmental microbiology* **78**, 1836-1845.

Okuyama, M., Saburi, W., Mori, H., and Kimura, A. (2016). α-Glucosidases and α-1, 4-glucan lyases: structures, functions, and physiological actions. *Cellular and Molecular Life Sciences*, 1-25.

Paigen, K., and Williams, B. (1969). Catabolite repression and other control mechanisms in carbohydrate utilization. *Advances in microbial physiology* **4**, 251-324.

Park, I., Lee, H., and Cha, J. (2014). Glycoconjugates synthesized via transglycosylation by a thermostable α-glucosidase from *Thermoplasma acidophilum* and its glycosynthase mutant. *Biotechnology Letters* **36**, 789-796.

Paulson, J. C. (1989). Glycoproteins: what are the sugar chains for? *Trends in biochemical sciences* **14**, 272-276.

Pontoh, J. (2001). Isolation, purification and characterization of glucosidases from three honey bee species *Apis mellifera*, *A. cerana* and *A. dorsata*.

Quezada, R., Sim, L., Ao, Z., Hamaker, B. R., Quaroni, A., Brayer, G. D., Sterchi, E. E., Robayo Torres, C. C., Rose, D. R., and Nichols, B. L. (2008). Luminal starch substrate "brake" on maltase-glucoamylase activity is located within the glucoamylase subunit. *The Journal of nutrition* **138**, 685-692.

Ravaud, S., Robert, X., Watzlawick, H., Haser, R., Mattes, R., and Aghajari, N. (2007). Trehalulose synthase native and carbohydrate complexed structures provide insights into sucrose isomerization. *Journal of Biological Chemistry* **282**, 28126-28136.

Ren, L., Qin, X., Cao, X., Wang, L., Bai, F., Bai, G., and Shen, Y. (2011). Structural insight into substrate specificity of human intestinal maltase-glucoamylase. *Protein & cell* **2**, 827-836.

Riordan, J. F. (1977). The role of metals in enzyme activity. *Annals of Clinical & Laboratory Science* **7**, 119-129.

Saburi, W., Kobayashi, M., Mori, H., Okuyama, M., and Kimura, A. (2013). Replacement of the catalytic nucleophile aspartyl residue of dextran glucosidase by cysteine sulfinate enhances transglycosylation activity. *Journal of Biological Chemistry* **288**, 31670-31677.

จุฬาลงกรณ์มหาวิทยาลัย
Chulalongkorn University

Saburi, W., Mori, H., Saito, S., Okuyama, M., and Kimura, A. (2006). Structural elements in dextran glucosidase responsible for high specificity to long chain substrate. *Biochimica et Biophysica Acta (BBA)-Proteins and Proteomics* **1764**, 688-698.

Saburi, W., Okuyama, M., Kumagai, Y., Kimura, A., and Mori, H. (2015). Biochemical properties and substrate recognition mechanism of GH31 α-glucosidase from *Bacillus* sp. AHU 2001 with broad substrate specificity. *Biochimie* **108**, 140-148.

Sato, T., Nakagawa, H., Kurosu, J., Yoshida, K., Tsugane, T., Shimura, S., Kirimura, K., Kino, K., and Usami, S. (2000). α-Anomer-selective glucosylation of (+)-catechin by the crude enzyme, showing glucosyl transfer activity, of *Xanthomonas campestris* WU-9701. *Journal of bioscience and bioengineering* **90**, 625-630.

Schauer, R. (1982). Cell Biology Monograph. *In* "Sialic Acids Chemistry, Metabolism and Function", Vol. 10. Springer Verlag Vienna.

Schmidt, R. R. (1986). New methods for the synthesis of glycosides and oligosaccharides—Are there alternatives to the Koenigs-Knorr method. *Angewandte Chemie International Edition* **25**, 212-235.

Shen, X., Saburi, W., Gai, Z., Kato, K., Ojima Kato, T., Yu, J., Komoda, K., Kido, Y., Matsui, H., and Mori, H. (2015). Structural analysis of the α-glucosidase HaG provides new insights into substrate specificity and catalytic mechanism. *Acta Crystallographica Section D: Biological Crystallography* **71**, 1382-1391.

Shimba, N., Shinagawa, M., Hoshino, W., Yamaguchi, H., Yamada, N., and Suzuki, E. (2009). Monitoring the hydrolysis and transglycosylation activity of α-glucosidase from *Aspergillus niger* by nuclear magnetic resonance spectroscopy and mass spectrometry. *Analytical Biochemistry* **393**, 23-28.

Shirai, T., Hung, V. S., Morinaka, K., Kobayashi, T., and Ito, S. (2008). Crystal structure of GH13 α-glucosidase GSJ from one of the deepest sea bacteria. *Proteins: Structure, Function, and Bioinformatics* **73**, 126-133.

Sim, L., Willemsma, C., Mohan, S., Naim, H. Y., Pinto, B. M., and Rose, D. R. (2010). Structural basis for substrate selectivity in human maltase-

จุฬาลงกรณ์มหาวิทยาลัย
Chulalongkorn University

glucoamylase and sucrase-isomaltase N-terminal domains. *Journal of Biological Chemistry* **285**, 17763-17770.

Stam, M. R., Danchin, E. G. J., Rancurel, C., Coutinho, P. M., and Henrissat, B. (2006). Dividing the large glycoside hydrolase family 13 into subfamilies: towards improved functional annotations of α-amylase-related proteins. *Protein Engineering, Design and Selection* **19**, 555-562.

Sugimoto, M., Furui, S., and Suzuki, Y. (1995). Multiple molecular forms of α-glucosidase from spinach seeds, *Spinacia oleracea* L. *Bioscience, Biotechnology, and Biochemistry* **59**, 673-677.

Suzuki, Y., and Uchida, K. (1984). Three forms of α-glucosidase from welsh onion (*Allium fistulosum* L.). *Agricultural and Biological Chemistry* **48**, 1343-1345.

Takesue, Y., Yokota, K., Oda, S., and Takesue, S. (2001). Comparison of sucrase-free isomaltase with sucrase-isomaltase purified from the house musk shrew *Suncus murinus*. *Biochimica et Biophysica Acta (BBA)-Protein Structure and Molecular Enzymology* **1544**, 341-349.

Takewaki, S., Kimura, A., Kubota, M., and Chiba, S. (1993). Substrate specificity and subsite affinities of honeybee α-glucosidase II. *Bioscience, biotechnology, and biochemistry* **57**, 1508-1513.

Takewaki, S. i., Chiba, S., Kimura, A., Matsui, H., and Koike, Y. (1980). Purification and properties of α-glucosidases of the honey bee *Apis mellifera* L. *Agricultural and Biological Chemistry* **44**, 731-740.

Tomasik, P., and Horton, D. (2012). Chapter 2 - Enzymatic conversions of starch. *In* "Advances in Carbohydrate Chemistry and Biochemistry" (D. Horton, ed.), Vol. 68, pp. 59-436. Academic Press.

Tombs, M. (1985). Stability of enzymes. *Journal of applied biochemistry* **7**, 3-24.

Ueno, T., Takeuchi, H., Kawasaki, K., and Kubo, T. (2015). Changes in the gene expression profiles of the hypopharyngeal gland of worker honeybees in association with worker behavior and hormonal factors. *PloS one* **10**, e0130206.

van den Eijnden, D. H., Blanken, W. M., and van Vliet, A. (1986). Branch specificity of β-d-galactosidase from *Escherichia coli*. *Carbohydrate research* **151**, 329-335.

จุฬาลงกรณ์มหาวิทยาลัย
CHULALONGKORN UNIVERSITY

Walter, J., Hertel, C., Tannock, G., Lis, C., Munro, K., and Hammes, W. (2001). Detection of *Lactobacillus, Pediococcus, Leuconostoc,* and *Weissella* species in human feces by using group-specific PCR primers and denaturing gradient gel electrophoresis. *Applied and Environmental Microbiology* **67**, 2578-2585.

Watanabe, K., Hata, Y., Kizaki, H., Katsube, Y., and Suzuki, Y. (1997). The refined crystal structure of *Bacillus cereus* oligo-1, 6-glucosidase at 2.0 Å resolution: structural characterization of proline-substitution sites for protein thermostabilization. *Journal of molecular biology* **269**, 142-153.

Wiegand, G., Epp, O., and Huber, R. (1995). The crystal structure of porcine pancreatic a-amylase in complex with the microbial inhibitor tendamistat. *Journal of Molecular Biology* **247**, 99-110.

Wongchawalit, J., Yamamoto, T., Nakai, H., Kim, Y., Sato, N., Nishimoto, M., Okuyama, M., Mori, H., Saji, O., and Chanchao, C. (2006). Purification and characterization of α-glucosidase I from Japanese honeybee (*Apis cerana japonica*) and molecular cloning of its cDNA. *Bioscience, Biotechnology and Biochemistry* **70**, 2889-2898.

Yamamoto, K., Miyake, H., Kusunoki, M., and Osaki, S. (2010). Crystal structures of isomaltase from *Saccharomyces cerevisiae* and in complex with its competitive inhibitor maltose. *The FEBS journal* **277**, 4205-4214.

Yamamoto, T., Unno, T., Watanabe, Y., Yamamoto, M., Okuyama, M., Mori, H., Chiba, S., and Kimura, A. (2004). Purification and characterization of *Acremonium implicatum* α-glucosidase having regioselectivity for α-1, 3-glucosidic linkage. *Biochimica et Biophysica Acta* **1700**, 189-198.

Yang, H., Liu, L., Wang, M., Li, J., Wang, N. S., Du, G., and Chen, J. (2012). Structure-based engineering of methionine residues in the catalytic cores of alkaline amylase from *Alkalimonas amylolytica* for improved oxidative stability. *Applied and environmental microbiology* **78**, 7519-7526.

Yoshinaga, K., Fujisue, M., Abe, J., Hanashiro, I., Takeda, Y., Muroya, K., and Hizukuri, S. (1999). Characterization of exo-(1, 4)-alpha glucan lyase from red alga *Gracilaria chorda.* Activation, inactivation and the kinetic properties of the enzyme. *Biochimica et Biophysica Acta* **1472**, 447-454.

จุฬาลงกรณ์มหาวิทยาลัย
Chulalongkorn University

Zhang, K., Li, W., Wu, Y., Chen, G., and Liang, Q. (2011). Purification and characterization of an intracellular α-glucosidase with high transglycosylation activity from *Aspergillus niger* M-1. *Preparative Biochemistry and Biotechnology* **41**, 201-17.

Zhou, C., Xue, Y., and Ma, Y. (2015). Evaluation and directed evolution for thermostability improvement of a GH 13 thermostable α-glucosidase from *Thermus thermophilus* TC11. *BMC Biotechnology* **15**, 1.

Zhou, K., Luan, H., Hu, Y., Ge, G., Liu, X., Ma, X., Hou, J., Wang, X., and Yang, L. (2012). Isolation and characterization of a novel α-glucosidase with transglycosylation activity from *Arthrobacter* sp. DL001. *Journal of Molecular Catalysis B: Enzymatic* **80**, 48-57.

จุฬาลงกรณ์มหาวิทยาลัย
CHULALONGKORN UNIVERSITY

APPENDICES

จุฬาลงกรณ์มหาวิทยาลัย
CHULALONGKORN UNIVERSITY

APPENDIX 1

Preparation of SDS-polyacrylamide gel electrophoresis

1) Stock reagents

2 M Tris-HCl pH 8.8

Tris (Hydroxymethyl)-aminomethane 24.2 g

Adjusted pH to 8.8 with 1 N HCl and adjusted volume to 100 ml with distilled water

1M Tris-HCl pH 6.8

Tris (Hydroxymethyl)-aminomethane 12.1 g

Adjusted pH to 6.8 with 1 N HCl and adjusted volume to 100 ml with distilled water

10% (w/v) SDS

Sodium dodecyl sulfate 10 g

Adjusted volume to 100 ml with distilled water

50% (v/v) glycerol

100% glycerol 50 ml

Adjusted volume to 100 ml by adding 50 ml of distilled water

1% (w/v) bromophenol blue

Bromophenol blue 100 mg

Adding 10 ml of distilled water and stir the solution overnight. The solution was filtered to remove aggregated dye prior to use

จุฬาลงกรณ์มหาวิทยาลัย
CHULALONGKORN UNIVERSITY

2) Working solutions

Solution A

30% acrylamide, 0.8% bis-acrylamind, 100 ml

Acrylamide	29.2 g
N,N'-methylene-bis-acrylamide	0.8 g

Adjusted volume to 100 ml with distilled water

Solution B

4X separating gel buffer

2 M Tris-HCl pH 8.8	75 ml
10 % SDS	4 ml
Distilled water	21 ml

Solution C

4X stacking gel buffer

1 M Tris-HCl pH 6.8	50 ml
10 % SDS	4 ml
Distilled water	46 ml

จุฬาลงกรณ์มหาวิทยาลัย
CHULALONGKORN UNIVERSITY

10% ammonium persulfate (APS)

Ammonium persulfate	0.5g
Distilled water	5 ml

Electrophoresis buffer

Tris (Hydroxymethyl)-aminomethane	3 g
Glycine	14.4 g

Sodium dodecyl sulfate	1 g
Adjusted volume to 1 litre with distilled water	

5X sample buffer

1 M Tris-HCl pH 6.8	0.6 ml
50 % glycerol	5 ml
10 % SDS	2 ml
2-β-mercaptoethanol	0.5 ml
1% bromophenol blue	1 ml
Distilled water	0.9 ml

Coomassie gel staining solution

Coomassie blue R-250	1 g
Methanol	450 ml
Glacial acetic acid	100 ml
Distilled water	450 ml

จุฬาลงกรณ์มหาวิทยาลัย
CHULALONGKORN UNIVERSITY

Coomassie gel destaining solution

Methanol	100 ml
Glacial acetic acid	100 ml
Distilled water	800 ml

APPENDIX 2

Preparation of buffer for crude enzyme preparation

1) Stock solution

0.5 M potassium phosphate buffer pH 7.4

Component 1

0.5 M dipotassium hydrogen phosphate

Dipotassium hydrogen phosphate	26.127 g

Adjusted volume to 300 ml with distilled water

Component 2

0.5 M potassium dihydrogen phosphate

Potassium dihydrogen phosphate	6.814 g

Adjusted volume to 100 ml with distilled water

Component 2 was added to component 1 until the pH of the solution was 7.4

Extraction buffer

0.5 M potassium phosphate buffer	50 ml
0.01% TritonX-100	400 ul
5 M NaCl	8 ml

Adjusted volume to 400 ml with distilled water

2.5 M NaCl

Sodium chloride	10 g

Adjusted the volume to 100 ml with distilled water

จุฬาลงกรณ์มหาวิทยาลัย
CHULALONGKORN UNIVERSITY

APPENDIX 3

Preparation of purification buffer

Buffer for His-Trap column purification

50 mM phosphate buffer pH 7.4

0.5 M phosphate buffer pH 7.4	50 ml

Adjusted the volume to 500 ml with distilled water

50 mM phosphate buffer pH 7.4 with 50 mM Nacl

0.5 M phosphate buffer pH 7.4	50 ml
2.5 M Sodium chloride	10 ml

Adjusted the volume to 500 ml with distilled water

50 mM phosphate buffer pH 7.4, 50 mM immidazole with 50 mM Nacl

0.5 M phosphate buffer pH 7.4	50 ml
2.5 M Sodium chloride	10 ml
2.5 M Imidazole	10 ml

Adjusted the volume to 500 ml with distilled water

จุฬาลงกรณ์มหาวิทยาลัย
CHULALONGKORN UNIVERSITY

50 mM phosphate buffer pH 7.4, 100 mM immidazole with 50 mM Nacl

0.5 M phosphate buffer pH 7.4	50 ml
2.5 M Sodium chloride	10 ml
2.5 M Imidazole	20 ml

Adjusted the volume to 500 ml with distilled water

50 mM phosphate buffer pH 7.4, 500 mM immidazole with 50 mM Nacl

0.5 M phosphate buffer pH 7.4	50 ml
2.5 M Sodium chloride	10 ml
2.5 M Imidazole	100 ml

Adjusted the volume to 500 ml with distilled water

จุฬาลงกรณ์มหาวิทยาลัย
CHULALONGKORN UNIVERSITY

APPENDIX 4

Preparation of Bradford' s solution

Stock solution

Ethanol	100 ml
Phosphoric acid	200 ml
Coomassie blue G-250	350 mg

Working solution

Ethanol	15 ml
Phosphoric acid	30 ml
Stock solution	30 ml
Distilled water	425 ml

Filtered through Whatman paper No.1 prior to use.

จุฬาลงกรณ์มหาวิทยาลัย
CHULALONGKORN UNIVERSITY

APPENDIX 5

Restriction map of modified pET-28b vector

Restriction map of modified pET-28b vector was kindly given by Mr. Thapanan Jatuyosporn which modified by remove region from *Nco* I to *Bam*H I.

pET-28a(+) sequence landmarks	
T7 promoter	370-386
T7 transcription start	369
His·Tag coding sequence	270-287
T7·Tag coding sequence	207-239
Multiple cloning sites (*Bam*H I · *Xho* I)	158-203
His·Tag coding sequence	140-157
T7 terminator	26-72
lacI coding sequence	773-1852
pBR322 origin	3286
Kan coding sequence	3995-4807
f1 origin	4903-5358

The maps for pET-28b(+) and pET-28c(+) are the same as pET-28a(+) (shown) with the following exceptions: pET-28b(+) is a 5368bp plasmid; subtract 1bp from each site beyond *Bam*H I at 198. pET-28c(+) is a 5367bp plasmid; subtract 2bp from each site beyond *Bam*H I at 198.

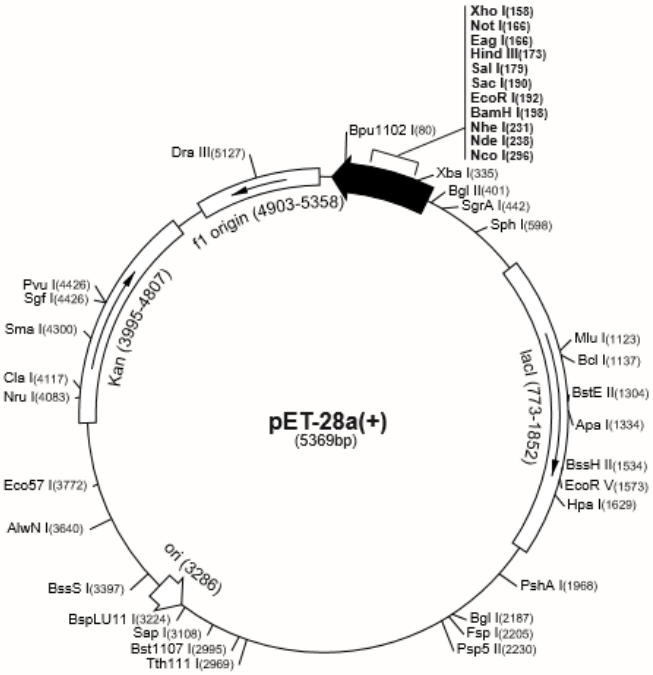

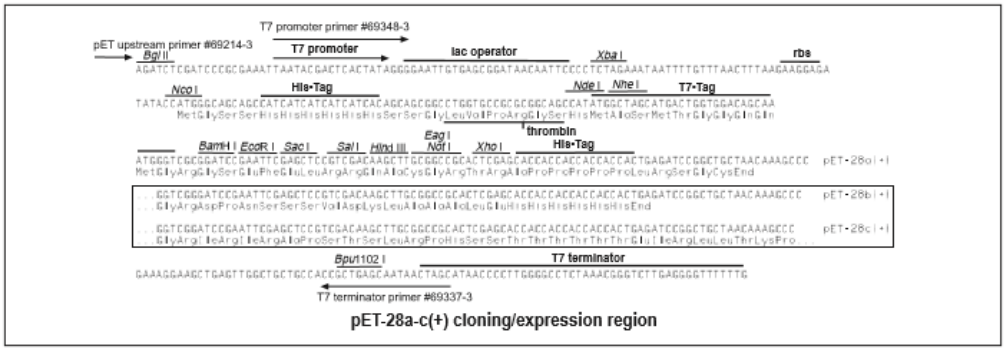

pET-28a-c(+) cloning/expression region

. . . . . CCATGGATCCGAATTC . . . . . .

*Nco*I *EcoR*I

Frame

Modified pET28b Map

จุฬาลงกรณ์มหาวิทยาลัย
CHULALONGKORN UNIVERSITY

APPENDIX 6

Standard curve for protein determination by Bradford's assay

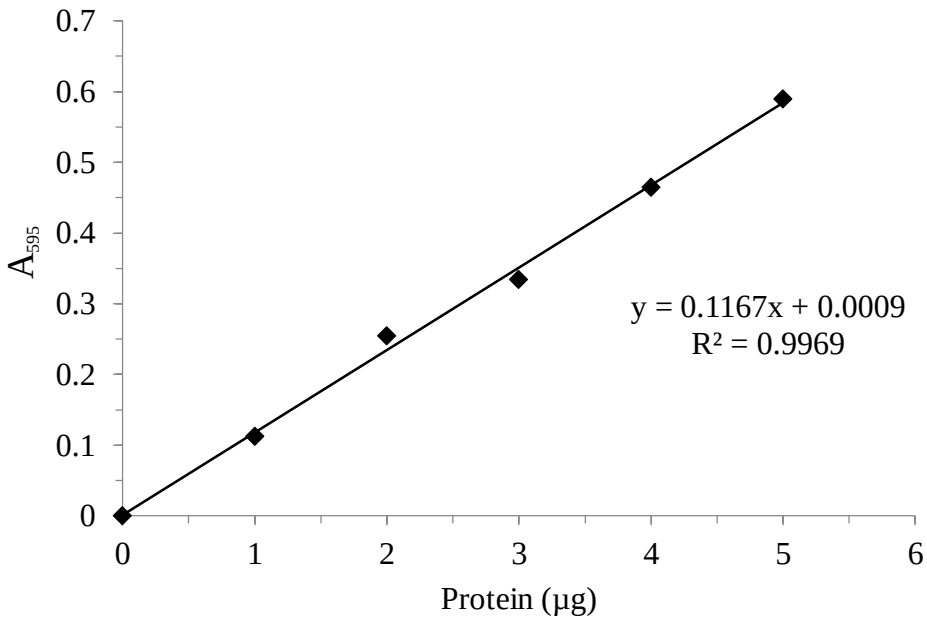

จุฬาลงกรณ์มหาวิทยาลัย
CHULALONGKORN UNIVERSITY

APPENDIX 7

Standard curve for protein determination by glucose oxidase assay

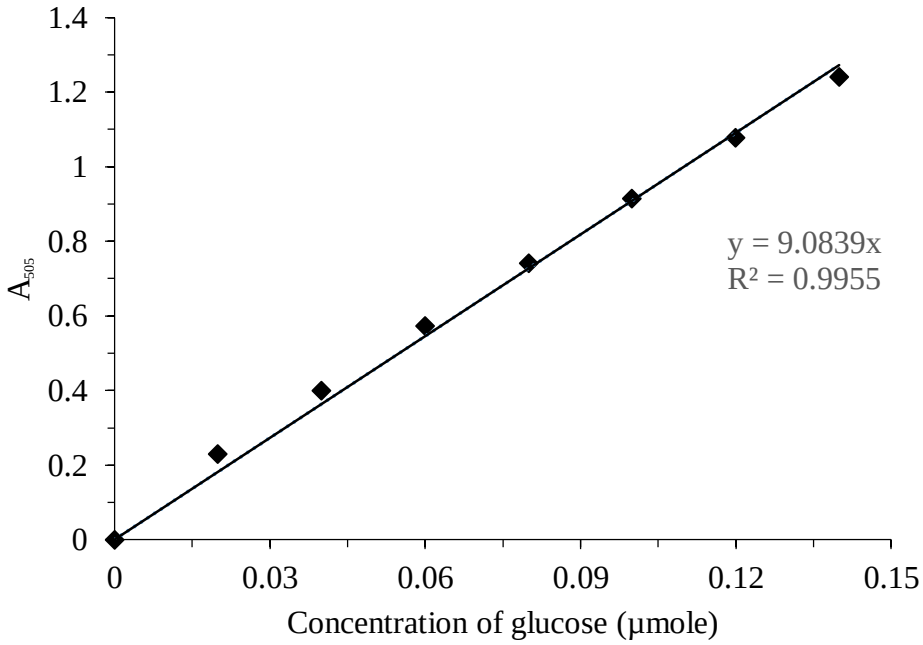

จุฬาลงกรณ์มหาวิทยาลัย
CHULALONGKORN UNIVERSITY

APPENDIX 8

Calculation for percentage relative activity

Substrate	$A_{Control}$	A_{505}			$A_{Average}$	$A_{Average}$-$A_{Control}$	Relative activity (%)
		1	2	3			
50 mM Maltose (G2)	0.194	0.216	0.217	0.217	0.2167	0.0227	2.80 ± 0.00
50 mM Maltotriose (G3)	0.338	1.188	1.115	1.138	1.1470	0.8090	100.00 ± 0.04
50 mM Maltotetraose (G4)	0.14	0.36	0.337	0.36	0.3523	0.2123	26.25 ± 0.01
50 mM Maltopentaose (G5)	0.148	0.263	0.255	0.253	0.2570	0.1090	13.47 ± 0.01
50 mM Maltohexaose (G6)	0.081	0.204	0.206	0.202	0.2040	0.1230	15.20 ± 0.00
50 mM Maltoheptaose (G7)	0.161	0.166	0.163	0.165	0.1647	0.0037	0.45 ± 0.00
1% Pullulan	0.081	0.081	0.081	0.081	0.0810	0.0000	0.00 ± 0.00
1% Dextrin	0.082	0.083	0.083	0.083	0.0830	0.0010	0.12 ± 0.00
1% Amylopectin	0.087	0.087	0.088	0.089	0.0880	0.0010	0.12 ± 0.00
0.5 mM pNPG	0.079	0.081	0.081	0.081	0.0810	0.0020	0.25 ± 0.00
50 mM Isomaltotriose	0.103	0.103	0.107	0.111	0.1070	0.0040	0.49 ± 0.00
50 mM Isomaltose	0.094	0.094	0.102	0.097	0.0977	0.0037	0.45 ± 0.00
2.5% Raffinose	0.079	0.081	0.082	0.081	0.0813	0.0023	0.29 ± 0.00
2.5% Cellobiose	0.172	0.174	0.172	0.175	0.1737	0.0017	0.21 ± 0.00
2.5% Melibiose	0.105	0.106	0.107	0.105	0.1060	0.0010	0.12 ± 0.00
2.5% Palatinose	0.118	0.119	0.126	0.12	0.1217	0.0037	0.45 ± 0.00

APPENDIX 9

Standard curve of molecular weight protein from SDS-PAGE

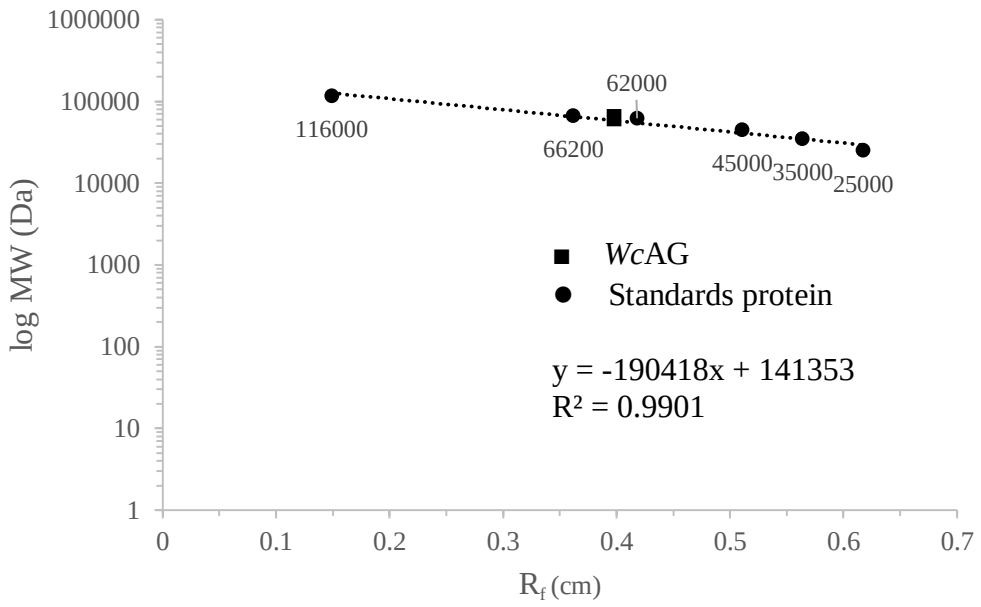

Calculation

From Figure 3.16 (A): Migration distance of *Wc*AG: 1.95 cm

Migration distance of dye front: 4.69 cm

So R_f = 1.95 cm/4.69 cm = 0.416 cm

From Figure 3.16 (B): y = -190418x + 141353

x = R_f of *Wc*AG = 0.416 cm

y = log MW

So molecular weight of *Wc*AG from SDS-PAGE $= 10^{y} = 10^{-190418x + 141353}$

= 62.1 kDa

APPENDIX 10

Standard curve for protein determination by gel filtration chromatography

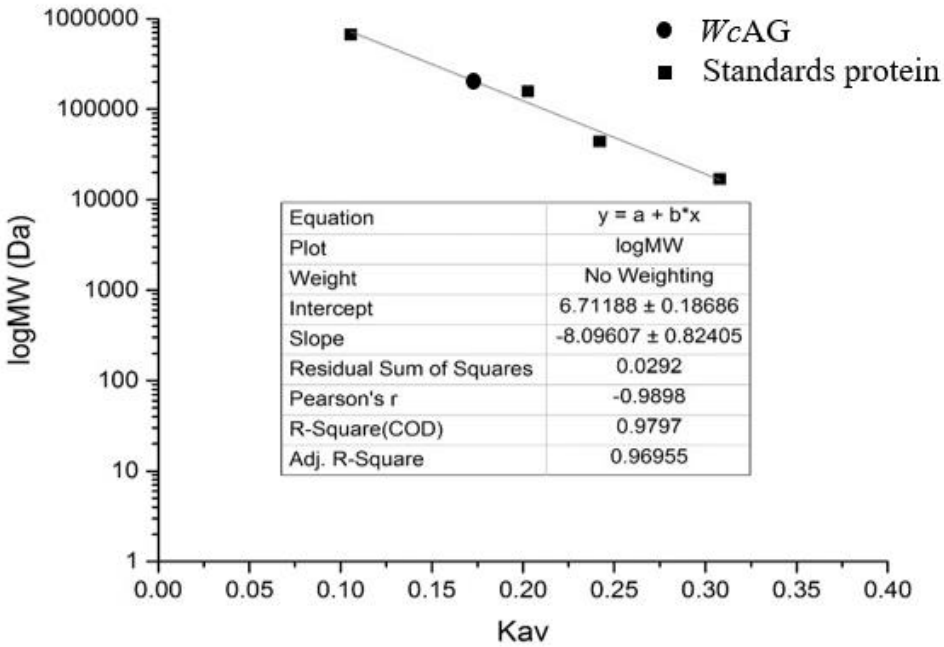

Calculation

V_e = 58.178 ml (From Figure 3.23 (A)), V_i = 120.103 ml, V_o = 42.724 ml,

$K_{av} = (V_e-V_o)/(V_i-V_o)$

$K_{av} = (58.187-42.724)/(120.103-42.724)$

$K_{av} = 0.1998$ ml

From Figure 3.23 (B): $y = -8.09607x + 6.71188$

$x = K_{av}$ of *Wc*AG = 0.1998 ml

y = log MW

So molecular weight of *Wc*AG $= 10^{y} = 10^{-8.09607x + 6.71188}$

= 124.2 kDa

APPENDIX 11

Abbreviation of amino acid residue found in protein

		Second base							
		T		C		A		G	
First base	T	TTT	Phe (F)	TCT	Ser (S)	TAT	Tyr (Y)	TGT	Cys (C)
		TTC	Phe (F)	TCC	Ser (S)	TAC		TGC	
		TTA	Leu (L)	TCA	Ser (S)	TAA	STOP	TGA	STOP
		TTG	Leu (L)	TCG	Ser (S)	TAG	STOP	TGG	Trp (W)
	C	CTT	Leu (L)	CCT	Pro (P)	CAT	His (H)	CGT	Arg (R)
		CTC	Leu (L)	CCC	Pro (P)	CAC	His (H)	CGC	Arg (R)
		CTA	Leu (L)	CCA	Pro (P)	CAA	Gln (Q)	CGA	Arg (R)
		CTG	Leu (L)	CCG	Pro (P)	CAG	Gln (Q)	CGG	Arg (R)
	A	ATT	Ile (I)	ACT	Thr (T)	AAT	Asn (N)	AGT	Ser (S)
		ATC	Ile (I)	ACC	Thr (T)	AAC	Asn (N)	AGC	Ser (S)
		ATA	Ile (I)	ACA	Thr (T)	AAA	Lys (K)	AGA	Arg (R)
		ATG	Met (M) START	ACG	Thr (T)	AAG	Lys (K)	AGG	Arg (R)
	G	GTT	Val (V)	GCT	Ala (A)	GAT	Asp (D)	GGT	Gly (G)
		GTC	Val (V)	GCC	Ala (A)	GAC	Asp (D)	GGC	Gly (G)
		GTA	Val (V)	GCA	Ala (A)	GAA	Glu (E)	GGA	Gly (G)
		GTG	Val (V)	GCG	Ala (A)	GAG	Glu (E)	GGG	Gly (G)

จุฬาลงกรณ์มหาวิทยาลัย
CHULALONGKORN UNIVERSITY

REFERENCES

จุฬาลงกรณ์มหาวิทยาลัย
CHULALONGKORN UNIVERSITY

APPENDIX

จุฬาลงกรณ์มหาวิทยาลัย
CHULALONGKORN UNIVERSITY

VITA

Miss Lalita Silapasom was born on August 18th, 1993. She has graduated the Bachelor's degree from Department of Biochemistry, Faculty of Science, Chulalongkorn University in 2015. Then, she has studied in Master's degree in the major field of Biochemistry and Molecular biology, Department of Biochemistry, Faculty of Science, Chulalongkorn University.

She attended the poster presentation and partticipating in the 5th Asia Pacific Protein Association Conference and the 12th International Symposium ot The Protein Society of Thailand at the Tide Resort, Bangsaen, Thailand. Her proceeding was published in the title of 'Cloning and expression of α–glucosidase from Weissella confusa BBK-1'.

จุฬาลงกรณ์มหาวิทยาลัย
CHULALONGKORN UNIVERSITY

จุฬาลงกรณ์มหาวิทยาลัย
CHULALONGKORN UNIVERSITY